Investigation of Wavelength Tunable Laser Modules for use in Future Optically Switched Dense Wavelength Division Multiplexed Networks

A THESIS FOR THE DEGREE OF DOCTOR OF PHILOSOPHY

Presented to

Dublin City University (DCU)

By

Eoin M.Connolly

B.Eng.

School of Electronic Engineering
Faculty of Engineering and Computing
Dublin City University

Research Supervisor
Prof. Liam P. Barry

December 2007

Declaration

I hereby certify that this material, which I now submit for assessment on the programme of study leading to the award of Doctor of Philosophy is entirely my own work, that I have exercised reasonable care to ensure that the work is original, and does not to the best of my knowledge breach any law of copyright, and has not been taken from the work of others save and to the extent that such work has been cited and acknowledged within the text of my work.

Signed: _____

ID No.: _____

Date: _____

Approval

Name: Eoin M. Connolly

Degree: Doctor of Philosophy

Title of Thesis: Investigation of Wavelength Tunable Laser Modules for use in Future Optically Switched Dense Wavelength Division Multiplexed Networks

Examining Committee:

Dr. Sean Marlow (Dublin City University)
Chair

_____

Dr. Pascal Landais (Dublin City University)
Internal Examiner

_____

Prof. Marian Marciniak (National Institute of Telecommunications, Warsaw, Poland)
External Examiner

_____

Date Approved: _____

Acknowledgements

I would foremost like to thank my supervisor Prof. Liam Barry for his guidance, enthusiasm and encouragement throughout my time in the lab. Thanks are also due to those, with whom I collaborated; in DCU – Ola, Philip, Frank, Prince, Rob and Antonia; and in Cork – Arvind, David and Andrew.

I would also like to thank all the other past and present members of the lab who have made my time here more enjoyable – Paul, Brendan, Marc, Krzy, Sylwester, Karl, Doug, Aisling, Celine and also the auxiliary members Damien and Eoin K.

Finally I would like to express my deep appreciation to all my friends and family, particularly my parents Mairéad and Jerome, and my girlfriend Laura who have helped me keep my sanity throughout the writing of this thesis.

Table of Contents

List of Figures

List of Tables

Abstract

This thesis investigates the use of fast wavelength tunable laser modules in future optically switched dense wavelength division multiplexed networks (DWDM). The worldwide demand for increasingly greater broadband access has thus far been satisfied by the use of DWDM networks, enabled by the development of the erbium doped amplifier. However as this demand continues to grow electronic switching at network nodes will become a limiting factor, creating a potential bandwidth mismatch between the fibre capacities and switching capacity. Optical switching has been proposed to overcome this electronic bottleneck and fully utilize the enormous bandwidth offered by fibre. Fast tunable lasers (TLs) are a key technology in this area, enabling fast wavelength switching.

Experimental work involving the fast wavelength switching of sampled grating distributed Bragg reflector TL modules is presented. Spurious mode generation during wavelength tuning is shown to cause severe cross-channel interference on other data channels in a DWDM test bed. Bit error rate (BER) results demonstrate that a integrated semiconductor optical amplifier can greatly reduce system degradation caused by asynchronous switching of multiple TLs. This is achieved by optically blanking the laser output during channel transition for a period of 60 ns.

Immediately after the blanking period a wavelength drift due to the TL module wavelength locking is found to cause cross channel interference and introduce an error floor >1 e-4 on the BER performance characteristic of an adjacent channel in a 12.5 GHz spaced DWDM network. This drift is characterised, using a self-heterodyne and a filter based approach – Error free performance is subsequently demonstrated by using an extended blanking period of 260 ns or by using sub-carrier multiplexing transmission and phase selective demodulation before detection.

A DWDM optical label switching system, utilizing 40 Gbit/s payload data with low data rate labels placed on a 40 GHz sub-carrier and using TL transmitters is presented. Channel performance is monitored on a static channel as a second data channel is tuned into an adjacent channel on a 100 GHz spaced grid. Error free performance is demonstrated only for the channel payload – Time resolved BER results in agreement with the TL wavelength drift are measured and demonstrate a detrimental influence of the drift on the sub-carrier label performance.

Introduction

The phenomenal growth of the Internet over the last decade has driven the evolution of telecommunications traffic from voice based real-time traffic to internet protocol (IP) based packet traffic. The associated growth in traffic volumes has, thus far led to the development of circuit switched reconfigurable dense wavelength division multiplexed systems (DWDM) to better utilize the enormous capacity offered by optical fibre originally deployed for single or multiple wavelength point-to-point links. With the continued growth of broadband demand and the introduction of new services such as voice-over-IP and IP television, the packet traffic is becoming increasingly sensitive to the high latency characteristic of today's reconfigurable circuit switched optical networks. The requirement for high throughput and reduced delay has therefore resulted in great interest in the development of optically packet switched systems.

Wavelength tunable lasers are quickly becoming a mainstream component in optical networks. In addition to providing immediate cost saving for deployed wavelength division multiplexed networks, in terms of back-up transmitters and inventory reduction, these devices also have an important role to play in future optically switched networks. The purpose of this thesis is to investigate the use of fast wavelength tunable lasers in such systems. In these systems a tunable laser (TL) can be used to generate optical packets at destination specific wavelengths, which can be routed to their appropriate network nodes by using simple optical wavelength filtering techniques. This thesis is based on experimental work carried out using a TL module developed by Intune Technologies Ltd. for such systems. The work was supported by Science Foundation Ireland and was carried out in the Radio and Optical Communications Laboratory, Dublin City University and in the Photonic Systems Laboratory at the Tyndall Institute, Cork

The main contributions of this work are:

- *Spurious Mode Blanking Investigation* – A semiconductor optical amplifier can be used to attenuate the spurious modes generated as a TL tunes. This blanking has been experimentally demonstrated to greatly reduce system performance degradation from the tuning of multiple TLs in a WDM system.

- *Characterisation and System Impact of TL Wavelength Drift* – The initial wavelength drift of a TL module, after tuning, has been characterised and two approaches (extended blanking & sub-carrier multiplexed transmission) have been demonstrated to overcome this drift, thus allowing for error free transmission in a 12.5 GHz spaced ultra-dense WDM system.

- *Optically Labelled Packet Switched System* – The bit error rate as a function of time was correlated with the wavelength drift from a TL module in a spectrally efficient (0.4 b/s/Hz) optically labelled packet switched system.

Report Structure

This thesis is structured into six chapters, which are laid out as described below:

Chapter 1: The first chapter provides an introduction to the subject of dense wavelength division multiplexed (DWDM) optical systems. After giving a brief overview of various multiplexing techniques, the main optical components and network topologies for DWDM systems are presented. Current and future switching schemes for wavelength routed optical networking are discussed, and the desire for optical wavelength tunability in such schemes is introduced.

Chapter 2: The focus of this chapter is on tunable laser semiconductor devices. The main applications for which TLs can be used and the specific requirements for their use in DWDM systems are given. The basic principles behind laser diode

wavelength tuning, particularly single mode tuning, are reviewed. A description of different types of electronically tuned fast TLs is given. The widely tunable sampled grating distributed Bragg reflector laser is covered in greater detail, as it is the basis of the TL module used in the experimental work presented in the later chapters of the thesis.

Chapter 3: This chapter is concerned with the integration of TL devices into modular form for use in DWDM systems. The device characterisation and control required for such modules is described and their related tuning dynamics are investigated. Particular attention is paid to the intermediate spurious modes generated as a TL module tunes between wavelength channels. In this regard an experimental investigation is carried out demonstrating the effectiveness of using a semiconductor optical amplifier (SOA), included in the TL module, to attenuate *or* blank the spurious modes generated during wavelength tuning.

Chapter 4: Two different methods are used to characterise the frequency drift of the TL module once the blanking time ends, and the module locks the laser wavelength to its target channel. The measured frequency drift is found to be detrimental to system performance of an ultra DWDM set-up using 12.5 GHz spacing. Experimental work detailing two different methods to overcome this drift and achieve error free performance are presented.

Chapter 5: This section turns the discussion to the use of TLs in future high capacity networks using optically labelled switched packets. A spectrally efficient scheme using sub-carrier optical labelling of a 40 Gbit/s payload is demonstrated for a 100 GHz spaced two channel set-up. The interference between the labels of two adjacent channels, during wavelength tuning, is then examined and characterised as a function of the initial wavelength drift of the TL module.

Chapter 6: A brief analysis is given of the work presented in the previous chapters, and the thesis conclusions are drawn.

Chapter 1 – Dense Wavelength Division Multiplexed Networks

The continued growth of internet usage and the introduction of new communication services and applications are driving the demand for greater broadband access. This chapter discusses the multiplexing techniques used to fully utilize the optical fibre capacity necessary to enable high speed networks to meet this growing demand. The two main optical multiplexing approaches, time domain and wavelength domain, are addressed along with an electrical modulation technique that can be applied to the optical domain. An overview of the main components used in dense wavelength division multiplexed (DWDM) systems is given followed by a description of the key network topologies in use. The chapter concludes with a description of current and emerging switching technologies necessary for such high capacity networks.

1.1 Multiplexing Techniques for High Speed Networks

The bandwidth offered by a single optical fibre in the low attenuation wavelength bands around 1.3μm and 1.5μm amounts to tens of terahertz. However in a basic optical communication system using a single laser transmitting over a single channel this huge bandwidth potential cannot be met. The capacity is ultimately limited by the speed at which light can be modulated at the transmitter and detected at the receiver (to around 40 Gbit/s). To overcome this limitation, set by the speed of available electronics, the temporal and wavelength domain have been utilized to increase the number of optical channels on the fibre, using optical time division multiplexing (OTDM) and wavelength division multiplexing (WDM) respectively.

1.1.1 Optical Time Division Multiplexing

One approach to overcome the electronic bandwidth limitation is to use time

division multiplexing (TDM) in optical networks, OTDM was first proposed by Tucker in 1988 [1]. This technique is used to create a high data rate optical signal by temporally combining a number of lower data rate optical signals that can be either processed by electronic, electro-optic or all optical techniques [2, 3, 4].

A simplified OTDM transmitter is shown in Fig 1.1. An optical pulse source generates a stream of very narrow pulses at a repetition rate B. The pulse stream is split into N separate paths which are each encoded with different electrical non return-to-zero (NRZ) signals of data rate B. Each path is passed through a progressively increasing fixed fibre delay. This is done in such a way that when all the paths are coupled together a pulse from each path is time interleaved into a dedicated temporal bit slot, generating a return-to-zero (RZ) signal at a data rate of N×B. At the receiver, in a similar manner the signal undergoes optical time division demultiplexing to separate the signals for detection by commercially available detectors.

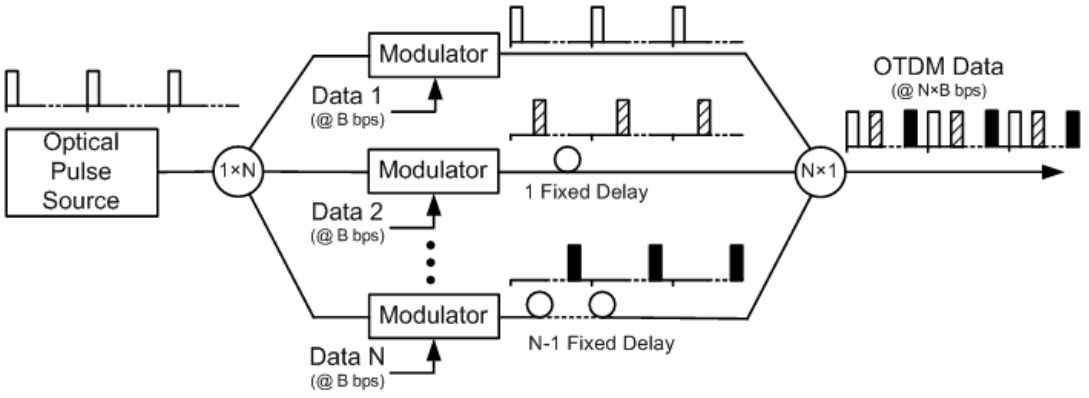

Figure 1.1 OTDM Transmitter Schematic

Using such an approach it is possible to send greater than a Tbit/s aggregate throughput on a single OTDM signal [5, 6], thus offering excellent spectral efficiency from a single optical source. There is however a number of problems associated with this multiplexing technique. Due to the interleaving process there is a need for strict time synchronization at the receiver, thus necessitating the need for

some part of the receiver to operate at the data rate of the multiplexed signal. Also the OTDM timing will dictate the framing format used and so reduce the electrical data protocol transparency.

1.1.2 Wavelength Division Multiplexing

The exploitation of the wavelength domain in approaching the opto-electronic bandwidth mismatch has generated the most attention, being the major multiplexing technology in current long haul optical communication networks [7, 8]. This technique, akin to electrical frequency division multiplexing (FDM) in the optical domain, termed wavelength division multiplexing (WDM), divides the fibre bandwidth into a number of non-overlapping wavelength windows. Conceptually each window supports individual data channels operating at nominal electronic speeds in such a way that the aggregate speed of the multiplexed signal is the sum of the individual wavelength channel speeds, allowing for vastly improved bandwidth utilization.

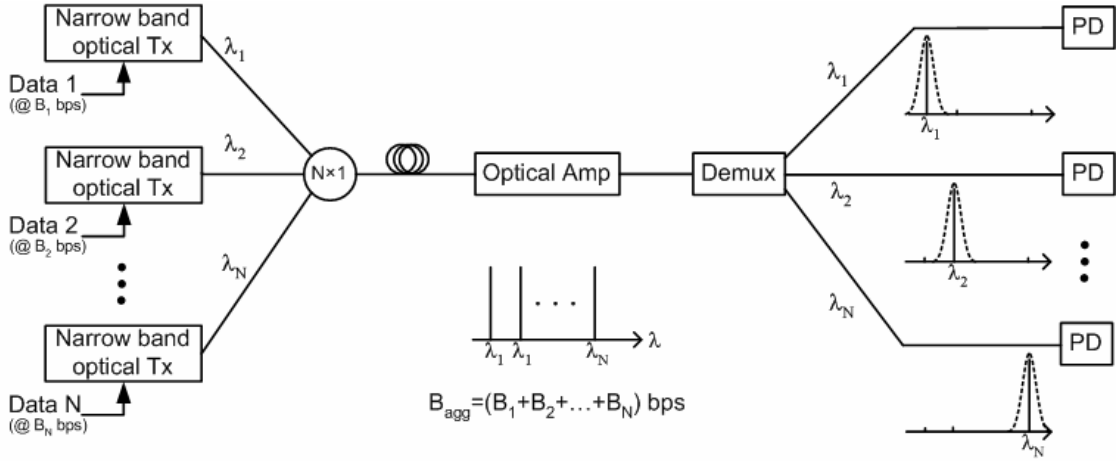

Figure 1.2 WDM Point-to-Point Link Schematic

In Figure 1.2, a simple WDM link is used to show the basic operation of a WDM system. Different electrical data signals at data rates B_N are encoded onto N narrow band optical sources transmitting simultaneously at different wavelengths. In this setup the wavelength channels are combined using a passive fibre coupler to make

the WDM signal with an aggregate data rate $B_{agg}= B_1+B_2+\ldots+B_N$ (different multiplexing techniques are discussed in section 1.3.4). Optical amplifiers can be used periodically to extend the link length. At the receiver end the signal is demultiplexed using optical bandpass filtering. This isolates the individual wavelength channels which are sent to photo-detectors (PD) for conversion back to electrical signals. Certain device, system and network issues will limit the full use of the fibre bandwidth e.g. fibre loss profile, optical amplification and optical source availability [9]. For identification purposes the optical transmission spectrum is divided into different wavelength bands as detailed in Table 1.1.

Band	Name	Range (nm)
O	Original	1260-1360
E	Extended	1360-1460
S	Short Wavelength	1460-1530
C	Conventional	1530-1565
L	Long Wavelength	1565-1625
U	Ultra-Long Wavelength	1625-1675

Table 1.1 Spectral Band Classification

WDM systems can be categorized based upon the specific wavelength or frequency separation between neighbouring wavelength channels. Systems with lower channel spacing will require higher specification, and therefore more costly components. Wide WDM (WWDM) is defined as systems with channels spaced by greater than or equal to 50 nm, with channels typically separated into different spectral bands [10]. Coarse WDM (CWDM) is characterized by channels placed across one or more spectral bands spaced by less than or equal to 20 nm and greater than 1000 GHz. Because of the wide channel spacing used, these systems are suitable for more cost effective applications that use relaxed wavelength selection accuracy and wide passband filters. They can be used for metropolitan area networks (MAN) which operate at lower bit rates and over shorter distances [11].

Dense WDM (DWDM) employs narrow channel spacing of less than or equal to 1000 GHz. Controlled transmitters are typically used to ensure that the wavelength

channels remain fixed to their assigned position, and not interfere with adjacent channels. DWDM systems will be discussed in greater detail in the following sections of this chapter.

Some of the key benefits of WDM systems are that they

- enable vastly improved utilization of the bandwidth of deployed optical fibre,
- offer the ability to transfer information on different wavelength channels independent of the data protocol and coding format of the electrical signal,
- offer great wavelength routing potential as information carried on different wavelengths can be routed using wavelength selective optical filtering,
- require no equipment that operates at speeds greater than the maximum data rate of any individual wavelength channel, and
- can benefit from the availability of optical amplification techniques.

1.1.3 Sub-Carrier Multiplexing

The enormous bandwidth made available by WDM has allowed for network capacity upgrade by simply increasing the wavelength channel count. These wavelength channels have generally used simple cost efficient but bandwidth inefficient on/off keyed direct detection modulation. As the individual channel data rates increase the electronic component speed required becomes economically limiting, with expense significantly increasing for operation beyond ~10 Gbit/s. Alternatively capacity can be increased while keeping a low 'cost per bit transmitted' figure by using advanced modulation techniques used in mature communication networks where bandwidth utilization has been more of a concern. Accordingly sub-carrier multiplexing (SCM), as established in cable TV, radio and satellite applications, can be applied to optical networking. [12, 13]

In optical SCM the available modulation bandwidth of a laser, whether from direct or external modulation, is subdivided into multiple narrow band channels. This is done with readily available low cost components using conventional microwave

techniques. Each channel can be encoded using bandwidth efficient modulation, such as phase shift keying or quadrature amplitude modulation [14], at relatively low data rates. This gives a combined signal with a high aggregate data rate requiring a receiver bandwidth only as high as the individual channels to be detected [15]. In a typical SCM transmitter, as shown in Fig. 1.3, individual digital signals undergo bandwidth efficient electrical modulation. Each signal is then up-converted or modulated onto a different radio frequency (RF) carrier. The channels are combined together in the frequency domain and used to modulate a laser. At a receiver the signal is detected using a photodiode, and the required channel is down-converted or demodulated by mixing with the appropriate channel specific carrier frequency.

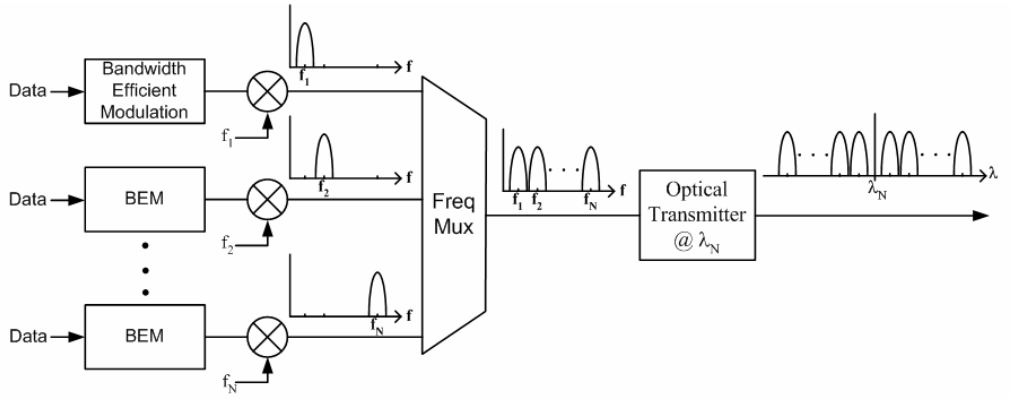

Figure 1.3 Optical SCM Transmitter Schematic

In this way SCM can keep costs down by offering increased bandwidth utilization for single and multi-wavelength (i.e. WDM) systems. Network flexibility will also be improved as many channels that would be available at all nodes can be transmitted using a single optical source. Unlike OTDM, the channels are combined together independent of time and so SCM is transparent to the data rate and protocol used.

1.2 Dense Wavelength Division Multiplexing

The advent of simultaneous optical amplification of multiple wavelengths over the

same wavelength range where currently deployed fibres have lowest loss, around 1550nm, has allowed for the development of DWDM in the C and L-band. The wavelength grid recommend by the International Telecommunication Union supports channel spacing ranging from 1000 GHz to 100 GHz (in steps of 100 GHz), 50 GHz, 25 GHz and as low as 12.5 GHz. A system operating at these channel separations will require high specification electrical, opto-electrical and optical components to perform the required data transmission across the network. In the following sections the opto-electrical and optical components will be described. However functions performed in the electrical domain, such as laser and modulator drivers, switching and regeneration elements will not be covered.

1.3 DWDM Components

1.3.1 Light Source

The light source used for DWDM channels is of fundamental importance and is often the most costly element in the network. The light emitters of choice are high resolution precision narrow band semiconductor lasers fabricated with Indium Gallium Arsenide Phosphide (InGaAsP) on Indium Phosphide substrate. In today's networks light is launched onto any of the supported wavelengths using precisely fabricated single wavelength distributed feedback lasers (DFBs). The DFBs operate on specific fixed wavelengths as set forth in the ITU recommendation G.694.1 [16] for DWDM networks with 100, 50, 25 and 12.5 GHz channel separation. The laser parameters that are important for network operation are output power, side mode suppression ratio (SMSR), wavelength stability, line width and lifetime. A description of current and future DWDM tunable semiconductor lasers is given in Chapter 2.

1.3.2 Modulators

Optical data modulation involves the conversion of an electrical data signal into an optical data signal by using the electrical data to temporally alter one or more physical properties of the optical signal. The intensity, phase and frequency of the optical signal can all be altered in this way [17]. The most widely used technique is

simple binary non-return-to-zero (NRZ) intensity or amplitude modulation using on-off keying. Using this technique a logic "1" is sent with the on keying and light is passed. A logic "0" is sent with the off keying and the light is blocked.

Direct and External Modulation

The laser source can be directly modulated by applying the electrical data signal (combined with a bias current) to the drive current, resulting in an intensity modulated optical signal. Using direct modulation the maximum data rate at which the laser can be modulated is limited by the speed of the laser. Also with the drive current varying, the changes in the carrier density in the laser cavity lead to changes in the cavity's refractive index. As the emitted wavelength depends on the refractive index, this results in a frequency variation known as chirp. The spectral broadening increases the dispersive effect on the signal as it propagates through fibre. Because of these effects and its inherent simplicity direct modulation is a low cost modulation option that is limited to short span and relatively low bandwidth applications (<10 Gbit/s) [9], e.g. Local Area Network (LAN) and Metropolitan Area Network (MAN) links.

External modulation can be used to overcome these problems, allowing modulation at higher data rates and transmission over longer fibre spans. In such a scheme the laser source operates in continuous-wave (CW) mode and the electrical data signal is then applied to an optical modulator external to the laser cavity. The main types of modulators are outlined below.

Mach Zender Modulators

Mach-Zehnder Modulators (MZM) are based on the electro-optic effect which occurs in certain crystal materials, whereby the refractive index of the material changes due to and in proportion to an applied electrical field. Lithium niobate is the most widely used material for the fabrication of MZMs due to its high electro-optic coefficient and optical transparency at the near infrared wavelengths [18]. A schematic of a typical MZM is shown in Fig. 1.4. After entering the lithium niobate

waveguide the input light is split into two paths. On recombination at the output there is either constructive or destructive interference between the optical signals depending on their relative phase difference. By applying a voltage to the electrode the refractive index of the upper path will increase due to the electro-optic effect. This has the effect of inducing a phase difference in the paths by slowing the light in the upper path. By controlling the applied voltage the phase shift can be set to give constructive interference, a logic "1", or destructive interference, a logic "0", at the output. Using this technique the electrical signal applied to the electrode can be modulated onto the optical carrier.

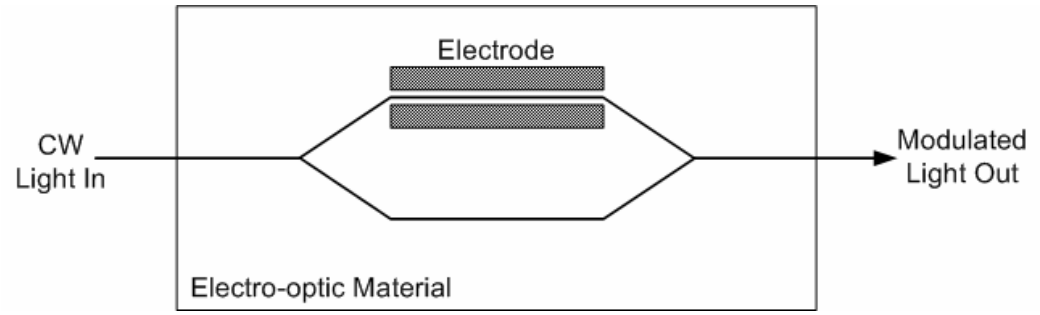

Figure 1.4 Mach-Zehender Modulator Schematic

Electroabsorption Modulators

Electoabsorption modulators (EAMs) are a type of external modulator made of similar materials to semiconductor lasers and so allow for simple integration with other optical devices. They are based on the electroabsorption effect, whereby photon absorption in a semiconductor material occurs for photons with energies above the bandgap energy, while the material is effectively transparent for photon energies below this absorption edge. This effect can be controlled in materials containing quantum wells and in bulk materials, respectively termed as the quantum confined Stark effect and the Franz-Keldysh effect. The absorption edge can be shifted to lower energies by application of an electric field – increasing the photon absorption in the material. Using this effect the material can be used as an on-off optical shutter controlled by the electrical signal to give an intensity modulated optical signal [19].

1.3.3 Receivers

Pin Photodiode:

The pin photodiode detector is fabricated with InGaAs and is connected with a GaAs pre amplifier. When reverse biased the internal impedance is effectively infinite and the input optical power falling on the photo-absorption layer is proportional to the output current, generated by creation of electron-hole pairs during photon absorption. With increasing channel data rates in DWDM networks pin diodes have had to improve. The typically used vertically illuminated pin detectors loose efficiency above 10 Gbit/s. Different detector designs that incorporate double pass techniques, waveguide photodiodes, distributed photodiodes and resonant photodiodes can to be used to overcome this bandwidth limit [20]. Saturation current improvements have also been needed to protect the photo diodes from the high optical powers falling on them due to the use of optical pre-amplification to improve receiver sensitivity.

Avalanche Photodiode:

Receiver sensitivity can be improved by using avalanche photodiodes (APD). The typical structure includes additional multiplication and grading layers compared to the pin. A multiplication process is used that produces avalanche gain of the electrons generated by photon absorption through impact ionisation in the multiplication layer. The avalanche gain is achieved by using very high reverse biasing (~90 V). However due to the additional layers through which the carriers must traverse and due to the multiplication process itself the carriers undergo increased transit time effects. These have the effect of reducing the bandwidth of the APD. The methods listed above to improve the pin bandwidth efficiency product can also be applied to APDs [20].

1.3.4 Multiplexers and Demultiplexers

Multiplexing and demultiplexing devices are used to, respectively, combine and separate the different wavelength channels in a DWDM signal. Optical couplers are passive devices which combine light from different fibre cores into the same core.

They can be used to build multiplexers by combining wavelength channels from different input fibres onto a single output fibre. Demultiplexing is however not as trivial a task, requiring the use of spectral selective components to isolate individual wavelength channels and output them on separate fibres. Demultiplexers function as multiplexers when operated in reverse, enabling their dual use in bi-directional communication systems.

Due to the narrow channel spacing in DWDM signals extremely precise filtering is required for channel isolation. A suitable filter should provide high transmission of the channel wavelength and near complete rejection of the other channels. A narrow flat topped, step edged passband that is stable over time and temperature is required to prevent interference in the form of cross talk from adjacent channels but should also be wide enough to accommodate any drift in the wavelength of the channel being filtered. Accordingly planar waveguides and fibre-based gratings provide the filtering in most DWDM multiplexers. Filtering is also used in DWDM networks for other functions such as gain equalisation and channel monitoring. The main filtering elements [21] are briefly described below.

Arrayed Waveguide Grating

The arrayed waveguide grating (AWG) is one of the most important filtering devices in use in DWDM networks, offering low cost precise demultiplexing of a large number of channels with low losses. Using an interference effect the wavelength channels from an incoming DWDM signal are passively routed to channel specific output fibre ports. Single AWGs with 25 GHz channel spacing covering the conventional (C-band, 1530 – 1565 nm) band and long (L-band, 1565 – 1625 nm) have been realised [22].

The AWG uses an array of silica based waveguides to diffract light into wavelength specific output fibres. As illustrated in Fig. 1.5 the incoming light is coupled to a free space region to illuminate a number of arrayed waveguides of progressively increasing fixed length difference. This causes a phase difference in the light

coming from each waveguide upon recombination at the output free space region, which results in a wavelength dependent diffraction pattern at the output plane. By positioning an output waveguide at the points where each wavelength is in phase it is possible to pick up each input channel – thus demultiplexing the composite wavelength signal and outputting the different wavelength channels on different fibres.

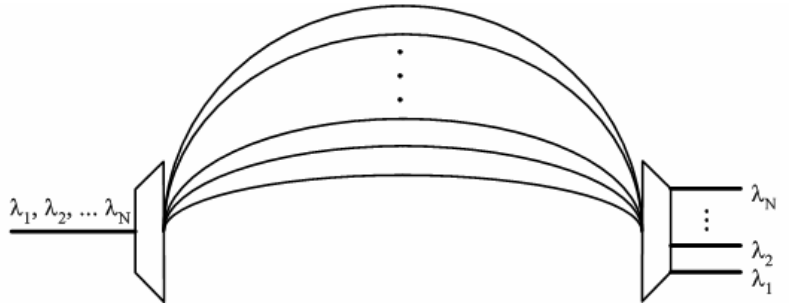

Figure 1.5 Arrayed Waveguide Grating

Etalon Filters

Etalons filters, of which the Fabry-Perot (FP) filter is an example, are based on the reflection of light in a cavity formed by two reflectors. Light of different wavelengths enters the cavity but only the wavelengths that meet the resonate condition of the cavity are transmitted. The distance between the reflectors can be set so that only a single wavelength is transmitted while all other wavelengths destructively interfere. Modifications can be made to increase the number of resolvable channels. FP filters can be made to give full coverage of the C and L-band. The narrow passband of the filter can be tuned by mechanically changing the distance between the reflectors.

Fibre Bragg Grating Filters

In a fibre Bragg grating (FBG) filter a segment of optical fibre is modified to reflect particular wavelengths while transmitting all others. The refractive index of the fibre core is permanently modified in a periodic fashion using a UV interference pattern. Light entering this grating is weakly reflected at each index change. Light

at a particular wavelength is reflected in phase and adds constructively to give strong reflection while light at all other wavelengths interferes destructively giving weak reflection. In this way the filter offers high reflectivity with a narrow spectral bandwidth capable of resolving very narrowly spaced wavelength channels [23]. Tunability of the FBG filter is possible by changing the reflection wavelength using mechanical stretching or heating of the fibre. Fibre grating FP filters can be assembled in a fibre using two narrowly separated identical FBG. These can be used as periodic wavelength references in controllers to fine-tune WDM channels to their intended wavelength [24].

Mach-Zehnder Filters

Mach-Zehnder interferometry, as described in section 1.3.2, can be used to construct Mach-Zehnder filters. An incoming DWDM signal is split into two paths and then recombined at the path outputs. By inducing a delay in one path relative to the other a phase difference is created between the signals at the path outputs. This will cause constructive and destructive interference for different wavelengths, resulting in a periodic passband. By cascading a number of these structures together a single wavelength channel can be isolated from a composite DWDM signal. In this way a tunable MZ Filter can be constructed.

Optical Add-Drop Multiplexers

The optical add-drop multiplexer (OADM) is used to selectively drop and add wavelength channels from and to a DWDM signal. It allows network nodes to optically pass wavelength channels that are not needed, while dropping only the channels that are destined for the node. The node can transmit by adding to the DWDM signal on the same wavelength channels that have been dropped. The optical demultiplexing at the drop port and multiplexing at the add port are performed at fixed wavelengths using passive filters such as FBGs.

1.3.5 Amplifiers

Erbium Doped Fibre Amplifiers

The erbium doped fibre amplifier (EDFA) has been a key enabling technology in the development of DWDM systems [25]. It has allowed increases in the distances of optical fibre links before 3R electronic regeneration[1] is necessary as they can be used as optical repeaters capable of optical 1R power regeneration. The EDFA can amplify multiple optical signal channels simultaneously and is data rate and format independent. This reduces costs by cutting down on expensive high-speed electronic circuitry thus enabling DWDM networks.

The EDFA is based on the material properties of rare earth elements such as trivalent erbium, which gives a wide bandwidth gain in the same wavelength region where silica fibres have lowest loss, around 1550nm. In a single amplifier only portions of the range can be accessed – an amplifier optimised for the C-band will not give good performance in the L-band. The doped fibre is pumped by a semiconductor laser at 980 or 1480 nm. This has the effect of raising electrons of the erbium atoms from ground energy band to an intermediate energy band. The lifetime in the intermediate band is ~10 μs, after which the atoms drop to a meta stable band through a non radiative transition. The lifetime at this band is longer, ~10 ms, which allows the build up of erbium atoms here. Optical signals (within the amplifier wavelength range of operation) entering the doped fibre stimulate the recombination of electron hole pair, which produces photons at the same wavelength as the optical signal, thus amplifing the signal. However the electrons can also return to the ground energy level by spontaneous emission. This produces photons at random wavelengths, which will also be amplified if in the amplifiers range. This results in a noise factor termed amplified spontaneous emission (ASE) noise. EDFAs can achieve gain of greater than 30 dB over a range of 50 nm, with

[1] 3R regeneration involves the restoration of the power, shape and timing of a data signal.

output powers up to 30 dBm.

Semiconductor Optical Amplifiers

The semiconductor optical amplifier (SOA) is based on the use of the gain mechanism of a semiconductor laser diode for optical amplification [26]. The SOA is not equipped with end mirrors and so does not allow the set up of an oscillation regime that causes lasing. The SOA is electrically pumped to create electron-hole pairs. An optical signal passing through the semiconductor will stimulate the exited electrons to return to the valence band. This will create photons of the same wavelength of the input signal and so will amplify the optical signal.

The semiconductor nature of the SOA, fabricated with InGaAsP, keeps the package size small and allows for integration with other optical components. The typical SOA gain is 15-25 dB [27], while lower than for EDFAs they are less expensive and operate over a wider bandwidth range. However, they do not operate well for multiple channels. Their main application in DWDM networks are as power boosters for low powered lasers and as in line single channel amplifiers. They also suffer from higher noise and experience strong optical non-linearities. This later problem can actually be used in wavelength conversion techniques.

Raman Amplifiers

Raman amplification [28] is an optical amplification technique based on stimulated Raman scattering by a pump laser in optical fibre. It involves the interaction of pumped photons with the fibre molecules which has the effect of amplifying a signal at a material specific wavelength offset from the pump wavelength. For amplification a pump wavelength is multiplexed with a signal wavelength in optical fibre and so the amplification gain medium is the transmission fibre itself. This allows the signal amplification to be distributed over significant fibre lengths and so the signal does not drop to as low a level as in lumped set-ups, i.e. with EDFAs, resulting in improved noise performance. The wavelength window over which the Raman amplifier provides gain can be set to different wavelengths or broadened by

selection of appropriate pump wavelength(s). This is advantageous for future DWDM networks, which may require access to wavelength channels outside the EDFA amplification window. Future networks may use distributed Raman amplification in conjunction with lumped EDFAs for improved optical signal to noise ratios [22].

1.4 DWDM Network Topologies

The job of any communications network is to route a client signal to its destination with an acceptable quality of service. From source to destination, a signal travels from an access network to progressively larger networks. Depending on its destination the signal may traverse a combination of access, metro, backbone and long haul networks [9] before it eventually reaches its destination client. To ensure network integrity various network architectures and designs are used. The choice of topology used is based on such factors as: the provision of network resiliency and restoration in event of failure, bandwidth efficiency, traffic capacity, network scalability and cost. The most common topologies used are point-to-point, ring and mesh.

1.4.1 Point to Point

A point-to-point network essentially consists of a DWDM link between two transceivers. This topology can be used for any range but is usually deployed for long haul links connecting continents and countries. Due to the costly nature of using one link to support only two nodes the maximum possible bandwidth is squeezed from the fibre. Accordingly these networks lead the drive for increased bandwidth utilization through increased channel count with narrower channel spacing, higher individual data rates per channel and the use of lossless fibre.

To increase cost efficiency the links can be equipped with intermediate nodes that offer channel adding and dropping functionality in the form of optical add drop multiplexers (OADM). Point-to-point networks are more sensitive to failure, due to fibre breaks or component failure bringing down the network. Restoration and

protection is achieved by using a back up fibre as a protection path and redundant components.

1.4.2 Ring

The ring topology comes in many different styles depending on the physical size of the network, the number of nodes served and the data capacity carried. In general the architecture takes on the form of a number of nodes serviced by a loop of fibre as shown in Fig. 1.6, with each node providing OADM functionality. At least one of the nodes operates as a hub, which provides connectivity to outside networks. The hub also performs flow control and management through the use of a supervisory channel.

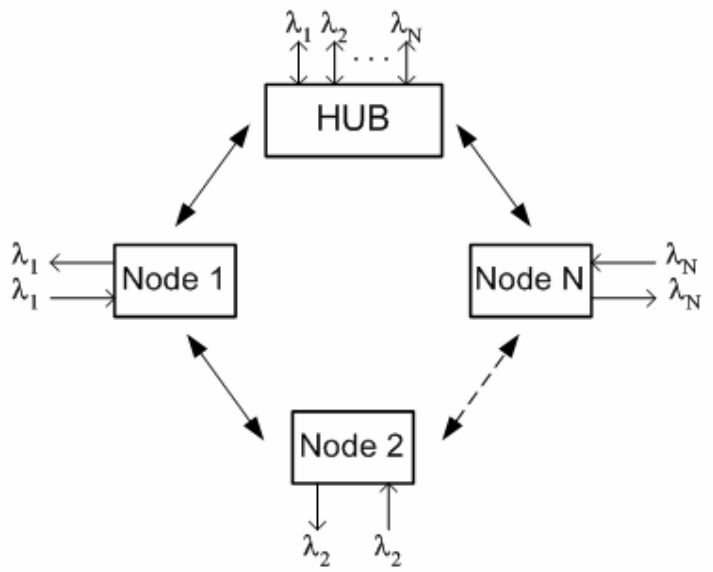

Figure 1.6 Ring Topology

Smaller rings are used at the access level carrying lower traffic capacities, on fewer channels over a single fibre with only one channel added and dropped at each node. As the ring size increases to cover metropolitan areas the aggregate traffic capacity increases and the necessary protection is provided by the use of dual or quad rings. The channel count also increases with the number of channels added and dropped at each node correspondingly increasing. Such metro rings are usually serviced by

more than one hub node.

1.4.3 Mesh

The mesh network as illustrated in Fig. 1.7 provides increased or full connectivity between different nodes and so can easily reroute optical channels around network faults, thus providing a network with increased survivability and protection from node and link failure. The mesh topology is also the most scaleable allowing for the simple integration of extra nodes when needed. This increased resiliency and restoration however is at the cost of laying increased amounts of fibre and the provision of over capacity in the network.

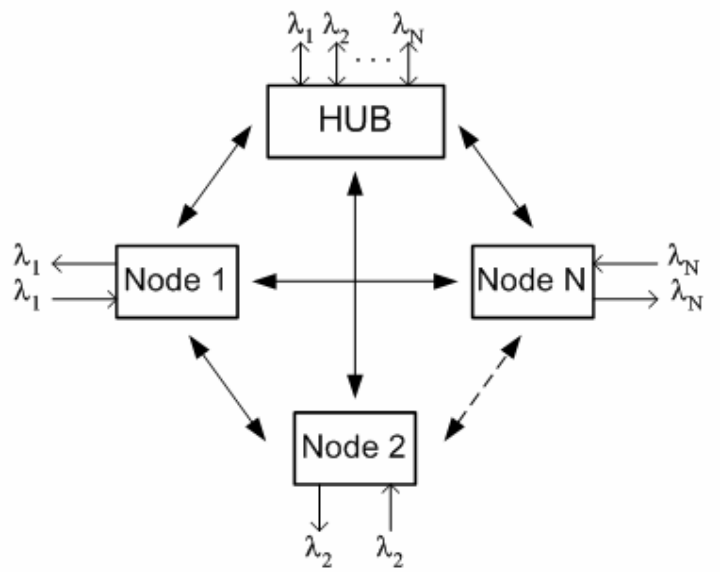

Figure 1.7 Mesh Topology

The mesh topology is used in metro networks as a development of the ring network but is more usually associated with long haul backbone networks. As different point-to-point networks expand and join together through the use of OADMs they begin to take on a mesh structure. These networks are characterised by links containing several fibres with large high capacity channel counts that transport data between different metro networks.

1.5 Optical Switching in WDM Systems

1.5.1 Optical Circuit Switching

Initial optical networks have used point-to-point fibre-optic links to transport data between electronic network nodes. With this setup, the conversion of the optical signal to electronic format for 3R regeneration and then conversion back to optical format for retransmission on the fibre link is necessary to extend the reach of the links. This optical-to-electronic-to-optical (OEO) conversion is also required at each node for electronic switching and routing.

The continued development of WDM components has allowed for the advancement of these initial networks giving potential for optical technology to play a greater role. The EDFA allows for greater distances between nodes before optoelectronic regeneration is necessary. The simultaneous operation of the EDFA on multiple wavelength channels has spurred the development of WDM stable sources and the advancement of filtering technologies. These advancements have greatly increased the number of wavelength channels and data rate per channel on the fibre links. The electronic nodes, however, have not been keeping up with this demand, creating a potential bandwidth mismatch between fibre capacity and router packet forwarding capacity [29].

Optical circuit switched (OCS) networks (which represent the current state of the art of deployed optical networks) may employ wavelength routing to overcome this electronic bottleneck. In such a scheme a dedicated source to destination wavelength connection, termed a lightpath, is set up to optically route information across the network. These networks can be either fixed-wavelength or wavelength reconfigurable. In the fixed wavelength network an OADM can be used at network nodes to perform the optical wavelength routing. At each node a fixed wavelength channel destined for the particular node is dropped from the fibre link, while the other channels are kept in the optical domain, avoiding unnecessary OEO conversion. The node can transmit on this same wavelength by using the OADM to

add a channel to the fibre link. In this scheme the same wavelength is used on each link of the light path. The wavelength reconfigurable scheme improves network functionality and management by using reconfigurable OADMs (ROADM) at the nodes. Each node can be tuned to add or drop any wavelength channel, thus allowing a light path to be made up of different wavelengths [30, 31].

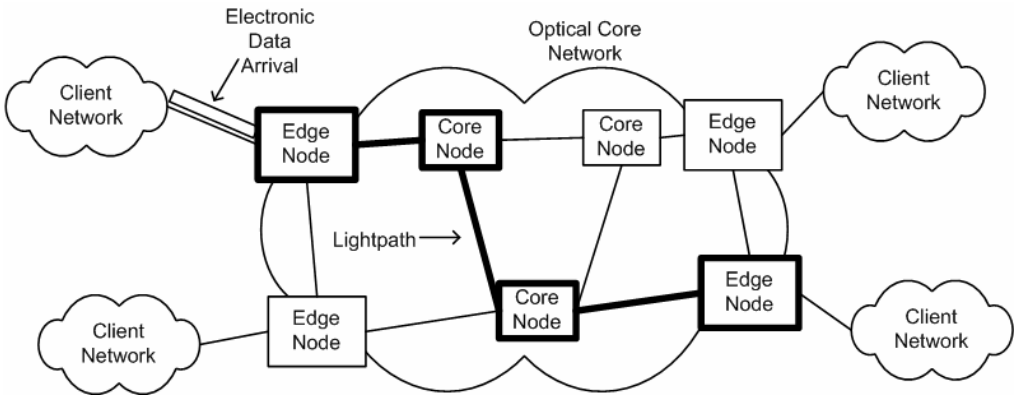

Figure 1.8 Network architecture of an optical circuit switched network

The circuit switched structure of the networks described above is inherited from legacy telecommunications networks which were designed to deal mainly with telephone traffic. As a result the current deployed optical networks are still based on the SONET/SDH architecture, which was established in the US and Europe respectively to accommodate the multiplexing of various data formats (voice, ATM, IP) to higher data rates. Due to the semi-permanent reservation of wavelengths and switching resources during the setup of light paths these networks have poor bandwidth utilization and high latency, as illustrated in Fig. 1.8 with the bold line representing the network resources in use. The networks have however remained, thus far, with packet oriented traffic transmitted on top of the OCS networks. Work is being carried out in two main areas, described below, in the development of next generation optical networks to overcome these problems [32].

1.5.2 Optical Burst Switching

Optical burst switching (OBS) is seen as an intermediary step, between OCS and

future optical packet switching (OPS), in the development of all optical networks. OBS offers improved bandwidth utilization over OCS while requiring less stringent optical device technology than OPS – switching on microsecond rather than nanosecond time scales with no requirement for optical buffering.

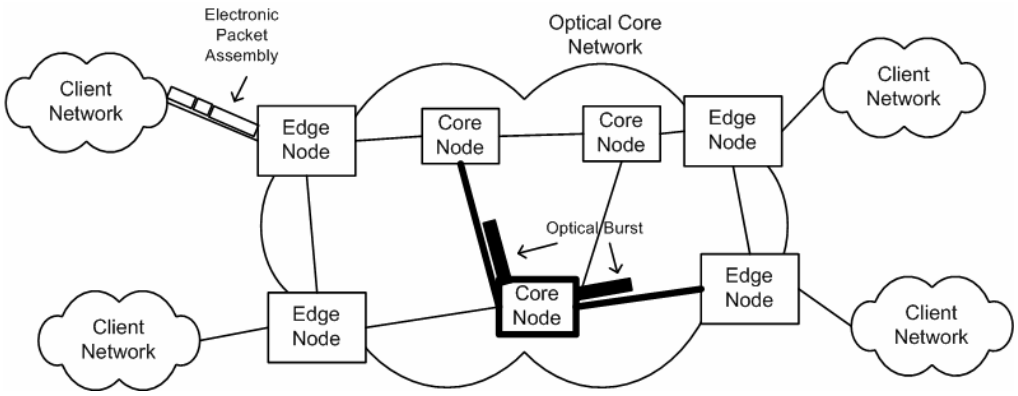

Figure 1.9 Network architecture of an optical burst switched network

Input nodes at the edge of the network (ingress nodes) electronically assemble incoming data into bursts of data. These bursts are optically routed through internal core nodes. The data is then converted back to electronic format when it reaches its destination output node at the edge of the network (egress node). The bursts of data are assembled from different types and sources of data that are destined for the same egress node. For each burst a control packet is sent out from the ingress node through the core nodes to the egress node. The control information is kept separate from the bursts, for example by sending it on a dedicated control channel. This packet is electronically processed at each node so as to set up the node for the imminent arrival of the burst, which is sent an offset time after the control packet either with or without waiting for acknowledgment that the path has been established. The timing is set so that the internal node resources are only configured for the time it takes for the burst to pass through them, after which they are freed for use by other bursts. This will increase the bandwidth utilization and reduce latency of the network, as shown by the reduction in the bold line in Fig.1.9 (representing the architecture for an OBS network) in comparison with that in

Fig.1.8. As the data burst is kept in optical format and only the control packet is electronically processed at core nodes, low cost electronics can be used by transmitting the control packet at low bit rates. There are currently no large scale functioning OBS networks deployed, with the technology still being at test-bed level [33, 34, 35].

1.5.3 Optical Packet Switching

Research into OPS is ongoing, with commercial development some way off, but is seen as the next step in the development of all optical networks, after OBS. Further gains in network granularity and bandwidth utilization can be achieved by the forwarding of data packets individually through the core network in the optical layer with each data packet containing its own control information. These optically labelled switched networks are covered in greater detail in Chapter 5.

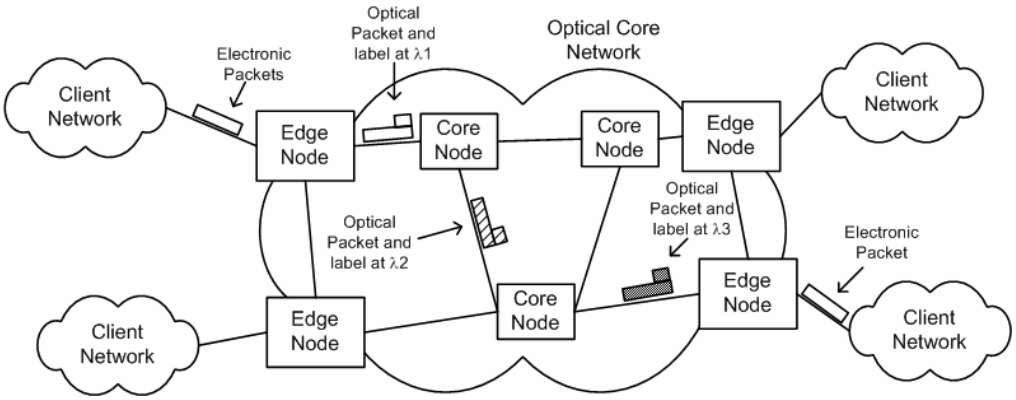

Figure 1.10 Network architecture of an optical packet switched network

In the all optical label swapping (AOLS) method of OPS [36] a label containing the control information is optically coded onto the data packet or optical payload at the ingress node, as shown in Fig. 1.10. At the core nodes the label is optically extracted and processed electronically. The label contains routing information for the optical packet routing layer only, and is not to be confused with the actual IP network data label, which remains part of the optical payload in optical format. During the time it takes the label to be read and updated the payload is buffered and

optically regenerated. The updated label is then reattached to the payload and the optical packet is wavelength converted and forwarded to the appropriate outgoing fibre link to get to the dynamically assigned node. The original data packet is kept in optical format throughout the core network and is only converted back to electronic format at the egress node.

1.5.4 Tunable Lasers in Optical Switched Networks

Tunable laser (TL) development will play a key role in the success of the potential optical networks described in the previous sections. Currently the primary applications of TLs in optical networks are sparing, dynamic provisioning and channel restoration. Tuning speeds for which are on millisecond timescales [37]. The introduction of OBS will increase this tuning requirement to the order of microseconds. Future networks using TLs to perform optical switching of individual packets (i.e. OPS), will increase the requirements even further. This could include the use of TLs as tunable transmitters on which packets will be encoded on destination dependent wavelengths [38]; or as local lasers in tunable wavelength converters to route packets by setting desired forwarding wavelengths [36]. Switching speeds in these types of networks will ultimately be limited by the tuning speed of the TL. To keep overhead respectable tuning times of the order of nanoseconds and below will be required [31, 39].

Tunable Laser demand is expected to grow rapidly at a compound annual growth rate of 37% over the next five years [40]. This market growth is being driven by WDM in long haul networks, with the transformation of point-to-point optical networks to agile networks using ROADMs [41], and in metro networks. In the following chapter we look at the technology that allows the tunable wavelength functionality that is necessary in TLs.

References

[1] R.S. Tucker, G. Eisenstein and S.K Korotky, "Optical time-division multiplexing for very high bit-rate transmission," *J. Lightw. Technol.*, vol. 6, pp. 1737-1749, Nov. 1988.

[2] D.M. Spirit, A.D. Ellis and P.E. Barnsley, "Optical time division multiplexing: systems and networks," *IEEE Commun. Mag*., vol. 32, pp. 56-62, Dec. 1994

[3] B. Kolner and D. Bloom, "Electrooptic sampling in GaAs integrated circuits," *IEEE J. Quantum Electron.*, vol. 22, pp. 79-93, Jan 1986.

[4] M. Westlund, H. Sunnerud, M. Karlsson and P.A. Andrekson, "Software-synchronized all-optical sampling for fiber communication systems," *J. Lightw. Technol.*, vol. 23, pp. 1088-1099, Mar. 2005.

[5] M. Nakazawa, "Tb/s OTDM technology," in *Proc. Eur. Conf. Optical Commun. (ECOC01)*, Amsterdam, Sep. 2001, vol. 5, pp. 184-187.

[6] H.G. Weber, R. Ludwig, S. Ferber, C. Schmidt-Langhorst, M. Kroh, v. Marembert, C. Boerner and C. Schubert, "Ultrahigh-Speed OTDM-Transmission Technology," *J. Lightw. Technol.*, vol. 24, pp. 4616-4627, Dec. 2006.

[7] B. Mukherjee, "WDM optical communication networks: progress and challenges", *IEEE J. Sel. Areas Commun*., vol. 18, pp. 1810-1824, Oct 2000.

[8] N.S. Bergano "Wavelength Division Multiplexing in Long-Haul Transoceanic Transmission Systems," *J. Lightw. Technol.*, vol. 23, pp. 4125-4139, Dec. 2005.

[9] S.V. Kartalopoulos, *DWDM: Networks, Devices, and Technology*. NJ: Wiley-Interscience, IEEE Press, 2003.

[10] ITU-T, Recommendation G.671, "Transmission characteristics of optical components and subsystems," Jan. 2005.

[11] ITU-T, Recommendation G.694.2, "Spectral grids for WDM applications: CWDM wavelength grid," Dec. 2003.

[12] R. Hui, B. Zhu, R. Huang, C.T. Allen, K.R. Demarest and D. Richards, "Subcarrier multiplexing for high-speed optical transmission," *J. Lightw. Technol.*, vol. 20, pp. 417-427, Mar. 2002.

[13] T. Wolcott and E. Schmidt, "Optical subcarrier multiplexing squeezes more capacity from bandwidth," Lightwave, 1 June 2000.

[14] T. Wolcott, S. Eleniak, and E. Schmidt, "SCM complements DWDM, increases capacity," WDM Solutions, 1 May 2001.

[15] T.E Darcie, "Subcarrier multiplexing for lightwave networks and video distribution systems," *IEEE J. Sel. Areas Commun.*, vol. 8, pp. 1240-1248, Sep. 1990.

[16] ITU-T, Recommendation G.694.1, "Spectral grids for WDM applications: DWDM frequency grid" June 2002.

[17] P J. Winzer and R-J Essiambre, "Advanced modulation formats for high-capacity optical transport networks," J. Lightw. Technol., vol. 24, pp. 4711-4728, Dec. 2006.

[18] R. Madabhushi, "Chapter 6 - Lithium niobate optical modulators," in *WDM Technologies: Active Optical Components,* A.K. Dutta, N.K. Dutta and M. Fujiwara, Ed. Academic Press, San Diego, CA. 2002, pp. 207-248

[19] R. Madabhushi, "Chapter 7 - Electroabsorption modulators," in *WDM Technologies: Active Optical Components,* A.K. Dutta, N.K. Dutta and M. Fujiwara, Ed. Academic Press, San Diego, CA. 2002, pp. 249-314.

[20] B.L. Kasper, O. Mizuhara and Y.K. Chen, "Chapter 16 - High bit rate receivers, transmitters, and electronics" in *Optical Fiber Telecommunications: IV A Components*, I.P Kaminow and T. Li, Ed. Academic Press, San Diego, CA, 2002 pp.784-852.

[21] D. Sadot, E. Boimovich, "Tunable optical filters for dense WDM networks," *IEEE Commun. Mag.*, vol. 36, pp. 50-55, Dec. 1998.

[22] Y. Hida, Y. Hibino, T. Kitoh, Y. Inoue, M. Itoh, T. Shibata, A. Sugita and A. Himeno, "400-channel arrayed-waveguide grating with 25 GHz spacing using 1.5% Δ waveguides on 6-inch Si wafer," *Electron. Lett.*, vol. 37, pp. 576-577, Apr. 2001 .

[23] B. Mukherjee, *Optical Communication Networks*. NY: McGraw-Hill, 1997.

[24] T.A. Strasser and T. Erdogan, "Chapter 10 - Fiber grating devices in high-performance optical communications systems," in *Optical Fiber Telecommunications: IV A Components*, I.P Kaminow and T. Li, Ed. Academic Press, San Diego, CA, 2002, pp. 477-462.

[25] D. Menashe, A Shlifer and U. Ghera, "Optical amplifiers for modern networks," in *Proc. Inter. Conf Transparent Optical Networks (ICTON 2006),* Nottingham, Jun. 2006, vol. 1, pp. 115-118.

[26] Bernard, J., and Renaud, M., "Tutorial: semiconductor optical amplifiers," *SPIE's OE Mag*., pp. 36-38, Sep. 2001.

[27] L.H Spiekman, "Chapter 14 - Semiconductor optical amplifiers," in *Optical Fiber Telecommunications: IV A Components*, I.P Kaminow and T. Li, Ed. Academic Press, San Diego, CA, 2002, pp. 699-731.

[28] J. Bromage, "Raman amplification for fiber communications systems," *J. Lightw. Technol.,* vol. 22, pp. 79, Jan.2004.

[29] D.J. Blumenthal, J. E. Bowers, L. Rau, Chou Hsu-Feng, S. Rangarajan, Wei Wang and K.N. Poulsen, "Optical signal processing for optical packet switching networks," *IEEE Commun. Mag*., vol. 41, pp. S23-S29, Feb 2003

[30] M. Klinkowski and M. Marciniak, "Development of IP/WDM optical networks", in *Proc. Inter. Conf Laser and Fiber-Optical Networks Modeling, 2001*. Kharkiv, Ukraine, 2001 Workshop, pp. 84-87.

[31] Jens Buus, Markus-Christian Amann and Daniel J. Blumenthal, *Tunable Laser Diodes and Related Optical Sources*, Wiley-Interscience, 2005, Chapter 10, "Communications applications and requirements" pp. 285-324.

[32] S. J. Ben Yoo, "Optical packet and burst switching technologies for the future photonic Internet," *J. Lightw. Technol.,* vol. 24, pp. 4468-4492, Dec. 2006.

[33] I. Baldine, M. Cassada, A. Bragg, G. Karmous-Edwards, and D. Stevenson. "Just-in-time optical burst switching implementation in the ATDnet all-optical networking testbed". in *Proc. Inter. Conf Global Telecomun. 2003*, San Francisco, Dec. 2003, vol. 5, pp. 2777-2781.

[34] K. Kitayama, M. Koga, H. Morikawa , S. Hara, and M. Kawai. "Optical burst switching network testbed in Japan," in *Proc. Optical Fiber Commun. Conf. (OFC 2005)*, Anaheim, Mar. 2005, vol. 1, pp. 178-180.

[35] Y. Sun, T. Hashiguchi, N. Yoshida, X. Wang, H. Morikawa, and T. Aoyama. "Architecture and design issues of an optical burst switched network testbed", in *Proc. Optoelectron. And Commoun. Conf. (OECC/COIN 2004),* Yokohama, July 2004, pp. 386-387.

[36] D. J. Blumenthal, B. E. Olsson, G. Rossi, T. E. Dimmick, L. Rau, M. Masanovic, O. Lavrova, R. Doshi, O. Jerphagnon, J. E. Bowers, V. Kaman, L. A. Coldren and J. Barton, "All-optical label swapping networks and technologies," *J. Lightw. Technol.,* vol. 18, pp. 2058-2075, Dec. 2000.

[37] S.-L. Lee, C.-Y. Chien, H.-W. Tsao, and J. Wu, "Practical considerations of using tunable lasers for packet routing in multiwavelength optical networks," in *Proc. Inter. Conf on Parallel Process. Workshops (ICPPW 2003)*, Kaohsiung, Oct. 2003, p. 325.

[38] I.M. White, M.S. Rogge, K. Shrikhande and L.G. Kazovsky, "A summary of the HORNET project: a next-generation metropolitan area network," *IEEE J. Sel. Areas Commun*., vol. 21, pp. 1478-1494, Nov. 2003.

[39] D. Sadot and I. Elhanany, "Optical switching speed requirements for terabit/second packet over WDM networks," *IEEE Photon. Technol. Lett.,* vol. 12, pp. 440-442, Apr. 2000.

[40] M. Hatcher, "Tunable lasers to star in fibre-optic 'mini-boom'," 5 April 2007, www.optics.org.

[41] Communications Industry Researchers, "Optical components markets: 2007-Vol 1," 3 April 2007, www.cir-inc.com.

Chapter 2 – Tunable Lasers

Chapter 2 is concerned with tunable lasers (TLs) for use in current and future DWDM systems as examined in Chapter 1. The TL applications and main requirements in such systems are presented. The basic tuning mechanisms and schemes are introduced for a generic tunable laser. The implementation of this tuning function in single wavelength electronic TLs is discussed. This discussion is carried forward to explore widely tunable electronic TLs with particular emphasis on the sampled grating distributed Bragg reflector laser.

2.1 Applications of Tunable Lasers

Research, development and deployment of TL technology has been ongoing for some time now [1]. The application of TLs in increased capacity optical telecommunications systems has driven much of the interest. Single frequency laser diodes with tunable wavelength functionality are important components in current and future wavelength multiplexed optical communication systems. The use of TLs in the areas of coherent optical communication, sensing and measurement is also of interest. These applications are however outside the scope of this thesis, which is focused on the use of TLs in WDM systems.

2.1.1 Sparing and Inventory Reduction

The most obvious application of TLs in current DWDM systems, where increasing numbers of wavelength channels are being used, is as optical sources to replace individual fixed frequency DFB lasers. This will reduce costs and improve simplicity of manufacturing and operating DWDM systems. By using the TLs it will be possible to reduce inventory, as a single TL product will be capable of operating at any wavelength required. Similarly it will not be necessary to keep a spare laser for each wavelength channel in the event of a laser failing, thus reducing

sparing costs.

2.1.2 Wavelength Routing

Some of the more interesting applications of TL technology are in the area of optical switching, routing and networking. TLs will be integral components in the future optical routing and networking architectures. In these schemes the information transmitted over the network will be encoded onto destination dependent wavelengths. The information will be routed to the desired location using passive wavelength selective filtering, such as N×N AWG. The ultimate goal of such networks is to perform routing for each packet of data. A TL could be used to generate a desired wavelength for each packet to be transmitted, requiring TLs with tuning times of nanoseconds or less [2].

2.1.3 Reconfigurable Optical Add-Drop Multiplexer

Reconfigurable OADMs (ROADMs) [3] are tunable OADMs capable of changing the wavelengths dropped and added to a set of DWDM signals on a fibre. They allow for the dynamic provisioning of wavelength channels as they can be remotely tuned to change the capacity dropped and added to each node, which will make networks more manageable and scaleable. The main functionality, of channel multiplexing and demultiplexing, is performed by tunable filters. However as the added wavelength is unknown in advance TLs will be needed to allow transmission on the wavelength desired.

2.1.2 Wavelength Converters

Tunable Wavelength Converters (WC) are critical elements in state of the art and future DWDM networks [4]. The ability to convert a high data rate signal from any input wavelength channel to a tunable output wavelength channel is an important feature for increasing network flexibility, allowing data to be routed along different paths in the network. There are various approaches to performing conversion; from optical-electronic-optical (OEO) WCs which detect the signal before retransmission on the new wavelength, to all optical WCs, which use optical nonlinearities of certain materials to optically modulate the new wavelength [4, 5].

Each method requires a local laser to set the new wavelength that the signal is converted to. To achieve tunable wavelength conversion therefore, it is necessary to have a TL to act as the local laser. Wavelength converters are important elements in optical switching. In WDM most of the switching to connect networks is wavelength switching. Tunable wavelength converters can be combined with N×N AWGs to form non-blocking optical wavelength switches.

2.1.3 DWDM Tunable Laser Requirements

	Attribute	**Specification**	**Comments**
Single Mode Operation	Mode suppression ratio	> 30 dB	
	Output power	13 dBm	
Tunability	Range	C-Band (minimum)	L-band eventually
	Channel to channel tuning time	~ 10 ms (short term) ~ 1 μs (medium term) ~ 10 ns (long term)	Application dependent
	Continuity	Quasi-continuous	Access to any wavelength in range will increase potential channel count
	Wavelength Accuracy	+/-5% channel spacing	
	Power uniformity	< +/- 0.5 dBm	
Simplicity	Fabrication		Allow for low cost mass production
	Characterisation		Low number of control currents
	Field Operation		Low number of control currents

Table 2.1 Primary Tunable Laser Requirements for DWDM Systems

The specific performance requirements that tunable lasers must meet for use in DWDM systems will vary from one application to the next. In general, though, they should give the same performance as fixed wavelength single mode lasers currently in use in DWDM systems (e.g. distributed feedback lasers) along with the added wavelength tuning functionality. The tunable laser requirements of primary concern for TLs are outlined in Table 2.1 [6, 7].

2.2 Generic Laser Tuning

The wavelength tuning operation of a generic laser diode as described in [8] and [9] is presented in this section. By referring to the basic laser spectra it is shown how the laser emission wavelength can be tuned by adjusting the cavity gain curve and/or the longitudinal mode positions.

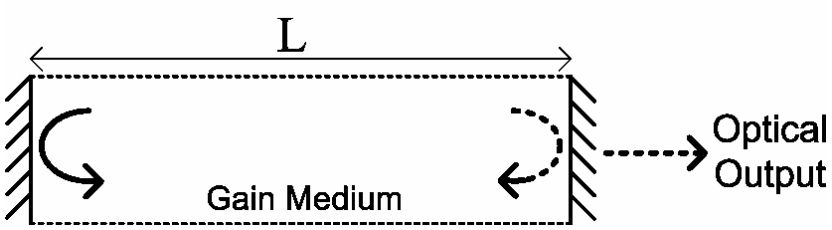

Figure 2.1 Basic Laser Structure

As current is injected into the active layer of a simplified laser, as shown in Figure 2.1, carriers are initially converted to photons by spontaneous emission. Mirror reflection at the cavity ends is used to reflect the photons back into the active region for amplification by stimulated emission – generating photons of the same wavelength and phase, which in turn are amplified. The steady state condition required for lasing to occur begins when the cavity roundtrip gain reaches unity. This happens when the wavelength dependent mode gain, given by the optical confinement (Γ) of the active medium gain (g_a), overcomes the internal losses (α_i) and the mirror losses (α_m), giving the gain condition,

$$\Gamma g_a(\lambda) - \alpha_i - \alpha_m = 0 . \qquad (2.1)$$

Above this gain threshold any additional injected carriers are converted directly to photons by stimulated emission. This gives the amplitude condition that defines the lasing regime of the laser, the cavity roundtrip gain characteristic,

$$g_c(\lambda) = \Gamma g_a(\lambda) - \alpha_i - \alpha_m, \qquad (2.2)$$

represented graphically in Fig 2.2(a). The phase condition of the cavity, dependent on the cavity length L and the effective refractive index ñ, is represented by,

$$\lambda_N = \frac{2\tilde{n}L}{N}, \qquad (2.3)$$

for the Nth mode centred at wavelength λ_N. This defines a set of longitudinal cavity modes, as shown in Fig 2.2(b), with mode spacing $\Delta\lambda_m$, at which lasing can occur if the gain condition is met. The laser wavelength is determined by the longitudinal mode closest to the gain peak, λ_p, of the cavity gain characteristic. In the case illustrated in Fig. 2.2(c), which is typical of a Fabry Perot (FP) Laser, the laser emission wavelength is centred at λ_N with side modes carrying a significant amount of the total laser power. Single mode operation can be achieved by making the mirror loss wavelength dependent (as is outlined in section 2.3).

The laser output wavelength can be tuned by varying the amplitude condition – spectrally shifting the peak (λ_p) of the the cavity gain characteristic; by varying the phase condition – spectrally shifting the longitudinal comb modes; or by a combination of both these methods. The tuning method used will impact the type of tuning achieved, giving continuous tuning, discontinuous tuning or quasi-continuous tuning. It is important to keep other laser parameters such as side mode suppression ratio (SMSR) and output power as constant as possible during wavelength tuning.

Continuous Tuning:

The laser wavelength is tuned smoothly in small steps remaining at the same longitudinal mode throughout the tuning range. Simultaneous control of the cavity gain peak wavelength and the comb mode spectrum is required. By keeping other laser parameters constant throughout tuning while maintaining the same dominant

longitudinal mode the tuning range is limited to around 15 nm.

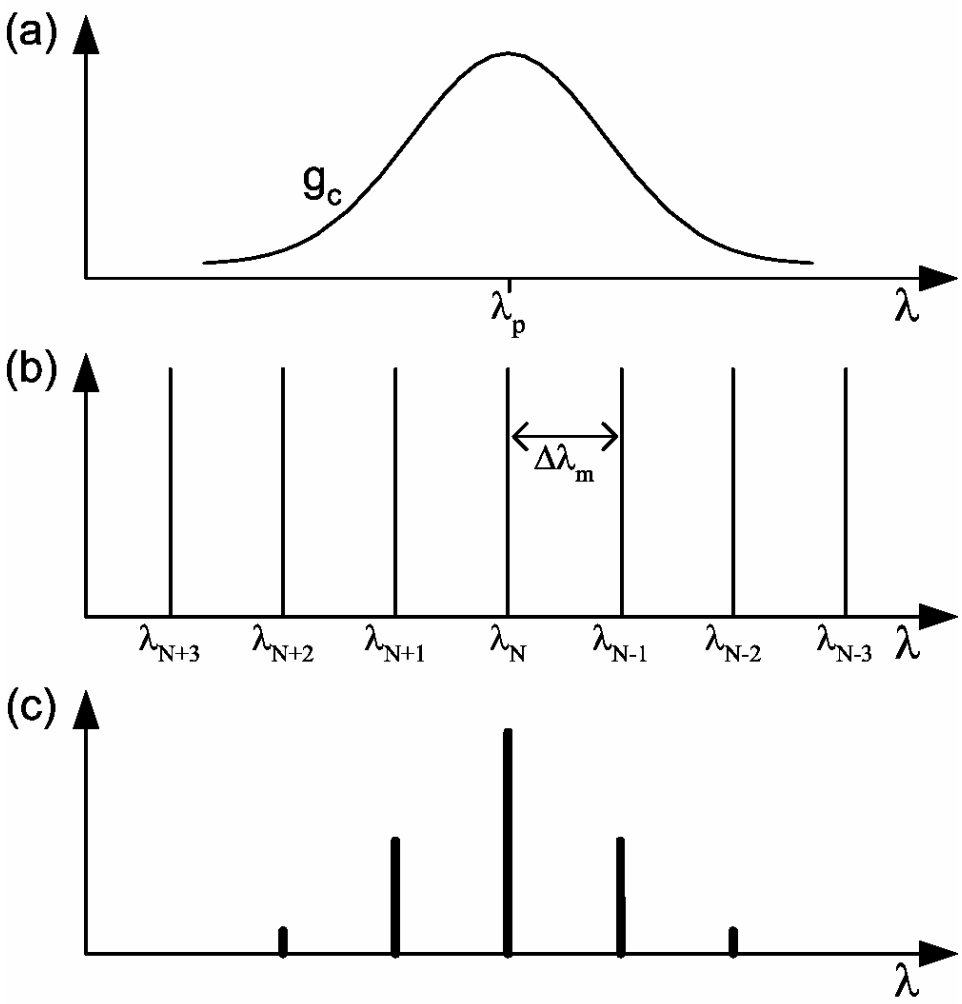

Figure 2.2 (a) Cavity gain characteristic spectrum (b) Longitudinal mode spectrum, (c) Longitudinal laser emission spectrum

Discontinuous Tuning:

If the laser is not confined to the same operational mode the wavelength can be tuned across the longitudinal modes of the laser. This mode hopping allows for an extended tuning range, up to around 100 nm, which is determined by the tuning range of the cavity gain characteristic. However with this scheme it is not possible to access every wavelength in the range.

Quasi-continuous Tuning:

This tuning scheme involves the amalgamation of a number of overlapping

continuously tunable ranges. Thus, by using mode hopping with continuous tuning within each mode, a large tuning range over which every wavelength is accessible can be achieved.

2.2.1 Cavity Gain Characteristic Tuning

The output wavelength of the laser can be tuned by the spectral adjustment of the cavity gain curve. This involves the movement of the gain peak wavelength, λ_p, by changing the wavelength dependence of the active medium gain, g_a, or by using the mirror loss α_m as a wavelength selective filtering element, (refer to equation (2.2)). Assuming no change in the comb mode spectrum the laser wavelength will change by mode hops of $\Delta\lambda_m$ as λ_p is varied. This results in discontinuous discrete tuning as shown in Fig. 2.3(a). However inspection of the output emission spectrum shows that the issue is more ambiguous, as the wavelength is tuned across different modes.

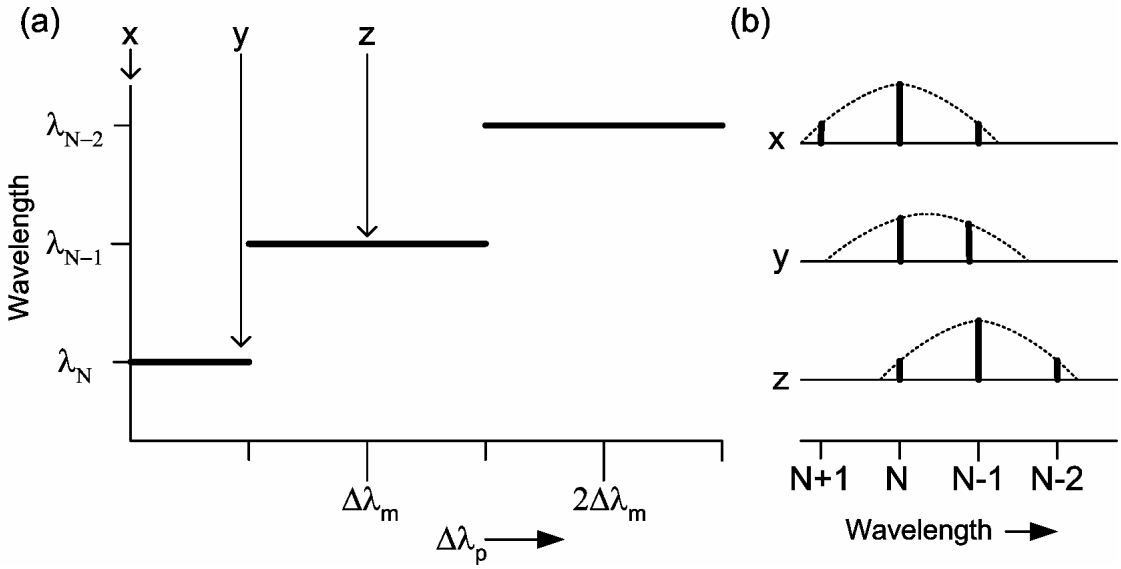

Figure 2.3 (a) Laser wavelength as a function of λ_p shift (b) Laser emission spectra at indicated λ_p positions

The SMSR varies during tuning due to the variation in the gain difference between the dominant mode and the second strongest mode. This wavelength ambiguity is

illustrated using the markers x, y and z in Fig. 2.3 for the mode transition from λ_N to λ_{N-1}. The best suppression is given when λ_p coincides with one of the comb modes, initially λ_N, position x. The gain difference between the two competing modes decreases, until the eventual dominance of the next mode; it then begins to increase until λ_p coincides with mode λ_{N-1}, position z. The lowest suppression value is given at the mode hop boundary, position y. This tuning method is ultimately limited by the tuning range over which λ_p can be tuned.

2.2.2 Comb Mode Spectrum Tuning

The laser wavelength can also be tuned by shifting the comb mode spectrum. With reference to equation (2.3) this can be achieved by either changing the length (L), or by changing the effective refractive index (ñ), of the laser cavity. Within the wavelength range of interest all the comb modes can be regarded as having an equal spectral shift. Assuming no change in the cavity gain peak the wavelength will change as the comb mode spectrum, λ_c, is varied as shown in Fig. 2.4, positional markers x, y and z are used again for illustration. At position x the comb mode is positioned such that mode N is in line with λ_p. As the comb is shifted, the wavelength changes in a continuous linear fashion up until position y. The laser then jumps mode to the neighbouring mode, N+1, resulting in a wavelength shift downwards equal to the mode spacing width. As the comb continues shifting the wavelength increases until it reaches z, where mode N+1 is in line with λ_p. The tuning continues in this way giving periodic continuous wavelength regimes of width $\Delta\lambda_m$, centred at the initial starting wavelength, λ_N, but successively jumping mode after every period, causing mode ambiguity. This happens in such a way that each previous period of continuous tuning drift is cancelled out. The same SMSR problems associated with tuning of the cavity gain curve are evident from Fig. 2.4 (b). Thus acceptable continuous tuning is only possible over a small wavelength range, i.e. a fraction of $\Delta\lambda_m$.

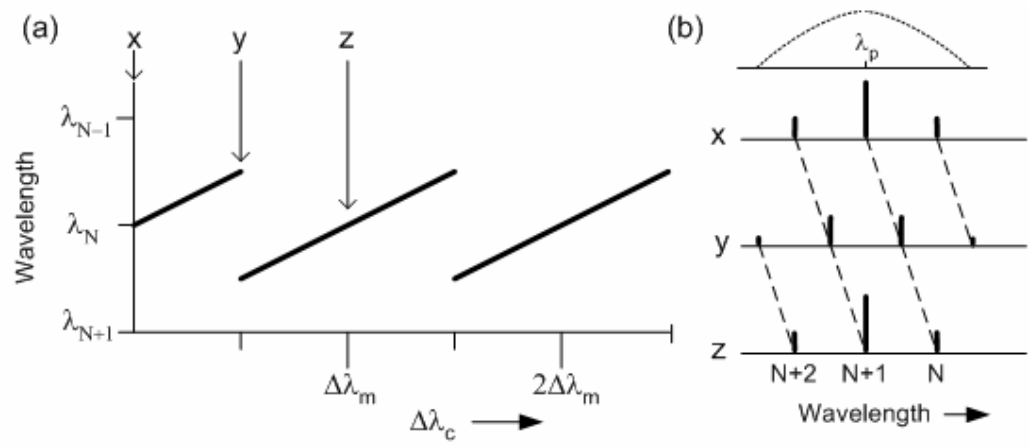

Figure 2.4 (a) Laser wavelength as a function of λ_c shift (b) Laser emission spectra at indicated λ_c positions

2.2.3 Combined Tuning

To achieve tuning performance that is superior to that already described, simultaneous control of both the cavity gain peak and the comb mode spectrum is required. By tuning the comb mode spectrum by the same amount as the cavity gain peak (i.e. $\Delta\lambda_p = \Delta\lambda_c$) it is possible to achieve a relatively wider tuning range. This scheme, as depicted in Fig. 2.5 (a), offers continuous tuning with fixed SMSR over the entire range. The tuning range will be determined by the smaller tuning range of λ_p or λ_c, generally being limited by the latter, which is still somewhat larger than the continuous tuning range described in section 2.2.2, which is a fraction of $\Delta\lambda_m$.

This range can be further increased by taking a quasi-continuous tuning approach. As before λ_p is monotonically increased while λ_c is changed in a stepwise manner over $\Delta\lambda_m$, then being reset to its initial value, resulting in a mode jump to a lower mode. The output wavelength increases smoothly as in the continuous scheme with fixed SMSR but mode jumps are permitted after each longitudinal mode. This periodic mode hopping however introduces ambiguity in terms of phase and wavelength around the mode boundaries, as shown in Fig. 2.5 (b). The emission spectrum is the same before the mode hop and directly after, despite the fact that the dominant mode has changed from mode N to mode N-1. This prevents the use of this scheme for certain applications such as coherent optical detection, however

it offers the widest tuning range and is therefore attractive for use in WDM applications.

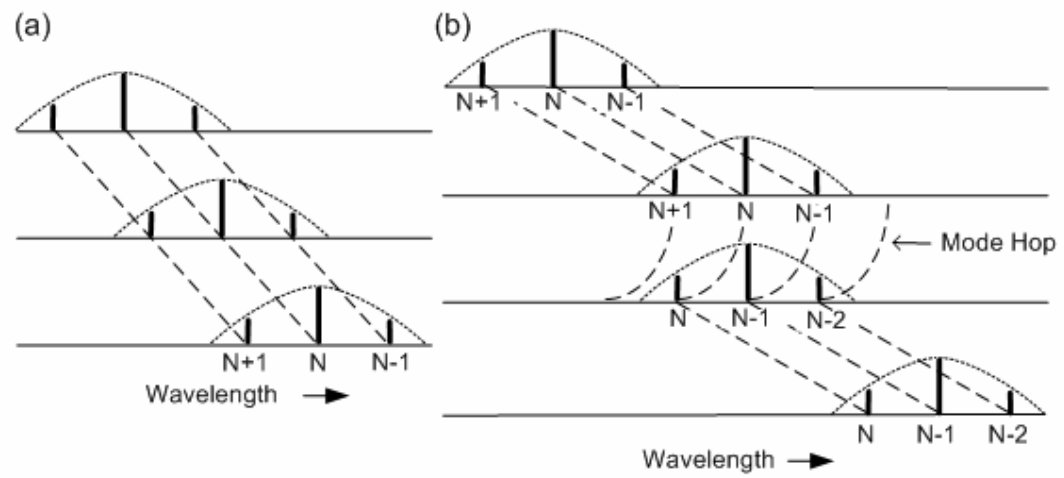

Figure 2.5 Laser emission spectra using combined tuning for (a) continuous tuning, and (b) quasi-continuous tuning

2.3 Single Mode Operation

As seen above, in an FP laser more than one mode reaches the lasing condition, resulting in a multimode emission spectrum. This is due to the wide spectral gain and the narrowly spaced longitudinal modes of the cavity. Single mode operation is required for DWDM systems as chromatic dispersion and SMSR are issues of concern. One important method to achieve single mode operation is by using shorter cavities to increase the mode spacing so that only one mode falls under the gain curve, as in the vertical cavity surface emitting laser (VCSEL). But the most widely used method is the use of periodic corrugated structures to provide mode selectivity.

In the FP laser mirror losses are wavelength independent and the spectral emission will consist of the modes that experience net gain, determined by the wide gain curve. The mode selection filtering can be enhanced by using periodic structures to create wavelength dependent mirror loss (α_m in equation 2.2) to suppress all the modes except the mode selected for lasing, thus providing mode selection filtering

as displayed in Fig. 2.6. In a waveguide with a periodically varying index grating the reflection coefficients for the different modes will be wavelength dependent. Distributed feedback occurs near the wavelength for which all the feedback or reflections from the grating add in phase. This is defined as the Bragg wavelength,

$$\lambda_B = 2\tilde{n}\Lambda\,, \qquad (2.4)$$

where Λ is the grating pitch and ñ is the effective refractive index. The mode closest to the Bragg wavelength (λ_B) will be reflected constructively as the reflections are in phase. For the modes away from λ_B the reflections will be out of phase and the modes will be suppressed. This results in single mode reflection at the λ_B allowing for lasing at this mode only [10].

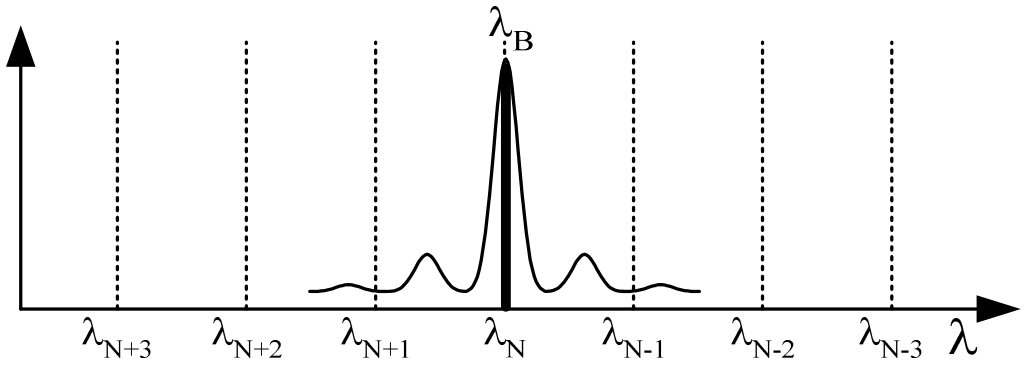

Figure 2.6 Laser emission using mode selective filtering centred at Bragg wavelength λ_B

2.4 Electronic Tunable Lasers

It has been shown that the lasing wavelength for a laser can be tuned by varying the phase condition and/or by varying the amplitude condition. From equation 2.3 representing the phase condition it can be seen that the comb mode positions can be spectrally shifted by varying the physical length (L) or by varying the effective refractive index (ñ) of the laser cavity. To achieve fast tunability it is not feasible to physically adjust L as the time required for mechanical (used in external cavity lasers) or electromechanical (as used in VCSELs) tuning will be limited to the order of milliseconds. A waveguide section of length L with an electronically

controllable ñ could function as a suitable tuning element.

With regards to the amplitude condition a Bragg grating reflector can be used to give wavelength selective loss so that lasing occurs only at the wavelength of minimum loss – the Bragg wavelength (λ_B). Referring to equation 2.4 the grating pitch of the reflector (Λ) cannot easily be dynamically changed as it is set at fabrication. However it is possible to tune the λ_B by electronically controlling the effective refractive index of the grating.

This approach could potentially yield a TL with sufficiently short tuning time for optical switching applications. To electronically tune the output wavelength therefore, it is necessary to vary the refractive index of a phase element and/or an amplitude element. Refractive index tuning can be achieved in semiconductors by field effects, thermal control and carrier injection.

2.4.1 Refractive Index Tuning

The application of an electric field can be used to change the refractive index of a material, as used for Mach-Zehnder modulation (introduced in section 1.3.2). This electro-optic effect, although capable of high speed tuning, can only give a small index shift [11]. Thus limiting the tuning range achievable and making it unsuitable for DWDM TL applications. Thermal control can also be used for wavelength control, as refractive index increases with temperature [12]. Although offering a relatively better tuning range excessive heating will ultimately limit the range achievable. The tuning speeds will also be limited to microsecond time scales due to thermal impedance.

Carrier injection is the most frequently used method to control the refractive index of a semiconductor waveguide for wavelength tuning, giving the largest index shift at nanosecond timescales [9]. Carriers injected into the waveguide by an external current source reduce the effective index in proportion to the excess carrier density, giving an effective index change (Δñ) approximated by,

$$\Delta\tilde{n} = -\Gamma\gamma N, \qquad (2.5)$$

where Γ is the optical mode confinement factor, γ is the index change per carrier density and N is the injected carrier density [13].

In the case of a Bragg reflector, carrier injection reduces the effective index giving the Bragg wavelength (λ_B) a negative wavelength shift, according to equation 2.4. For λ_B to stay at this wavelength the current source must be sustained at the appropriate level, or changed for a different wavelength shift. The wavelength tuning range of λ_B will be limited by the amount of effective index change achievable in the grating,

$$\Delta\lambda = \lambda_B \frac{\Delta\tilde{n}}{\tilde{n}}. \qquad (2.6)$$

The index change becomes less efficient at large injection current levels as non-radiative recombination increases at higher carrier densities. The tuning range will also be limited by excessive heating of the laser due to the sustained current injection. Besides affecting laser parameters such as power and threshold current the heating will also cause a parasitic refractive index increase that will counteract the carrier injection index change to a certain extent.

2.4.2 Distributed Feedback (DFB) Laser

The distributed feedback (DFB) laser combines an active and grating region over the length of the laser cavity. It was developed as a fixed wavelength single mode laser, now being one of the most prevalent, and was not originally intended for tunability. The transverse integration of the wavelength selective and gain functionality, as shown in Fig. 2.7, allows for relatively simple fabrication with no active/passive interface. Only wavelengths around the Bragg wavelength are reflected back into the cavity and so this is the only range of light that builds up within the active layer and reaches the lasing threshold.

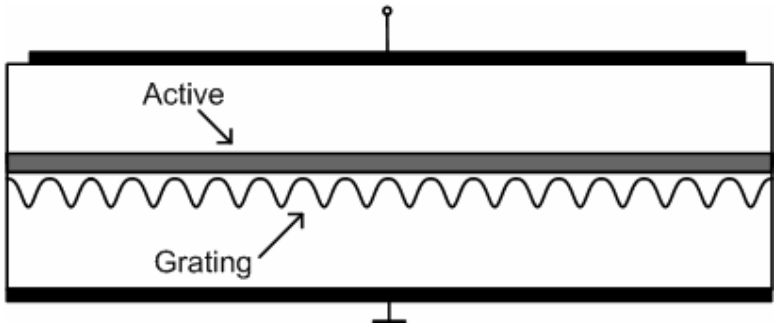

Figure 2.7 Distributed Feedback (DFB) Laser Schematic

Some of the first TLs were DFB based with the electrode split into two or three tuning sections. The operation of these devices is complicated and wavelength control is difficult while offering only modest tuning ranges of ~3 nm [13, 14]. The use of thermally controlled DFBs as TLs is more common, offering a stable mode-hop free, easily controllable wavelength tuning based on reliable standard DFB technology. As the emission wavelength of a DFB changes by about 0.1 nm/^{o}C [12], a tuning range of 3-4 nm is possible with a temperature tuning of 30 – 40 ^{o}C. To offer wider tuning ranges various component vendors have developed selectable arrays of 8 – 12 DFB lasers which can operate at any wavelength across the C-band or large portions of it. Either optical coupling [15, 16] or an external micro-electro-mechanical (MEM) mirror [17] is used to output the operating wavelength of the array. Using DFBs with different grating periods (Δ) to give different default output wavelengths separated by ~3nm it is possible to cover the C-band with a thermally controlled 12 DFB array. The main drawback of using arrays is the power loss associated with the coupler option or the moving part associated with the MEM mirror option. Also the slow tuning times reported, measured in seconds, limit their use for future dynamic functionality.

2.4.3 Distributed Bragg Reflector (DBR) Laser

The development of distributed Bragg reflector (DBR) lasers with separate active and passive regions was originally, as with DFBs, for fixed wavelength single frequency operation, but in comparison DBRs are better suited than DFBs for wavelength tunability. This is because of the inherent active/passive separation of

the gain function and the wavelength or mode selective function in the DBR, thus reducing the influence of the wavelength tuning on the gain functionality.

The most important DBR laser, a three-section device with a passive waveguide region separated from the active region is illustrated in Fig. 2.8. A Bragg grating etched into the waveguide at one end of the device operates as a passive wavelength selective mirror. Anti reflection (AR) coating is used at this end of the device to reduce reflections at the end of the grating. The cleaved facet provides the mirroring at the other end of the device. A passive phase control section separates the grating section from the active section, which provides the optical gain. The passive region is fabricated with a higher bandgap material than the active region to prevent photon absorption in the phase and grating section. This allows for current injection carrier density change in the passive region without interfering with the photon generation of the active region, thus allowing for the near independent control of the optical gain and wavelength.

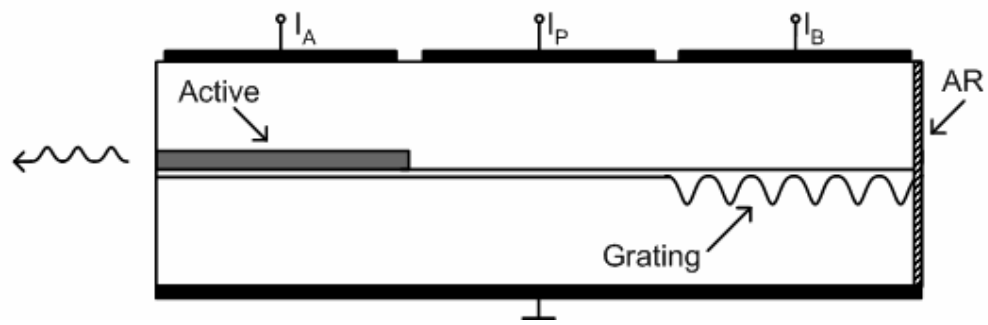

Figure 2.8 Distributed Bragg Reflector (DBR) Laser Schematic

Currents applied to each section control the laser operation. The current to the gain section, I_A, controls the optical output power. The cavity gain peak wavelength of the narrowband reflection, which can be approximated well by the Bragg wavelength [18], is controlled by current injection I_B into the Bragg grating. The longitudinal comb mode positions can be aligned with the Bragg peak by current injection to the phase section, I_P. In this way the laser wavelength can be fine-tuned,

giving better SMSR. Using simultaneous control of the phase section and grating section it is possible to achieve continuous tuning ranges of ~4 nm and quasi-continuous tuning ranges of ~10 nm [19]. A tuning range of 17 nm using discontinuous tuning was achieved in [20].

DBR lasers are suitable TLs for many telecom applications; based on mature technology they offer reliability and efficiency with high output powers and fast tuning times. However even at record tuning ranges they can still not offer full C-band coverage. Ultimately the tuning range of the DBR will be limited by the extent to which the Bragg wavelength can be tuned – this will be determined by the maximum achievable index change in the grating section,

$$\frac{\Delta\lambda}{\lambda} = \frac{\Delta n}{n}, \qquad (2.7)$$

and when using carrier injection is limited to ~ 5% [7].

2.4.4 Widely Tunable Lasers

Due to the limitation of the refractive index achievable in a waveguide, the tuning range of a device based on such a change will be limited to around ~15 nm. This is in contrast to the broad gain curve of semiconductor materials and the EDFA amplifying bandwidth. For DWDM systems it is desirable to have a single device which can offer at least full C-band coverage. To achieve wide tunability it is necessary to be able to change the relative index, and thus the relative wavelength, by a multiple of the amount that any single waveguide index can be changed. This can be achieved by changing an index difference as opposed to the index itself. Various devices capable of this wide tuning can be structurally arranged into the following groups.

Interferometric Structures:

Lasers based on MZ interferometry can offer extend tuning ranges by using a semi-MZ interferometer setup or a 'Y' structure. The longitudinal modes from two cavities of different lengths interfere constructively and destructively at the Y junction to give single mode operation. The output wavelength can be tuned by

varying the refractive index of one or more of the cavities. Y-branch lasers and vertical-Mach-Zehnder lasers are examples of this technology. Since these devices do not contain a grating structure their fabrication is somewhat simplified. This however also limits the side mode filtering giving low SMSR. A special case of this group is the modulated grating Y-branch (MGY) laser in which passive branches with modulated gratings are used. The gratings have different comb reflection spectra which can significantly improve mode selectivity, giving SMSR of 40 dB over a tuning range of 40 nm [21].

Co-directional Coupler Structures:

The use of co-directional coupling between two waveguides can be used to filter out a single longitudinal cavity mode. The difference in refractive index of two waveguides allows for an enhanced tuning range. In the grating assisted vertical coupler filter laser [22] two waveguides are vertically stacked with a grating placed on the upper waveguide which gives coupling at the Bragg wavelength. The laser can be tuned by carrier injection into the grating section. The tuning range is proportional to the passband of the filtering and so in achieving a wide tuning range mode selection will be compromised, leading to reduced SMSR.

This condition is improved in the **g**rating assisted **c**o-directional coupler with **s**ampled **r**eflector (GCSR) laser by using a second filtering element. A second grating with a modified comb like reflection spectrum is placed at the back end of the laser. The reflection peaks are narrow enough to pass only one cavity mode while the co-directional coupling filters out only one peak. In this way a wider tuning range can be achieved with coarse tuning performed by the original grating and fine tuning performed by the sampled grating. A 74 nm tuning range with good SMSR was achieved using this design in [23]. A disadvantage of this laser is the complex fabrication process involved, due to the use of different waveguides and two grating sections.

Grating Based Structures:

These structures operate on the same principle as DBR and DFB lasers, in that grating reflection is used to select out a longitudinal cavity mode for lasing. The tuning range is increased by using two separate gratings in the laser structure. The gratings are modified to give comb like reflection spectra, with each grating having slightly different comb spacing. By tuning one mirror relative to the other it is possible to achieve a Vernier tuning enhancement. Devices based on this technology offer tuning ranges of over 40 nm with high SMSR levels.

A laser from this group, the sampled grating distributed Bragg reflector (SGDBR), is the subject of experimental work in the following chapters and so will be explained in greater detail in the following section, along with an outline of other lasers in this group.

2.5 Widely Tunable Grating Based Tunable Lasers

In a standard DBR laser as presented in section 2.4.3 wavelength tuning is performed by varying the Bragg wavelength of a single grating section to adjust the reflection window of minimum cavity loss. A phase section was then used to place a mode at the centre of this window. In this scheme the tuning range is limited by the amount that the Bragg wavelength can be varied. It was first proposed by Coldren in [24] that this limitation could be overcome by using the variation in the beating between the reflection spectra of two multi element mirrors. The reflections of which, have periodic maxima, with the maxima differently spaced in each. This Vernier tuning enhancement is illustrated in Fig. 2.9 using two reflection spectrums, R_1 and R_2, with the comb maxima or peaks spaced by different amounts. Due to the different peak spacing used only one set of reflection peaks can be in alignment at any one time, within a wide range, to give an overall reflection $R_1.R_2$. By shifting the comb position of R_2 by a small amount ΔR_2 a different set of peaks come into alignment. The new point of alignment is a relatively large distance away, ΔR_1R_2, from the original point of alignment – thus by varying the comb positions of one of the reflection spectrums relative to the

other, a small change in the comb positions gives a large change in the combined reflection.

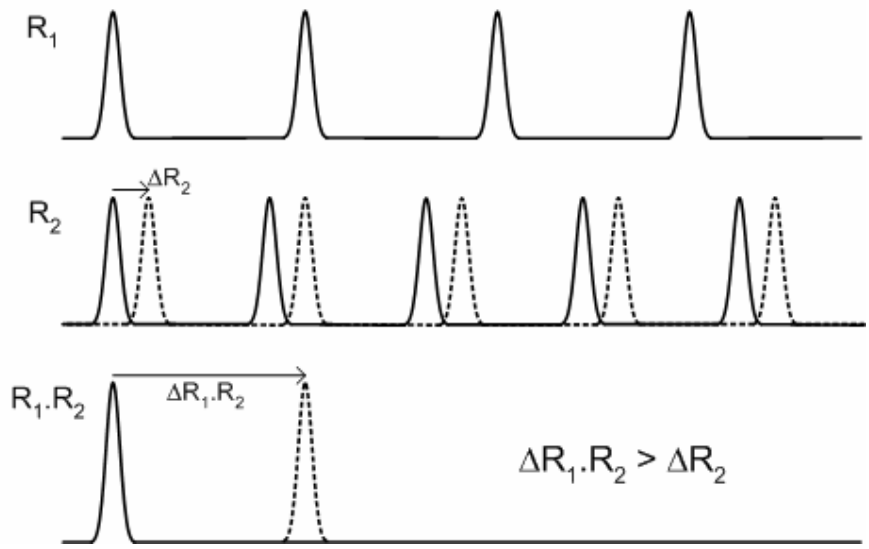

Figure 2.9 Vernier Tuning Enhancement

2.5.1 Sampled Grating Distributed Bragg Reflector (SGDBR)

A method to incorporate this tuning enhancement using multi element mirrors, in the form of the sampled grating distributed Bragg reflector (SGDBR), was proposed in 1991 [25, 26] and first demonstrated shortly after in [27, 28]. The SGDBR, as illustrated in Fig. 2.10, has two sampled grating mirror sections, with comb like reflection spectra, etched into the waveguide at either end of an active gain section and passive phase section. Its structural similarity to a conventional DBR laser is evident.

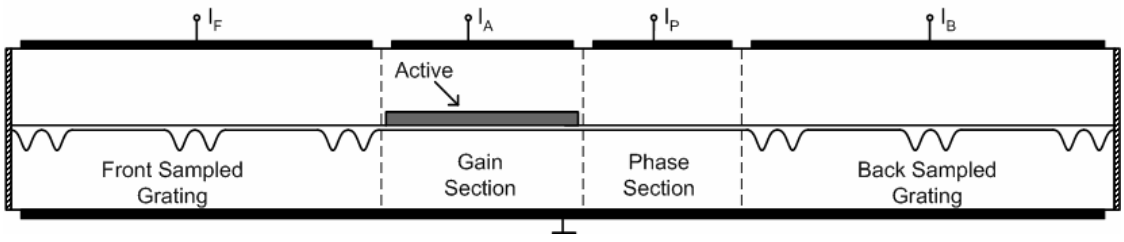

Figure 2.10 Sampled Grating Distributed Bragg Grating (SGDBR) Laser Schematic

The SG mirror is essentially a standard DBR mirror with grating elements blanked out in a periodic manner. In Fig. 2.11 a grating with the pitch (Λ) set to give Bragg reflection at 1550nm is sampled with a sampling period L_S and a grating length L_G to give the sampled grating structure of length $L=N_S L_S$, where N_S is the number of samples used. Sampled gratings are fabricated in a similar method to conventional Bragg gratings with only the extra step of using lithography to sample the gratings.

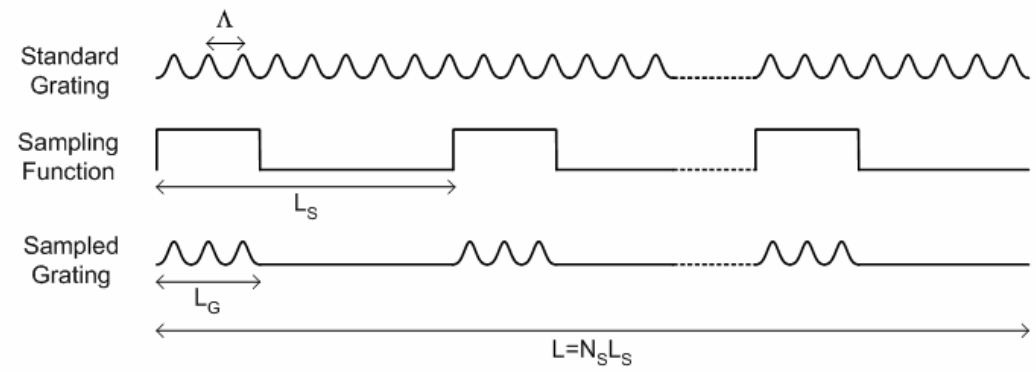

Figure 2.11 Sampled Grating Schematic

The SG has a comb shaped reflection spectrum with narrow peaks spaced around a centre peak which is at the Bragg wavelength [29, 30]. These side peaks occur where the reflection from the individual gratings are in phase which happens at wavelength separated by,

$$\Delta\lambda_S = \frac{\lambda^2}{2n_g L_S}, \qquad (2.8)$$

where n_g is the group refractive index in the material [31]. The peak amplitudes are unequal, with the reflection strengths symmetrically reducing from the centre wavelength. The full wave half maximum (FWHM) of the roll off envelope is a good measure of the usable reflection peaks and is approximately equal to $\frac{L_S}{L_G}\Delta\lambda_S$ [31]. Using a lower duty cycle of grating length to sampling length will give a wider roll off envelope. However as can be seen from work carried out on sampled grating reflectivity in [32] (reproduced in Fig. 2.12) keeping the same sampling

period but reducing the grating burst length reduces the reflection peak amplitude from each grating section. So a trade off is needed between tuning range, reflection amplitude and chip length. In [7, 29] duty cycles of 6-10% have been used in sampled gratings of lengths of ~500 μm made up of 10 and 13 samples respectively.

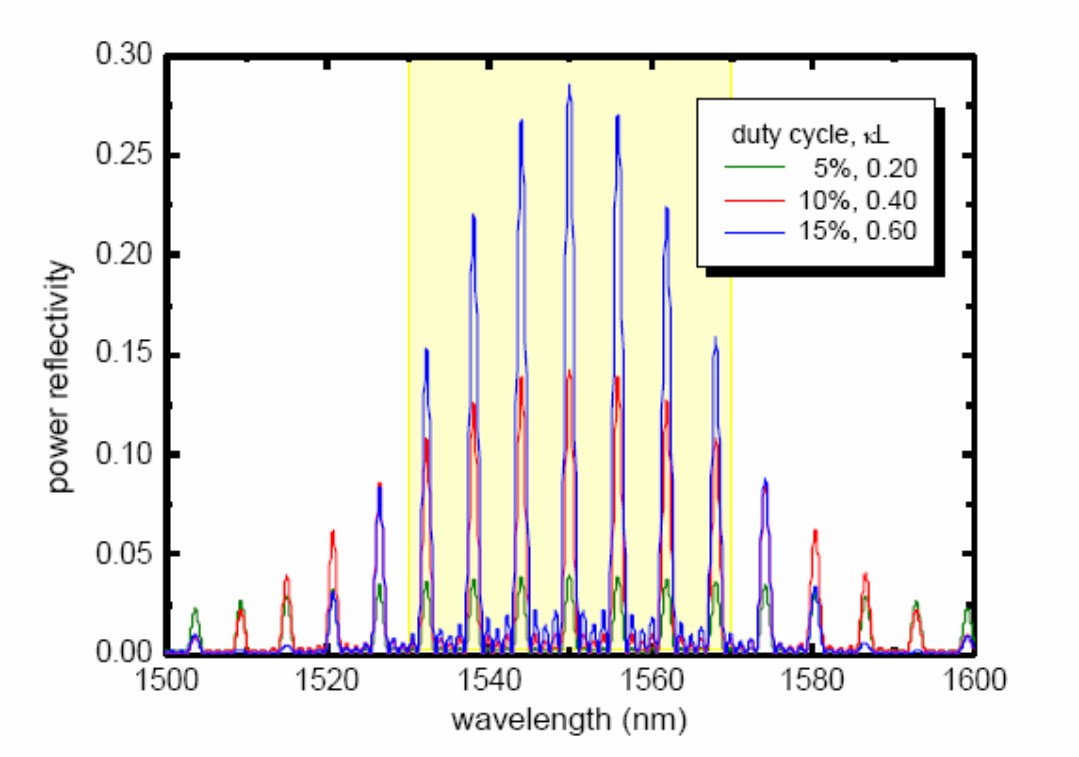

Figure 2.12 Simulated reflection spectra of sampled gratings of uniform length but with different duty cycles. [32]

In the SGDBR two sampled grating mirrors are used to provide comb shaped reflection from either end of the laser. Different sampling periods are used in the gratings to give a mismatch in the peak spacing of each grating, thus allowing only one set of peaks to come into alignment within in the range of interest. The mirror loss seen by the propagating modes is the product of the front mirror reflection and the back mirror reflection. The wavelength of peak alignment therefore experiences minimum mirror loss allowing a mode placed at this wavelength to laze. Anti reflection coating is applied to suppress any reflection from the grating ends [33].

As with the three-section DBR, the laser wavelength can be tuned by using carrier injection to vary the refractive index of the grating and phase sections to tune the wavelength of minimum loss and the longitudinal mode positions, respectively. Enhanced Vernier tuning can be achieved in the SGDBR by varying the reflection combs relative to each other.

Through using the same grating pitch (Λ) in both mirror sections the comb reflections are centred at the same Bragg wavelength as seen in Fig. 2.13(a). With no current applied to the mirror sections, lasing can occur at this wavelength. The phase section can be used to fine tune the longitudinal mode to the centre of the reflection window. The combined reflectivity of the comb peaks, R1.R2, is shown in Fig. 2.13(b). Discontinuous tuning over a wide tuning range can be achieved by tuning one of the mirrors relative to the other. By tuning the reflection R2 to a higher wavelength by $\Delta\lambda_M$ (the mismatch in peak spacing between the two mirror reflections) the peak alignment will jump to the next peak or super mode. This differential tuning picks out widely space longitudinal modes and can be continued across the tuning range in either direction. The maximum peak spacing is set less than or equal to the available direct index tuning of the mirror sections to enable tuning to wavelengths between the reflection peaks. This is possible by tuning both mirror sections simultaneously to keep the same peak alignment. This mode tuning picks out closely spaced neighbouring longitudinal modes and can be used in a stepwise manner to tune to modes between the reflection peaks across the tuning range. The phase section is used throughout to ensure that the modes are positioned at the centre of the reflection window. The tuning enhancement achieved is given by,

$$\frac{\Delta\lambda}{\lambda} = \frac{\Delta\lambda_{S,ave}}{\Delta\lambda_M} \times \frac{\Delta\tilde{n}}{\tilde{n}} = F\frac{\Delta\tilde{n}}{\tilde{n}}, \qquad (2.9)$$

where, F is the average peak spacing of the two mirrors ($\Delta\lambda_{S,ave}$) divided by the peak spacing mismatch $\Delta\lambda_M$.

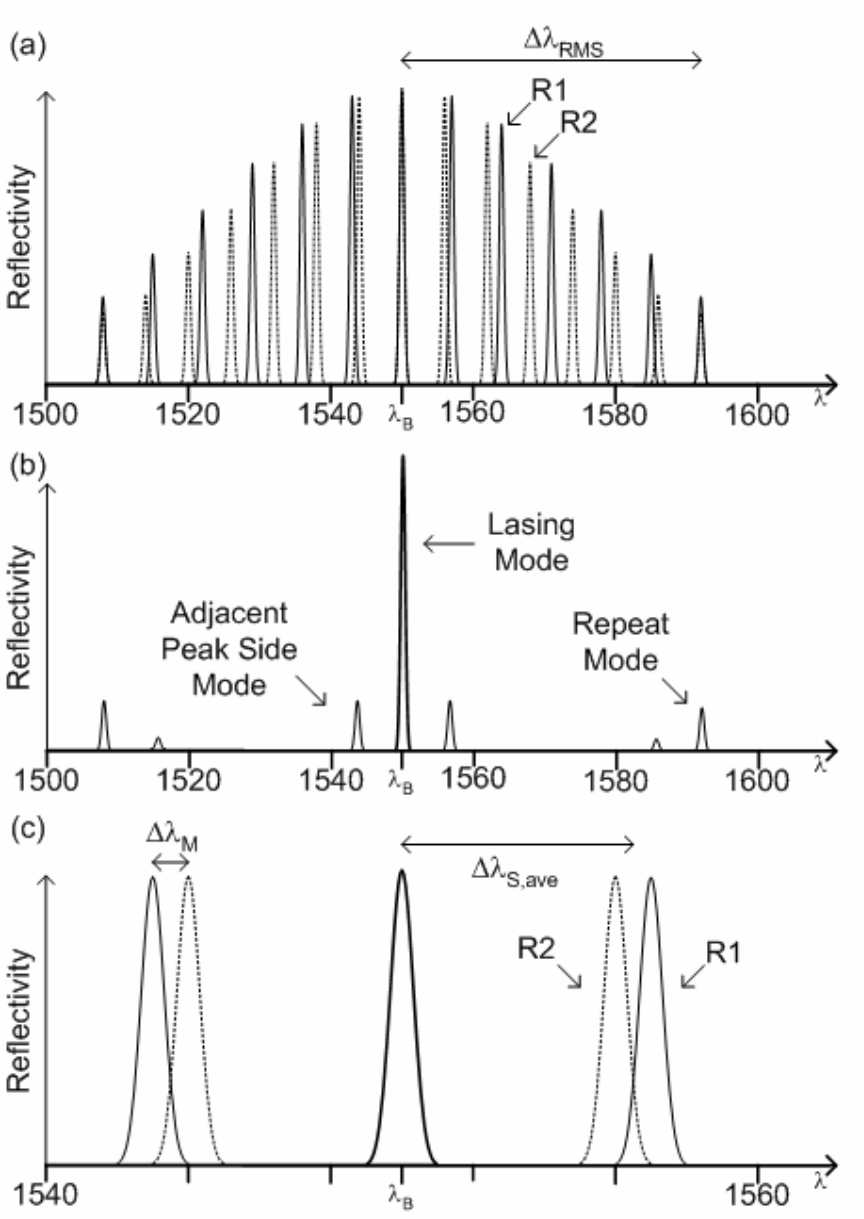

Figure 2.13 Typical power vs. wavelength plots of (a) individual reflections from both mirror sections R1and R2, (b) combined reflection of both mirror sections, i.e. R1.R2 and (c) individual reflections from both mirror sections R1and R2 at greater resolution.

Mode suppression is an issue that influences the tuning range achievable in the design of an SGDBR. Suppression of adjacent longitudinal modes is of less concern than that of adjacent supermodes. Due to the narrow reflection peaks the

former can be sufficiently reduced by the alignment of the comb peaks, through mirror control, and the lasing mode position through phase section control. The later however can be problematic and their suppression will limit the tuning range.

Referring to equation (2.9), increasing the tuning range enhancement (F) is possible through reduction in the peak spacing mismatch ($\Delta\lambda_M$). This will however reduce the SMSR due to the increasing overlap of the peaks adjacent to the peak of alignment. This is related to the repeat mode spacing ($\Delta\lambda_{RMS}$), marked in Fig. 2.13(a) as the distance between which reflection peaks are aligned, and will generally limit the maximum tuning range. When one of the reflection combs is tuned by this amount relative to the other, a repeat mode can become the dominant wavelength due to its position under the material gain spectrum, resulting in mode hopping across the wavelength range to this mode. The SMSR will also be significantly reduced due to lasing at both points of mirror alignment. Analytic expressions for the loss difference between the lasing mode and the various side modes have been derived in [29]. If tuning range is of primary concern F can be increased at the expense of quasi-continuous tuning across the range. This can be done by setting the peak spacing of the mirror sections greater than the available direct index tuning of the grating. A discontinuous tuning range of 72 nm was reported in [34].

Interferometric lasers and co-directional coupled lasers generally have greater output powers than the SGDBR for a given drive current due to the positioning of the active gain section at the front of the laser structure. In the SGDBR the optical output power from the gain section is reduced by carrier induced absorption losses in the passive front mirror section. This loss can increase for wavelengths at the edge of the tuning range which require high mirror tuning currents, leading to a power variation across the range for a fixed drive current of ~6 dB. This variation can be reduced and output powers can be increased by using gain control during tuning and integration of the laser with an SOA [34].

With regards to the SOA integration, the gain section positioning in the SGDBR is advantageous in comparison to the other widely tunable leasers, requiring no front facet reflections for operation. This allows for monolithic integration of the SGDBR and SOA with only minimal increase in fabrication complexity. Fibre coupled powers of 13 dBm (20 mW) have been reported for packaged devices offering full C-band or L-band coverage with high SMSR [35]. Component integration has expanded beyond meeting the power concerns to include the integration of electro-absorption modulators and MZ modulators [36, 37]. This has allowed for the development of low-cost, low-size and low-power single chip transmitter and wavelength converter photonic integrated circuits [38].

2.5.2 Super Structure Grating Distributed Bragg Reflector (SSGDBR)

The use of sampled grating structures is the simplest method to achieve comb like reflection spectra. The sampled gratings however do not possess the optimum "top hat like" reflection of equal peak power within a limited bandwidth and no peaks outside that bandwidth; instead they have non uniform reflection peaks with power reducing symmetrically around a centre peak. Super structure gratings (SSG) using a frequency or phase modulation rather than an amplitude modulation give improved reflection spectra and are used in super structure grating distributed Bragg reflector (SSGDBR) lasers [39]. This allows for improved tuning operation and more levelled output powers across the tuning range. The SSGDBR is structurally similar to the SGDBR with the only difference being the different grating design. The frequency varied gratings give reflection spectra with near uniform peak magnitude across a chosen range and significantly reduced reflection outside this range. Higher reflectivity is also achieved, in comparison to sampled grating reflections, as the grating covers the whole tuning element. These improvements however are at the expense of increased fabrication complexity for the gratings. Discontinuous tuning of over 100 nm [40] and quasi-continuous tuning over 62 nm [41] with good SMSR has been reported.

2.5.3 Digital Supermode Distributed Bragg Reflector (DSDBR)

The digital supermode distributed Bragg reflector (DSDBR) laser is a 4 section device similar to the SGDBR with a gain section and a phase section but with different front and back mirror sections. A phase grating is used in the back mirror to provide a comb reflection. This is essentially a uniform grating separated by π phase shifts to achieve improved reflection, over the sampled grating, with a fixed number of peaks with equal strength and spacing [42]. The front mirror is a continuously chirped grating with relativity low reflection across the entire tuning range. Eight short electrical contacts are positioned on the mirror for current injection into different sections of the grating.

By controlling the current to neighbouring contacts on the front mirror the reflection is enhanced over a broad wavelength range. This enhancement peak range is set at ~7 nm to ensure it overlaps with only one peak from the back mirror reflection. In this way the front mirror can provide course or supermode wavelength tuning. The strong, narrow rear reflection peaks ensure single mode operation, while the phase section is used for fine-tuning of the longitudinal mode positions. Quasi-continuous tuning can be achieved by controlling all three sections to give SMSR > 40 dB across a tuning range of 45 nm [43]. Wavelength dependent losses are reduced in the DSDBR, as only small tuning currents are required to control the front mirror section. High current accuracy is also not necessary for the front mirror tuning as only the rear mirror controls the mode selection. This reduction the number of high accuracy tuning currents is however at the cost of an increased number of overall control currents.

2.5.4 Widely Tunable Twin Guide Lasers

A disadvantage of the four-section DBR devices described above is the need for control of three or more tuning currents to achieve complete wavelength coverage. The wavelength tuning characterisation and control can be simplified by a reduction in the number of control currents, as is the case in widely tunable twin guide lasers. These lasers are based on the distributed feedback tunable twin guide

(DFB-TTG) laser [44] in which there is a transverse electrical separation between the active and tuning section that cover the length of the laser. As is the case with the conventional DFB laser a phase section is not needed, thus reducing the number of control currents.

The sampled grating and super structure grating tunable twin guide ((S)SG-TTG) lasers are examples of such devices, with the former exhibiting quasi-continuous wavelength coverage with 10 mW output powers and greater than 35 dB SMSR across 40 nm [45]. The tuning region is split into two sections, with slightly different gratings in each, giving differently spaced reflection combs. Vernier tuning is possible through differential and simultaneous control of the refractive index of both sections. Single mode lasing is achieved at the wavelength of comb peak alignment with no additional phase control needed. Thus wide wavelength tuning can be achieved with only two control currents (one current to each grating section) and a constant current to the active section. A disadvantage of these lasers is their transverse structure which is more complex than the longitudinal integration of the four section devices, leading to increased fabrication costs.

Summary

This chapter has looked at semiconductor tunable lasers in terms of their main applications in DWDM systems and the associated device requirements. A review of the wavelength tuning of a generic laser was given, and more specific information was given on different varieties of TL semiconductor devices. The following chapters are concerned with the use of such devices in actual system modules, and thus covers device characterisation and control, and experimentally examines the impact of their use, both when fixed and when tuning, on system performance.

References

[1] Larry A. Coldren, "Monolithic tunable diode lasers" *IEEE J Sel Topics Quant Electron*., vol. 6, pp. 988-999, Nov./Dec. 2000.

[2] M. Deulk, J. Gripp, J. Simsarian, A. Bhardwaj, P. Bernasconi, M. Zirngibl, and O. Laznicka, "Fast packet routing in a 2.5 Tb/s optical switch fabric with 40 Gb/s duobinary signals at 0.8 b/s/Hz spectral efficiency" in *Proc. Optical Fiber Commun. Conf. (OFC 2003)*, Georgia, Mar. 2003, vol. 3, postdeadline paper PD8-1-3.

[3] B.P Keyworth, "ROADM subsystems and technologies," in *Proc. Optical Fiber Commun. Conf. and National Fiber Optic Eng. Conf. (OFC /NFOEC 2005),* Anaheim, Mar. 2005, vol. 3, pp. 4.

[4] J.M.H. Elmirghani and H.T. Mouftah, "All-optical wavelength conversion: technologies and applications in DWDM networks," *IEEE Commun. Mag*., vol. 38, pp. 86 – 92, Mar. 2000.

[5] I. White, R. Penty, M. Webster, Yew Jun Chai, A. Wonfor and S. Shahkooh, "Wavelength switching components for future photonic networks," *IEEE Commun. Mag.,* vol. 40, pp. 74 –81, Sep. 2002.

[6] J. Buus and E.J. Murphy, "Tunable lasers in optical networks" , *J. Lightw. Technol.,* vol. 24, pp. 5- 11, Jan. 2006.

[7] Franck Delorme, "Widely tunable 1.55-μm lasers for wavelength-division-multiplexed optical fiber communications," *IEEE J. Quantum Electron.*, vol. 34, pp. 1706-1716, Sep. 1998.

[8] Larry A. Coldren, G. A. Fish, Y. Akulova, J. S. Barton, L. Johansson, and C.W. Coldren, "Tunable Semiconductor Lasers: A Tutorial," *J. Lightw. Technol.,* vol. 22, pp. 106-125, Jan. 2004.

[9] Jens Buus, Markus-Christian Amann and Daniel J. Blumenthal, *Tunable Laser Diodes and Related Optical Sources*, Wiley-Interscience, 2005, Chapter 4, "Basic concepts of tunable laser diodes" pp. 79 – 106

[10] Jens Buus, Markus-Christian Amann and Daniel J. Blumenthal, *Tunable Laser Diodes and Related Optical Sources*, Wiley-Interscience, 2005,

Chapter 3, “Single-mode laser diodes” pp. 43 – 78

[11] Franck Delorme, Serge Slempkes, Abderrahim Ramdane, Benoft Rose, and Hisao Nakajima, “Subnanosecond tunable distributed Bragg reflector lasers with an electrooptical Bragg section,” *IEEE J. Sel. Topics Quant. Electron*., vol. 1, pp. 396-400, Jun. 1995.

[12] K. Chinen, K. Gen-ei, H. Suhara, A. Tanaka, T. Matsuyama, K. Konno, and Y. Muto Toshiba, “Low-threshold 1.55-μm InGaAsP/InP buried heterostructure distributed feedback lasers,” *Applied Physics Letters* , vol. 51, pp. 273-275, Jul. 1987.

[13] C.E. Zah and T.P. Lee, “Wavelength-tunable semiconductor lasers for optical fiber communications” in *Proc. of Global Telecommun. Conf*., San Diego USA, 1990, vol. 2, pp.1286-1290.

[14] Y. Kotaki, S. Ogita, M. Matsude, Y. Kuwahara, H. Ishikawa, “Tunable, narrow-linewidth and high-power λ/4-shifted DFB laser,” *Electron. Lett*., vol. 25, pp. 990-992, July 1989.

[15] T. Mukaihara, Y. Nakagawa, H. Nasu, H. Kambayashi, M. Oike, S. Yoshimi, T. Kurobe, T. Kimoto, K. Muranushi, T. Nomura and A. Kasukawa, “High power, low noise, low power consumption, 25 GHz × 180 ch thermally tunable DFB laser module integrated with stable wavelength monitor,” in *Proc. Eur. Conf. Optical Commun. (ECOC03),* Rimini, Sep. 2003, paper We.4.P.81, pp. 718-719.

[16] M. Bouda, M. Matsuda, K. Morito, S. Hara, T. Watanabe, T. Fujii and Y. Kotaki, “Compact high-power wavelength selectable lasers for WDM applications,” in *Proc. Optical Fiber Commun. Conf. (OFC 2000)*, Baltimore, Mar. 2000, vol. 1, pp. 178-180.

[17] B. Pezeshki, E. Vail, J. Kubicky, G. Yoffe, S. Zou, J. Heanue, P. Epp, S. Rishton, D. Ton, B. Faraji, M. Emanuel, X. Hong, M. Sherback, V. Agrawal, C. Chipman, and T. Razazan “20-mW widely tunable laser module using DFB array and MEMS Selection,” *IEEE Photon. Technol. Lett.,* vol. 14, pp. 1457-1459, Oct. 2002.

[18] Jens Buus, Markus-Christian Amann and Daniel J. Blumenthal, *Tunable*

Laser Diodes and Related Optical Sources, Wiley-Interscience, 2005, Chapter 5, "Wavelength-tunable single-mode laser diodes" pp. 107 – 150.

[19] S. Murata, I. Mito and K. Kobayashi, "Tuning ranges for 1.5 μm wavelength tunable DBR lasers," *Electron. Lett.*, vol. 24, pp. 577-579, May 1988.

[20] Franck Delorme, Guilhem Alibert, Pierre Boulet, Serge Grosmaire, Serge Slempkes, and Abdallah Ougazzaden, "High reliability of high-power and widely tunable 1.55- m distributed Bragg reflector lasers for WDM applications," *IEEE J. Sel. Topics Quant. Electron*., vol. 3, pp 193-202 Apr. 1997.

[21] M. Isaksson, M. Chacinski, O. Kjebon, R. Schatz, and J.-O. Wesström, "10 Gb/s direct modulation of 40 nm tunable modulated grating Y-branch laser" in *Proc. Optical Fiber Commun. Conf. and National Fiber Optic Eng. Conf. (OFC /NFOEC 2005),* Anaheim, Mar. 2005, vol. 2, paper OTuE2.

[22] R. C. Alferness, U. Koren, L. L. Buhl, B. I. Miller, M. G. Young, T.L. Koch, G Raybon and C. A. Burrus, "Broadly tunable InGaAsP/InP laser based on a vertical coupler filter with 57-nm tuning range" *Applied Physics Letters*, vol 60, pp.3209-3211, Jun. 1992.

[23] M. Oberg, S. Nilsson, K. Streubel, J. Wallin, L. Backbom, and T. Klinga, "74 nm wavelength tuning range of an InGaAsP/InP vertical grating assisted codirectional coupler laser with rear sampled grating reflector," *IEEE Photon. Technol. Lett.*, vol. 5, pp. 735-738, Jul. 1993.

[24] Larry A.Coldren, "Multi-section tunable laser with differing multi element mirrors," United States Patent 4,896,325, January 23, 1990.

[25] V. Jayaraman, D.A. Cohen and L.A. Coldren, "Extended tuning range semiconductor lasers with sampled gratings," in *Lasers and Electro-Optics Society Ann. Meet. (LEOS 1991)*, San Jose, Nov. 1991, Paper No. SDL15.5.

[26] V. Jayaraman, D.A. Cohen and L.A. Coldren, "Demonstration of broadband tunability in a semiconductor laser using sampled gratings," *Applied Physics Letters*. , vol. 60, (19), pp. 2321-2323, May 1992.

[27] V. Jayaraman, A. Mathur, L.A. Coldren and P.D. Dapkus, "Very wide

tuning range in a sampled grating DBR laser," in *Proc. 13th IEEE Int. Semiconductor Laser Conf.,* Takamatsu, Japan , Sep. 1992 , pp. 108-109.

[28] V. Jayaraman, A. Mathur, L.A. Coldren, and P.D. Dapkus,"Extended tuning range in sampled grating DBR lasers," *IEEE Photon. Technol. Lett.*, vol. 5, pp. 489-491, May 1993.

[29] Vijaysekhar Jayaraman, Zuon-Min Chuang, and Larry A. Coldren, "Theory, design, and performance of extended tuning range semiconductor lasers with sampled gratings," *IEEE J. Quantum Electron*, vol. 29, pp.1824-1834, Jun. 1993.

[30] Xi-Hua Zou, Wei Pan, Bin Luo, Wei-Li Zhang, and Meng-Yao Wang, "Accurate Analytical Expression for Reflection-Peak Wavelengths of Sampled Bragg Grating," *IEEE Photon. Technol. Lett.*, vol. 18, pp. 529-531, Feb. 2006.

[31] Jens Buus, Markus-Christian Amann and Daniel J. Blumenthal, *Tunable Laser Diodes and Related Optical Sources*, Wiley-Interscience, 2005, Chapter 7, "Widely tunable monolithic laser diodes," pp. 169–220.

[32] René Todt, Reinhard Laroy, Geert Morthier, and Markus-Christian Amann, "New widely tunable lasers for optical networks (NEWTON) project, Deliverable 2: device concepts for the SG-TTG laser," Sep. 2002, http://intecweb.intec.ugent.be/newton/download/D21.pdf

[33] René Todt and Markus-Christian Amann, "Influence of facet reflections on monolithic widely tunable laser diodes," *IEEE Photon. Technol. Lett.*, vol. 17, pp. 2520-2522, Dec. 2005.

[34] Beck Mason, Jonathon Barton, Greg A. Fish, Larry A. Coldren and Steven P. DenBaars "Design of sampled grating DBR lasers with integrated semiconductor optical amplifiers," *IEEE Photon. Technol. Lett.*, vol. 12, pp. 1-3, Jul. 2000.

[35] T. Wipiejewski, Y.A. Akulova, G.A. Fish, P.C. Koh, C. Schow, P. Kozodoy, A. Dahl, M. Larson, M. Mack, T. Strand, C. Coldren, E. Hegblom, S. Penniman, T. Liljeberg and L.A. Coldren, "Performance and reliability of widely tunable laser diodes" in *Proc. Electron. Compon. and*

Technol. Conf., New Orleans, May 2003, pp. 789-795.

[36] Y. A. Akulova, G. A. Fish, P. Koh, C. L. Schow, P. Kozodoy, A. P. Dahl, Shigeru Nakagawa, M. C. Larson, ,M. P. Mack, T. A. Strand, C. W. Coldren, E. Hegblom, S. K. Penniman, T. Wipiejewski and L. A. Coldren, "Widely tunable electroabsorption-modulated sampled-grating DBR laser transmitter," *IEEE J. Sel. Topics Quant. Electron*., vol. 8, pp. 1349-1357, Nov./Dec. 2002.

[37] J. S. Barton, E. J. Skogen, L. Masanovic´, S. P. Denbaars, and L. A. Coldren, "A widely tunable high-speed transmitter using an integrated SGDBR laser-semiconductor optical amplifier and Mach–Zehnder modulator," *IEEE J. Sel. Topics Quant. Electron*., vol. 9, pp. 1113- 1117, Sep./Oct. 2003.

[38] L.A. Coldren, J.W. Raring, J.S. Barton, M.N. Sysak, and L.A. Johansson, "Improved functionality and performance in photonic integrated circuits"in *Proc. Indium Phosphide and Related Materials Conf.* , Princeton, May 2006, paper no. PLE1 1-6.

[39] H. Ishii, H. Tanobe, F. Kano, Y. Tohmori, Y. Kondo, and Y. Yoshikuni, "Quasicontinuous wavelength tuning in super-structure grating (SSG) DBR lasers," *IEEE J. Quantum Electron*, vol.32, pp.433–441, Mar. 1996.

[40] H. Ishii, Y. Tohmori, Y. Yoshikuni, T. Tamamura and Y. Kondo, "Multiple-phase shift super structure grating DBR lasers for broad wavelength tuning," *IEEE Photon. Technol. Lett.*, vol. 5 , pp. 613–615, Jun. 1993

[41] H. Ishii, H. Tanobe, F. Kano, Y. Tohmori, Y. Kondo and Y. Yoshikuni, "Broad-range wavelength coverage (62.4nm) with superstructure-grating DBR laser," *Electron. Lett.,*vol. 32, pp. 454-455, Feb. 1996.

[42] A.J. Ward, D.J. Robbins, D.C.J. Reid, N.D. Whitbread, G. Busico, P.J. Williams, J.P. Duck, D. Childs and A.C. Carter, "Realization of phase grating comb reflectors and their application to widely tunable DBR lasers," *IEEE Photon. Technol. Lett.,* vol. 16, pp. 2427-2429, Nov. 2004.

[43] A.J. Ward, D.J. Robbins, G. Busico, E. Barton, L. Ponnampalam, J.P. Duck,

N.D. Whitbread, P.J. Williams, D.C.J. Reid, A.C. Carter and M.J. Wale, "Widely tunable DS-DBR laser with monolithically integrated SOA: design and performance," *IEEE J. Sel. Topics Quant. Electron*., vol. 11, pp. 149-156, Jan./Feb. 2005

[44] M. C. Amann, S. Illek, C. Schanen and W. Thulke, "Tunable twin-guide laser: A novel laser diode with improved tuning performance.," *Applied Physics Letters* , vol. 54, pp. 2532-2533, Jun. 1989.

[45] René Todt, Thomas Jacke, Ralf Meyer, Jörg Adler, Reinhard Laroy, Geert Morthier, and Markus-Christian Amann, "Sampled grating tunable twin-guide laser diodes with over 40-nm electronic tuning range," *IEEE Photon Technol. Lett.*, vol.17, pp. 2514-2516, Dec. 2005.

Chapter 3 – TL Module Investigation

As was seen in the previous chapter the SGDBR is a four section device with three passive sections – *front grating/mirror*, *rear grating/mirror*, and *phase*, and an active *gain* section. The operation wavelength of the laser is coarsely tuned by the application of appropriate analogue currents to the grating sections and fine tuned by current control of the phase sections. The active section is used for gain control. This chapter is concerned with the wavelength tuning of the SGDBR to ITU defined wavelength channels, operational stability at these channels and the wavelength switching behaviour during channel transition. Particular attention is paid to the latter section with experimental work presented on intermediate or spurious modes generated during wavelength switching.

3.1 Characterisation and Control

The characterisation and control of the SGDBR is similar to that used for other TLs such as the GCSR and the SSGDBR, hence the inclusion of references to work based on such. Static tuning characterisation of the SGDBR can be performed to provide a visual representation of the mirror Vernier tuning function. In [1] the wavelength of an SGDBR is measured, using an optical spectrum analyser (OSA), as a function of the current applied to the mirror sections. The current to the phase section and the gain section are kept constant throughout. The data is displayed in a wavelength tuning map in Fig. 3.1 with the wavelength variation represented by a colour scaling.

Two types of wavelength transition are visible from the plot, super mode changes and smaller longitudinal mode changes. The former are due to super mode jumps, which occur due to the realignment of peaks of the mirror reflection spectra. These

coarse wavelength changes of ~7 nm (approximate peak spacing) result from tuning the mirrors relative to each other and their boundaries produce a fan like layout on the plot. The changes within these supermode boundaries are representative of the smaller longitudinal mode changes (of around 0.5 nm) and are due to the lasing mode jumping to an adjacent longitudinal cavity mode as the mirror currents are tuned simultaneously. Fine tuning of the laser wavelength can be achieved by current control of the phase section, which shifts the positions of the longitudinal modes themselves. Through correct control of the three tuning currents (front mirror, back mirror and phase) the laser can be tuned to any wavelength within its tuning range, assuming quasi-continuous wavelength coverage as outlined in section 2.5.1.

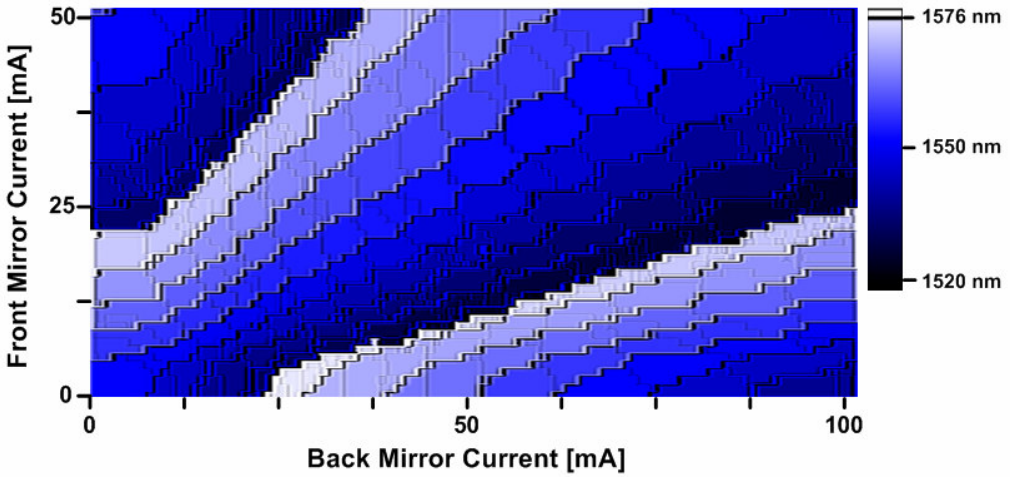

Figure 3.1 SGDBR wavelength tuning map

3.1.1 Look-up Table Generation

Static spectral tuning characterisation as outlined above can be used to determine the current settings required for each wavelength channel of the laser. The particular wavelength channels will be determined by the ITU DWDM grid recommendation [2] and the channel spacing selected. Tuning maps for several different phase currents are recorded. The output power at each wavelength is also recorded. To ensure stable mode hop free lasing potential operating points within each region defined by the longitudinal and super mode boundaries with good

SMSR are selected from each tuning map. Through simple interpolation of the points in the corresponding regions of each tuning map the required currents for any wavelength can be found. The three tuning currents for each wavelength are stored in a look-up table. For the case of channels accessible by multiple tuning current combinations, the combination that requires the smallest total tuning current is used as this will give the lowest absorption losses in the passive sections [3].

In commercially available TL modules [4, 5, 6] the current sources to set the laser wavelength channels are controlled by a microprocessor. The control electronics of a typical module setup [7], are based around a field programmable gate array (FPGA) containing a microprocessor and a look-up table. To set the laser to a particular channel, a request for that channel is sent via a control bus to the FPGA. The current value for each tuning section is read from the look-up table and sent to digital to analogue circuits (DAC). The analogue currents produced are amplified and sent to the appropriate tuning sections of the laser. It is advantageous to keep the gain current, also supplied by the module, at a constant value and only use an integrated SOA [8] for output power control. This is because adjusting the gain current can also impact the laser wavelength, reducing wavelength stability [9]. A block diagram of such a setup is given in Fig. 3.2.

Due to fabrication tolerances the wavelength channel tuning currents will be different for each TL, necessitating individual look up table generation. This requires wavelength and output power measurement for hundreds of thousands of different current settings [10] which are costly and time consuming, requiring several days of expensive equipment use i.e. an optical spectrum analyser (OSA). Thus high resolution spectral characterisation is unpractical for large scale device fabrication. The characterisation time and cost can be significantly reduced by using a reduced number of spectral measurements. This has been done in [11] by using output power measurements, as a function of mirror currents, and low resolution wavelength measurement, using a filter based wavelength discriminator, to locate the mode boundaries. Stable operating points are selected within these

boundaries on which high spectral measurements are performed. In [3] the stable operating points were identified by measuring the voltage across the gain section as a function of the mirror currents. This voltage varies as the mirror alignment is shifted relative to the cavity modes, yielding a local minimum at the point of perfect alignment. In both cases the measurements are repeated for various phase values to allow for the location of stable operating points for all wavelength channels through interpolation as outlined previously. Reduction in the characterisation time also facilitates simpler recalibration that may be required due to ageing of the laser.

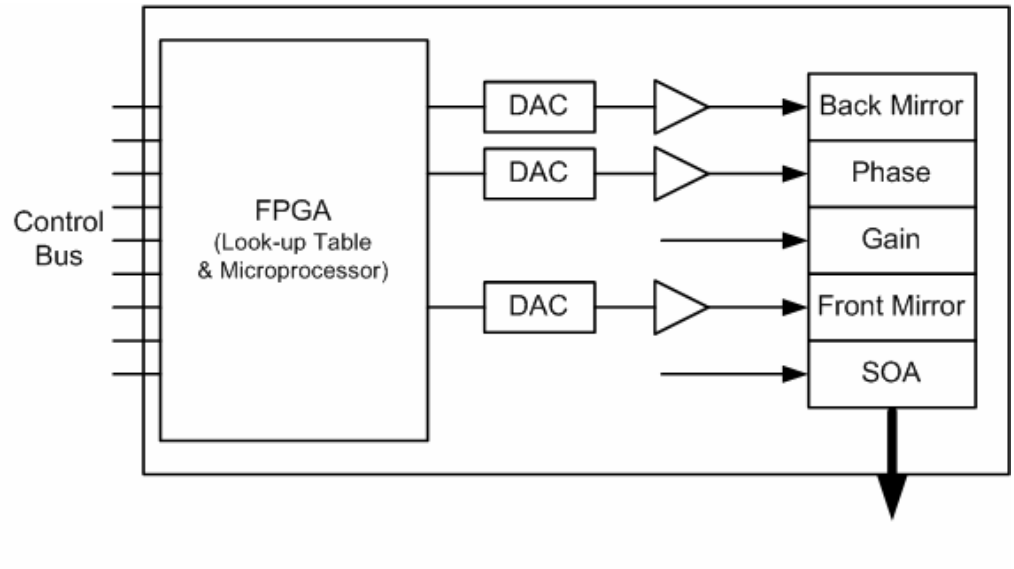

Figure 3.2 SGDBR TL module block diagram

3.1.2 Feedback Control

Once the laser has been set to a desired channel, by the application of the tuning currents given in the look-up table, it must remain at this wavelength for an indefinite amount of time, generally until the next channel transition is requested. The accuracy within which the wavelength remains stable will determine the maximum number of channels achievable from the TL, as according to [12] the frequency deviation should be no greater than $(f_S\text{-}2B)/4$, where f_S is the channel spacing and B is the channel bit rate. Due to environmental or ageing induced

wavelength drift, for DWDM applications the initial operating currents may have to be dynamically modified to satisfy this ITU recommendation. Accordingly wavelength feedback control is used in TL modules to ensure adequate wavelength stability. Aside from wavelength control, feedback may also be required to ensure mode and power stability.

In DWDM systems with channel spacing of less than 100 GHZ, wavelength stability cannot be maintained by tight temperature control alone. Also in comparison with fixed channel lasers, TL wavelength locking is required across more than just a single channel. Subsequently, in addition to internal temperature control, wavelength lockers built around filters with narrow periodic transmission peaks have been developed for multiple channel TL modules with narrow channel spacing. A block diagram of a TL module with feedback control from an internal Fábry-Perot etalon wavelength locker [13] is given in Fig. 3.3. The etalon cavity length is designed to suit the channel spacing of the DWDM system for which the TL is intended, giving peak transmission at each ITU defined wavelength channel.

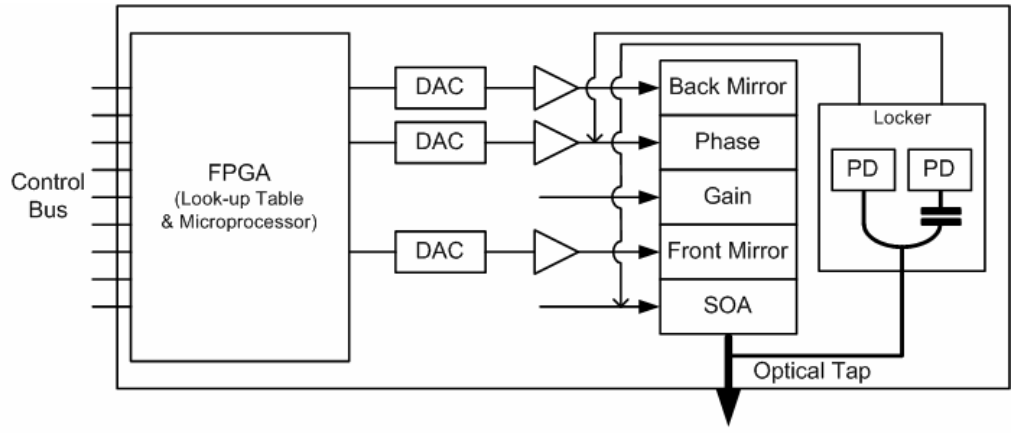

Figure 3.3 SGDBR TL module with wavelength and power feedback control block diagram

In the module a small portion of the laser output power is diverted to the locker. This tap is then split between two paths, one of which is passed through the etalon

and detected by a photodiode. The other path is detected directly by a second photodiode to provide a reference power measurement. The electrical signals produced, one depending on the laser wavelength and the other depending on only the laser power, are used to generate an error signal. This signal is fed back to the phase current to smoothly fine-tune the lasing wavelength by adjusting its longitudinal mode position. As the reference output power path signal depends only on the laser output power it can be used to independently generate an error signal to be fed back to the SOA section of the laser to lock the output power. A TL module using a digital feedback loop, in which the wavelength error signal is sent to the FPGA, was presented in [14]. The phase section current adjustment is achieved in this case by modification of the look up table. This could potentially allow for dynamic updating of the look up table based on the feedback from a single channel.

The feedback control described above is capable of capturing wavelength channels within the transmission band of the filter peaks and locking them to the corresponding peak transmission wavelengths, which are fixed on the ITU channel wavelength. This gives a wavelength locker range of about $^1/_3$ of the system channel spacing either side of each channel. However as this feedback does not provide mirror control, SMSR can be impaired due to misalignment of the mirror reflection peaks and the cavity mode. This mirror reflection drift could eventually lead to mode hopping and potentially locking of the laser wavelength at an adjacent channel, if the lasing cavity mode hops into an adjacent etalon transmission peak [3]. Although according to SGDBR reliability results for a 50 GHZ spaced TL module presented in [9], mirror control is not necessary as phase control provides adequate wavelength accuracy over the laser lifetime.

Mode hopping and adjacent channel locking have been observed in SSGDBR TLs as a result of induced temperature variation, used to simulate aging or environmental variation [15]. Mirror control has been demonstrated to prevent this by locking the reflection peaks to the selected cavity mode. This feedback control can be based on knowledge of mirror and cavity mode misalignment derived either

from output power measurements [16] or active section voltage measurements [3, 15] (Operating on the same principle as the characterisation time reduction techniques described previously). Similar mirror control has also been demonstrated for the SGDBR [17]. In actual SGDBR modules, temperature variation should not be a problem due to internal temperature control of the module. In addition, aging related mirror reflection drift is not as significant a problem for sampled gratings, of which ~90% of the mirror section is free from actual grating, as opposed to standard gratings, for which the grating covers the full length of the mirror section [9].

3.2 Tuning Dynamics

The investigation of the wavelength tuning behaviour of tunable laser modules is important for their deployment in DWDM networks. Understanding the limitations and obstacles to achieving fast channel to channel transition will be of concern for their application in future optically switched networks, while the wavelength tuning evolution of the laser emission as the module tunes will be critical to the integrity of other wavelength channels in use.

3.2.1 Wavelength Tuning Time

The tuning time for a wavelength channel transition is an important characteristic for TL modules to be used in future optically switched networks. The tuning time is made up of two time components;

1) the module latency is the time required for the laser wavelength to begin switching after receiving a trigger request, and will generally be stable for different channel transitions,
2) the wavelength switching time is the time interval between the laser wavelength leaving a source channel and settling at a destination channel within a specified wavelength and power accuracy, and will vary for different channel transitions [7].

Through efficient circuit and system design data can be transmitted during the module latency time, the laser however becomes inoperable for data transmission

during the wavelength switching time. For system simplicity a fixed overhead time, sufficiently long to accommodate any possible channel transition, should be used. This system overhead will be dictated by the maximum tuning time of all possible channel transitions. To achieve efficient network throughput minimum overhead is required and should be short compared with the data burst or packet to be transmitted. In future optical networks based on burst or packet switching, with respectively decreasing data transmission lengths [18] TL modules with tuning times on nanosecond timescales will be required [19, 20].

The electro-optic effect offers the fastest tuning times; the limited tuning range achievable however makes it unpractical for use in DWDM TL modules. Carrier injection tuning, as outlined in section 2.4.1, allows for an extended tuning range and the development of TL modules suitable for DWDM systems. The tuning time in such modules will depend on and be limited by the following:

Carrier Lifetime:

In multi section tunable lasers such as the SGDBR the wavelength is tuned by changing the refractive index of a passive waveguide (i.e. phase) section and/or filter (mirror) sections. This can be achieved through current injection to change the carrier density of a section. The speed of this change will inherently be limited to several nanoseconds by the spontaneous carrier lifetime in the tuning sections [21]. For a particular channel transition the switching time will be impacted by the carrier density required in the tuning sections for the source and destination wavelength, with the switching time being greater for transitions that require larger carrier density variation in a tuning section.

Laser Structure:

The electrical properties of the laser chip are important with regard to the tuning time as the dynamic impedance can be large for operation below threshold [7], as is the case for the passive tuning sections. The switching time is therefore limited by the section capacitances resulting in slow electrical carrier settling times. Parasitic thermal effects in the tuning sections will also impact the switching time due to a

reduction in the wavelength accuracy. These points are addressed in [18] to achieve sub 5 ns wavelength switching between all transition combinations of 64 channel a SGDBR through controlled tuning currents and superior design of the laser structure. Pre-distorted tuning currents [22] are used to improve the capacitance limited switching times – the carrier settling time is sped up by overshooting the current required for a particular wavelength channel for a short period of time (<5 ns) before stabilizing at the usual tuning current. Thermal impedance of the laser is reduced by using more efficient heat extraction in the tuning sections. The switching current variation for channel transitions is also reduced by using grating sections with narrower peak separation.

Module Electronics:

The TL module must be able to handle channel requests at irregular time intervals and, using high speed circuitry, apply accurate channel specific analogue currents to the laser tuning sections. The module electronics can contribute significantly to the overall channel tuning time in terms of module latency and feedback control circuitry (as described in section 3.1.2). The optical output requirements will be important in DWDM networks with closer channel spacing requiring greater wavelength accuracy. Sub 50 ns wavelength switching was reported in [14] for an FPGA based module, with transitions between a large number of random combinations of a 64 channel system on a 50 GHz spaced grid.

3.2.2 Spurious Mode Generation

An important feature of widely tunable lasers is the emission of unwanted optical components during channel transition. These intermediate or spurious modes could potentially coincide with, and corrupt data transmitted on other wavelength channels [23, 24, 25]. As explained previously, when a channel request is received the analogue currents to the laser tuning sections are modified as per digital information stored in the module look up table. After the module latency or *wavelength setup* time the current to each section will continuously change the carrier concentration in each section, until the appropriate levels are reached for the new channel. However, as can be understood from the wavelength-tuning map in

Fig. 3.1 and the tuning mechanism of the laser, the module emission wavelength will not change in a strictly continuous manner but will rather include discrete mode hops to the new wavelength channel [26].

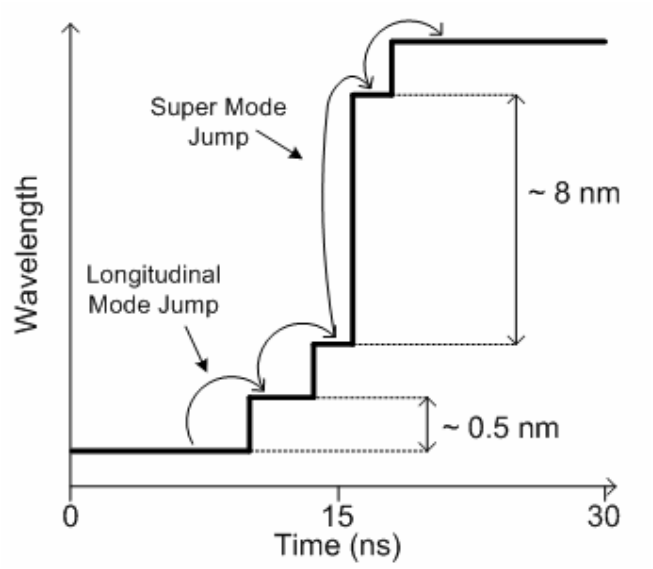

Figure 3.4 Wavelength variation versus time for channel transition

In [27] time resolved spectral characterization was performed on the channel transition behaviour of an SGDBR. It was shown that during wavelength switching the laser output switches between modes with time. The wavelength tuning evolution can be understood from Fig. 3.4 in which the laser emission wavelength is plotted versus time for a sample channel transition. The laser is initially lasing at the source channel wavelength. When the currents to the tuning sections begin to change, the source channel looses mode dominance, as the point of mirror alignment is tuned, and the laser mode-hops. This mode hopping continues, and can include longitudinal and super mode jumps (as indicated in the diagram), until the laser stabilizes at the destination channel. Depending on the wavelength of these spurious modes, bursts of errors may occur on data transmitted on different wavelength channels due to coherent interference. In [28] a switching SGDBR was shown to cause cross channel interference on an intermediate wavelength channel resulting in a severe degradation of the channel performance.

To prevent the spurious modes generated during the channel-to-channel transition of a TL module interfering with other channels in a DWDM system it is necessary to ensure that the light emitted during the wavelength switch does not enter the multiplexed channel. It is a better option to suppress the laser output during a switching event rather than simply turning off the laser gain current. This is because turning the current to the gain section back on again may introduce a transient on the wavelength tuning accuracy [29]. The output suppression during switching could be achieved by using an external amplitude modulator in the off state. A simpler solution however would be to use an integrated SOA, already in place to boost the output power [8, 30], as an optical shutter during switching. By reducing the SOA bias condition, from the saturated state used for power boosting, the laser output was reduced to -30 dBm during wavelength switching for an SGDBR in [31] and for a DSDBR in [32].

3.3 Spurious Mode Investigation

System Performance Measurement:

In the following experimental work bit error rate (BER) testing and eye diagram observation is used to measure the integrity of data detected in a pseudo DWDM system. The BER is a quantitative measurement of system performance which is the ratio of the number of bits received in error to the total number of bits received. Data from a pattern generator in the form of a programmed test pattern or a pseudo random bit sequence (PRBS) is transmitted across the system. An error detector at the receiver, synchronised to the transmitted pattern, compares each bit transmitted to the corresponding bit received, giving a bit error for differing bits, this allows for a fundamental measure of system performance. The eye diagram is a synchronised superposition of possible bit transitions and is used to give a qualitative measurement of system performance. The eye pattern provides an accessible method to quickly judge the quality of a digital signal with the eye opening relating to the BER of the system. Eye diagram analysis however does not give logical

information about the signal, with only parametric information, such as rise-time, overshoot, noise, jitter and inter symbol interference, provided [33].

In previous work [28], the characterisation of cross-channel interference from a single TL module that was switched between two wavelengths was presented. The spurious components generated during the switching event placed an error floor on the BER of a channel transmitted at the same wavelength as the spurious components. It was also shown that in order to achieve an acceptable BER the output of the TL must be attenuated by a certain level during the transition. Similar SGDBR based nanosecond wavelength switched tunable laser modules are used in the work presented here.

3.3.1 Tunable Laser Module

Tunable laser modules [4] built around a monolithically integrated SGDBR-SOA chip are used in this work. The continuous wave (CW) module output power is ~ 8.5 dBm; however a more important characteristic is the Side Mode Suppression Ratio (SMSR) of each individual wavelength channel. Normally the SMSR should be greater than 30 dB for correct use of the module in a DWDM system, as if it is any higher significant cross channel interference from the side mode of one source at the same wavelength as the output from a second source, can cause serious degradation in system performance. However, with advanced DWDM design and a large number of channels, the allowed SMSR of the wavelength tuneable sources may become more stringent than 30 dB. The optical spectrum of each channel was measured using an optical spectrum analyser (OSA). As can be seen from the superimposed spectra in Fig. 3.5 the TL exhibits very good SMSR over the entire range (33.4 nm) of 85 channels with 50 GHz spacing. The channel with the worst SMSR, at the extreme of the tuning range, is highlighted and can be seen to give a SMSR greater than 40 dB. The optical output variation as a function of wavelength can also be observed from the superimposed optical spectra, and is within requirements at ~ +/-1 dB.

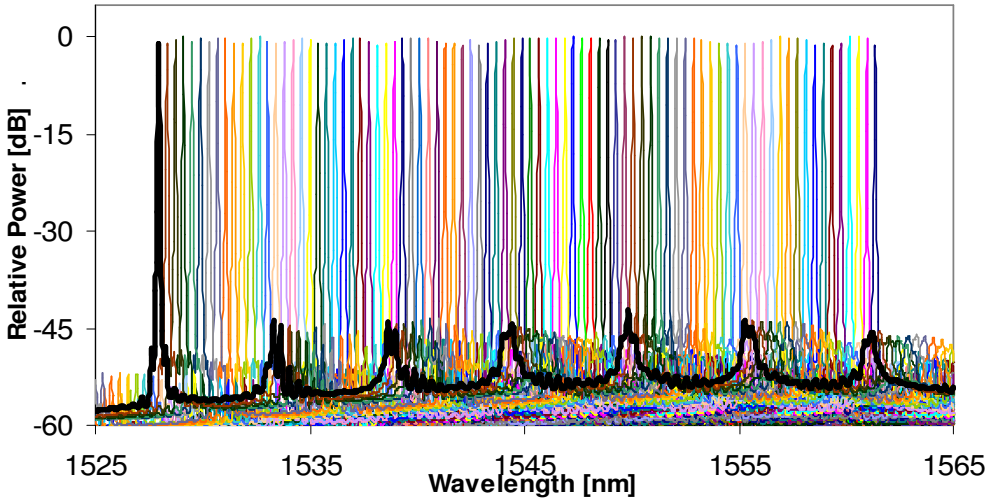

Figure 3.5 Superimposed spectra of 85, 50 GHz spaced TL module channels showing a tuning range of 33.4 nm

The TL modules can be switched between any set of 50 GHz spaced ITU channels within the C-band with a wavelength setup time of 200 ns and a maximum switching time of 200 ns, after which the laser output is specified to be within +/- 2.5 GHz of the intended frequency. Within this switching time and depending on the particular channel transition the time taken to be within +/-15 GHz of the final frequency is typically in the order of 20-50 ns, during which spurious output wavelengths may be generated due to mode hopping of the TL emission wavelength. The main difference in comparison to the TL module used in [28] is the integrated Semiconductor Optical Amplifier (SOA) at the output of the tunable laser. The SOA is zero biased to blank the laser output for a period of ~60 ns starting from the moment the laser tuning (to a different wavelength) is initialised. The effectiveness of the optical shuttering is investigated by detecting the output from the TL module as it switches wavelength channel. The detected signal is sent to an oscilloscope, displayed in Fig. 3.6, and shows output power suppression during the blanking period of greater than 35 dB. This should attenuate any spurious components that are generated during the switching event.

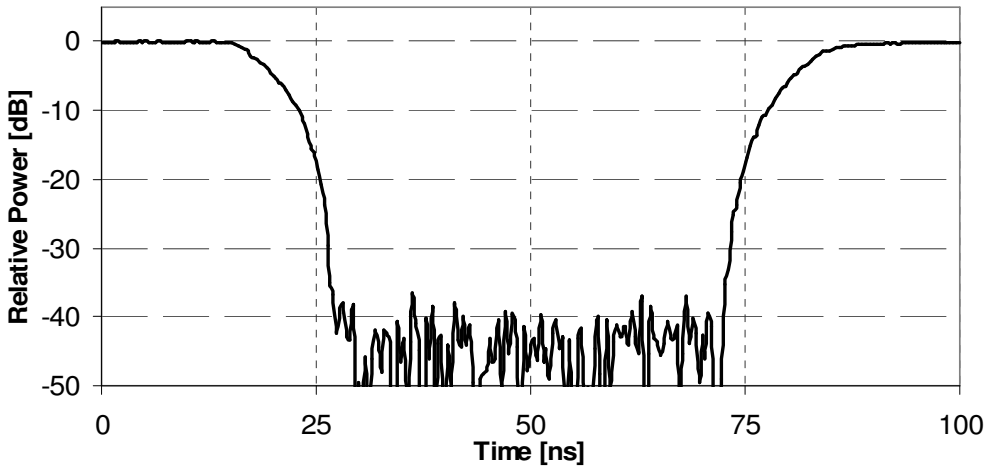

Figure 3.6 SOA optical blanking for channel transition displayed on oscilloscope

The blanking attenuation level will change with the bias condition of the SOA as a function of wavelength. This is due to the wavelength dependent absorption of the SOA. The spurious mode power at different wavelengths was measured using an OSA for different biasing conditions of the SOA. The bias condition of the SOA could be varied from arbitrary set values of 0 to 16383, corresponding to the zero biased setting and a point beyond the saturation of the SOA respectively.

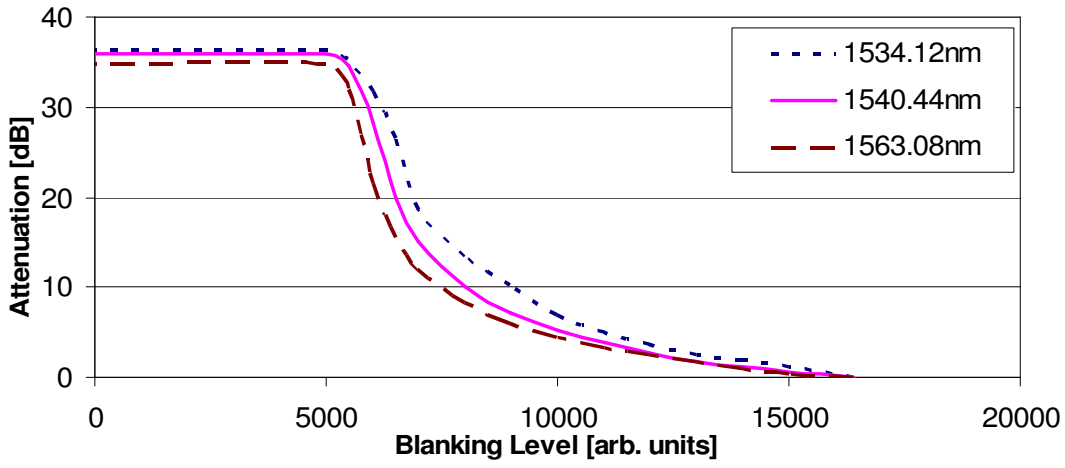

Figure 3.7 Power Blanking Depth of SOA for different bias settings

From the results presented in Fig. 3.7, of a number of different modes generated during different channel transitions, it can be seen that the attenuation achieved is wavelength dependent. Longer wavelengths experience slightly less attenuation due to the position of the SOA absorption peak at lower wavelengths. Setting the blanking level to less than 5000 effectively turns off the SOA, giving blanking of ~35 dB across the entire wavelength range of the TL.

3.3.2 Spurious Mode Blanking Experiment

Work was carried out in [32] in which it was shown that an SOA can be used to blank the spurious modes generated by a DS-DBR laser during channel switches. In the experiment presented here the effectiveness of this method of reducing the cross-channel interference caused by multiple TLs in wavelength packet-switched WDM networks is verified by presenting Bit-Error-Rate measurements.

Experimental Setup:

The experimental set-up used is shown in Fig. 3.8. It consists of three computer controlled TL modules. Each TL is switched between two wavelengths. A Pattern Generator (PG) is used to generate a non return to zero Pseudo Random Bit Sequence (PRBS) of length 2^7-1 at 2.5 Gbit/s, which is then externally modulated onto an optical carrier generated by a Continuous Wave (CW) Laser. The combined output power of the three TLs is adjusted using a Variable Optical Attenuator (VOA) before being coupled with the data channel. This ensures that the powers of the four lasers (from the three TLs and the externally modulated CW laser) are equalised after coupling. The receiver consists of an EDFA to boost the optical power on the detector, an Optical Band Pass Filter (OBPF) with a 3 dB bandwidth of 27.5 GHz to filter out the data channel, a VOA to vary the optical power falling on the receiver, which consists of a photodiode, an electrical amplifier and a low pass filter. An error analyser is used to measure the BER of the recovered data channel.

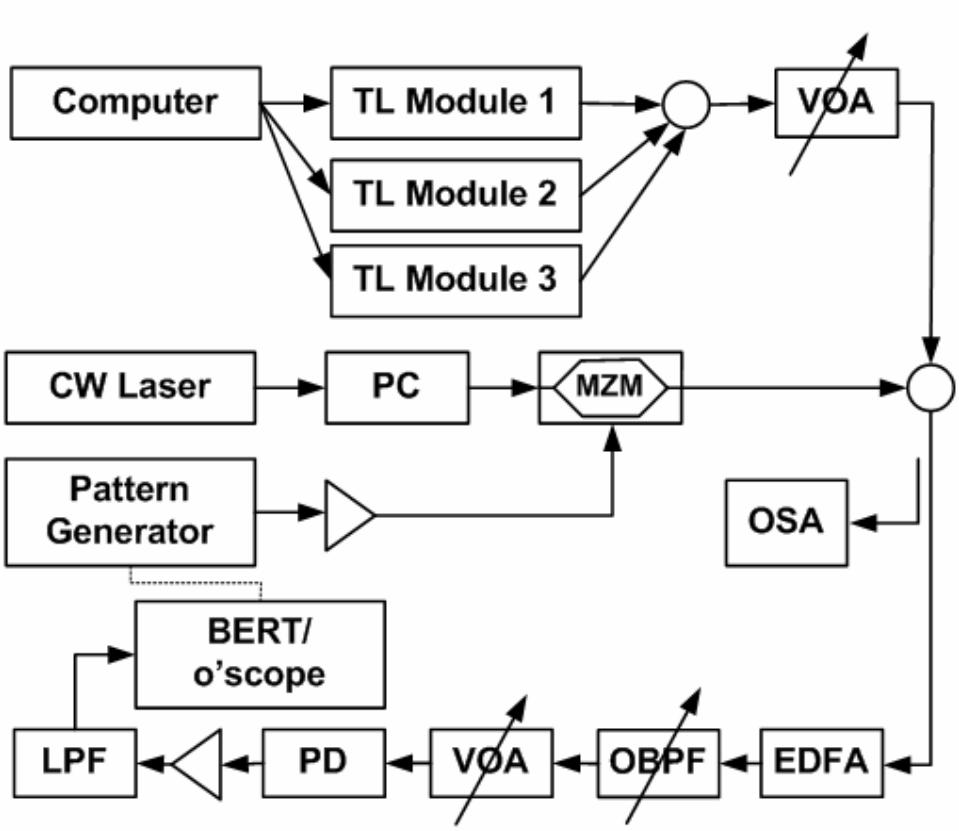

Figure 3.8 Experimental configuration to determine how the spurious wavelength signals emitted during switching of the TL modules affect a multiplexed data channel lying between the TLs' output wavelengths.

In order to characterise the cross channel interference, the TLs are switched continuously between different pairs of wavelengths: TL1 between channel (ch.) 86 (1531.5 nm) and ch. 28 (1554.5 nm), TL2 between ch. 57 (1542.9 nm) and ch. 13 (1560.6 nm) and TL3 between ch. 52 (1544.9 nm) and ch. 26 (1555.3 nm). Using these particular transitions it is found that significant spurious modes are generated around the same wavelength, 1548.04 nm (within a window of 0.16 nm). As it would be in an actual system the three TL modules switch independently of each other. In order to verify how these undesired modes would influence the performance of a WDM system, the wavelength of an individual probe data channel is set in the middle of this window at 1548.04 nm. The time averaged optical spectrum of the TL outputs with blanking disabled is shown in Fig. 3.9. From the

figure it can be seen that the TLs produce a series of spurious components during the transition between wavelengths – especially at the location where the data channel is to be multiplexed in.

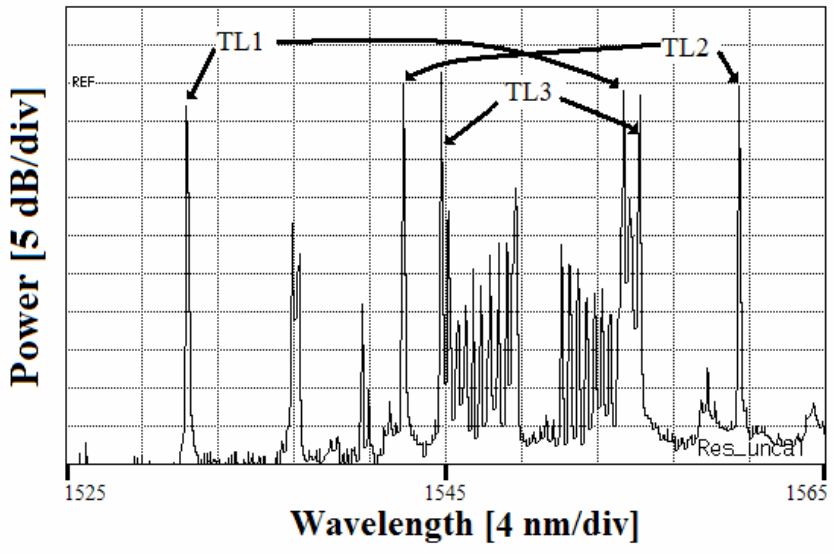

Figure 3.9 Optical Spectrum of TLs switching with blanking disabled

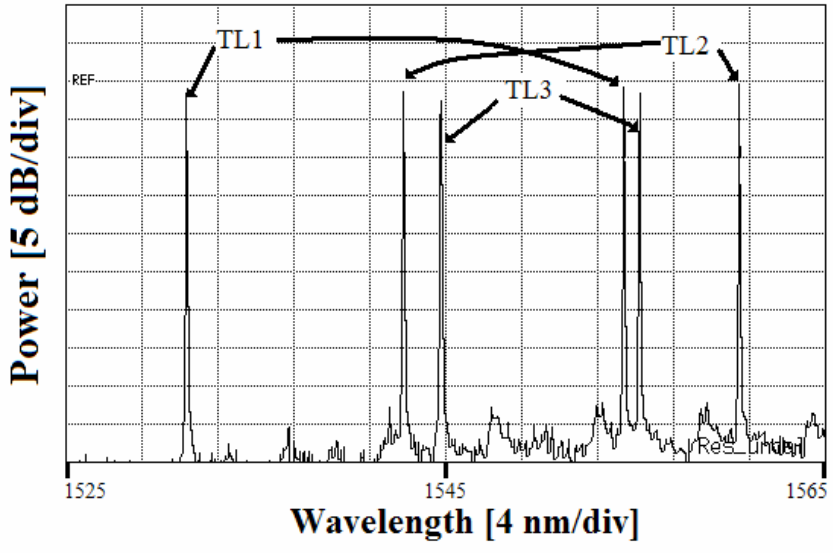

Figure 3.10 Optical Spectrum of TLs switching with blanking enabled

The optical spectrum of the TLs with the blanking enabled is presented in Fig. 3.10. In this case the spurious components are attenuated since the SOAs at the output of

the TLs are momentarily zero biased (for a period of ~60 ns from the moment the lasers begin to tune).

Experimental Procedure and Results:

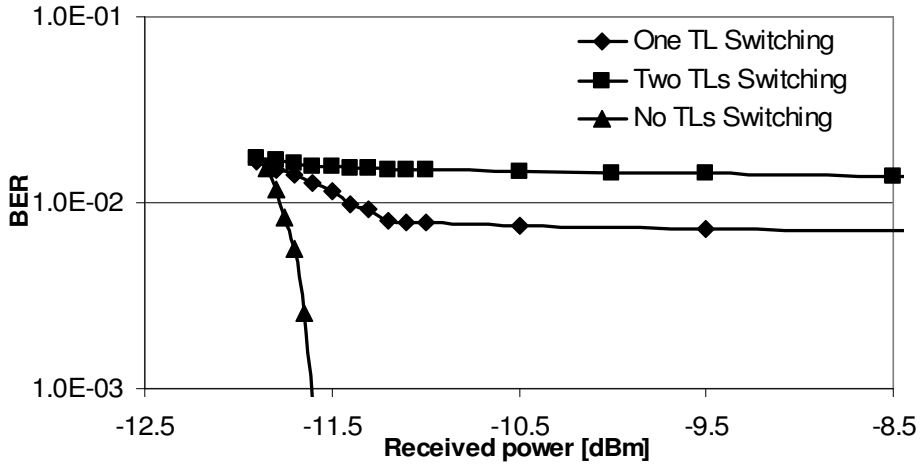

Figure 3.11 Average BER vs. received optical power measurements for the case when the data channel is multiplexed with the combined TL module output with blanking disabled (i) when one TL Module is switching, (ii) when two TL Modules are switching, and (iii) when no TLs are switching.

In order to verify the impact of the spurious components generated by the TLs on the data channel, the BER of the latter is measured as function of the received optical power for various TL switching configurations (with blanking enabled and disabled). Fig. 3.11 presents the results when the blanking is disabled for: (i) the average BER of the data channel multiplexed with one TL switching, (ii) the average BER of the data channel multiplexed with two TLs switching, and (iii) the BER when the TLs are on but not switching. The effect of multiplexing the switching TLs onto the same fibre as the data channel is to place an error floor on the performance of the monitored data channel. The average error floor for one TL switching is 7.5×10^{-3}. This increases to 1.5×10^{-2} when a second TL is added. The BER of the data channel multiplexed with the three TLs switching cannot be measured due to such a high level of noise. The error floors are a result of burst of errors on the received data channel at the time when the TLs are switching and

generating spurious emissions at the same wavelength as the monitored data channel.

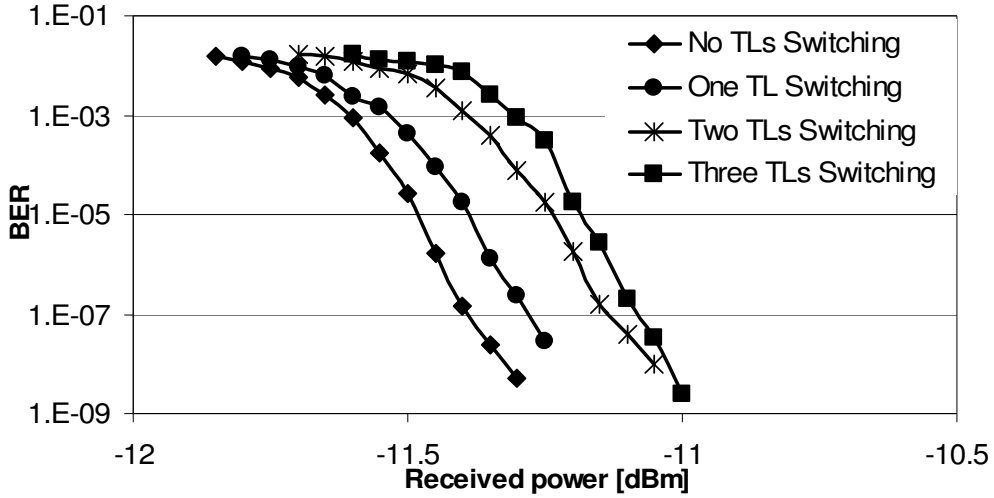

Figure 3.12 Average BER vs. received optical power measurements for the case when the data channel is multiplexed with the combined TL module output with blanking enabled (i) when no TLs are switching, (ii) when one TL Module is switching, (iii) when two TL Modules are switching, and (iv) when the three TL Modules are switching

Zero biasing the SOA for ~60 ns from the moment that the transition is initiated reduces the interference from the TL as the laser is specified to be within +/- 15 GHz of the final wavelength typically 20-50 ns after the wavelength switching begins. This can be seen in Fig. 3.12 which presents the results when the blanking is enabled for: (i) the BER of the data channel when the TLs are on but not switching (ii) the average BER of the data channel with one TL switching, (iii) the average BER of the data channel with two TLs switching and (iv) the BER of the data channel with the three TLs switching. However, it can also be seen that for such a scenario there is a slight power penalty incurred due to coupling the data channel with the output of the TLs that are switching, even though blanking is enabled for 60 ns after the switching begins. This gets progressively worse with the addition of more TLs, giving a penalty of ~0.4 dB for coupling with the three TLs switching. This may be due to the attenuation blanking level of the SOA not being high enough. The power penalty may also be attributed to not all the spurious

modes being blanked as the TL blanking may not continue long enough after the switch occurs.

The eye diagrams of the received data signals, when the data channel is multiplexed with the three TLs, for the case when the TLs are on but not switching and for the case when they are switching, between different pairs of wavelengths, are shown in Fig. 3.13(a) and Fig. 3.13(b) respectively. It can clearly be seen that the optical filter selects out both the data channel and the spurious emissions generated within the filter window by the switching TLs. It is these spurious emissions that cause the measured errors on the data channel during the switching time of the TLs. An optimised optical filter for 2.5 Gbit/s data with a narrower passband may reduce the interference falling on the detector, and thus improve system performance.

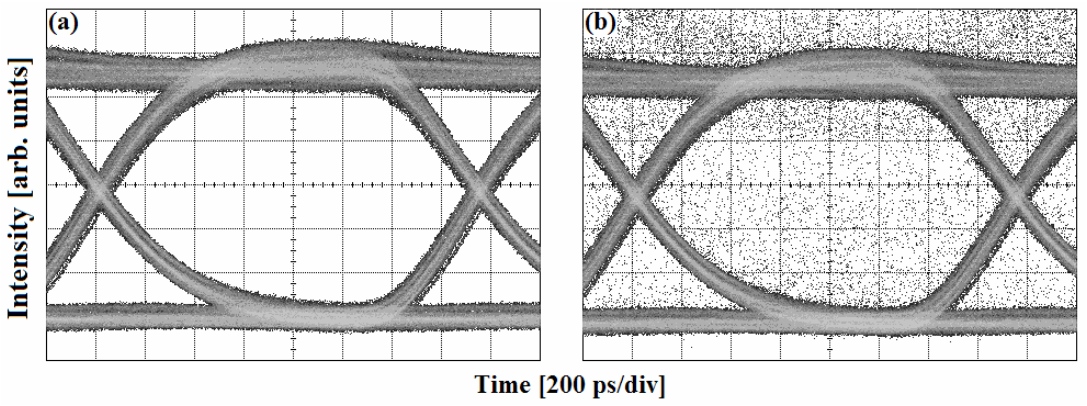

Figure 3.13 Eye diagrams of the received data signals, when the data channel is multiplexed with the three TLs before being filtered out, for (a) the case when the TLs are on but not switching, and (b) for the case when the TLs are switching between different pairs of wavelengths

Based on calculations in [28] it is possible to estimate the length of time that the TL module is transmitting at the same wavelength as the monitored data channel as it undergoes channel transition. The TL is transitioning between two output wavelengths every 200 ns, and since the data is modulated at 2.5 Gbit/s, this means that 500 bits are transmitted in each burst. With an average BER of 7.5×10^{-3} for the case when one TL is switching with blanking disabled, this means that ~4 of the

500 bits sent in 200 ns is received in error due to the excitation of a spurious mode. However given that the interference from the spurious mode only gives an error for a sent "0", and given that unbiased data is used (equal number of "1's" and "0's"), it can be assumed that the intermediary wavelength is on for approx. 8 bit periods of the 2.5 Gbit/s data signal, or for a time of 3.2 ns. As the wavelength switching only interferes with the monitored data channel for this short period of time it may be feasible to use forward error correction to achieve error free performance without the need for blanking. System performance degradation however will be dependent on the frequency of wavelength switching.

In order to characterise how the switching interval time (i.e. the time the TL remains tuned to a particular wavelength before switching) impacts the performance of the system, the BER (averaged over both switching event and interval between switching event) of the data channel as a function of the switching interval time is measured. The results acquired for one TL switching with blanking disabled, are plotted in Fig. 3.14.

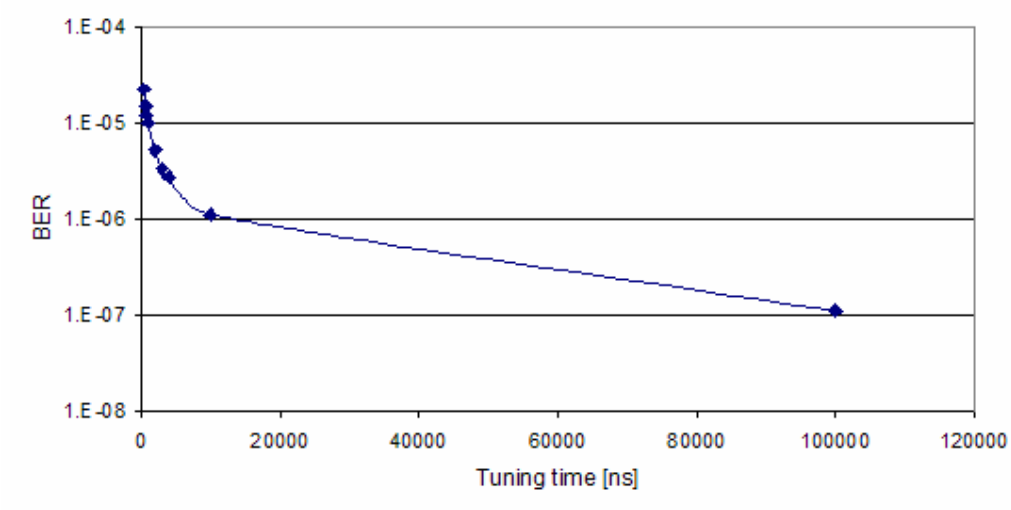

Figure 3.14 BER of the data channel vs. the switching time interval of TL module

As expected the BER improves as the switching interval time is increased. This is due to the fact that the spurious components, which degrade the quality of the data

signal, are generated less often as the TL remains tuned to one wavelength for a longer time. The degradation in performance of a wavelength packet-switched WDM system, due to the spurious wavelengths emitted from the TL, will be determined by how often the TL switches. This in turn will be strongly dependent on the packet length used in such systems. Thus, in future optically switched systems, with increasingly smaller burst and packet transmission times spurious mode blanking will be necessary.

Conclusion

Wavelength tunable lasers are becoming more and more important for the development of future WDM wavelength switched networks. In this chapter it has been shown that a significant problem associated with these devices is the generation of undesired spectral components during the switching event. This issue becomes more important as the switching interval time is reduced. It has been demonstrated that the solution to this problem is to use an SOA at the output of the TL. The SOA effectively blanks the output during the transition to attenuate the spurious components that may be generated during that time. However, if a large number of TL's are employed in a network, then the system penalties due to this effect maybe non-negligible, as shown in our work with three TLs. In WDM networks employing a large number of TLs it may be necessary to increase blanking levels or reduce switching times to prevent performance degradation due to wavelength switching events.

In the following chapter particular focus is placed on the output of the TL Modules once the blanking time ends. The wavelength evolution, in terms of deviance from the target channel, and how this drift may affect system performance will be investigated.

References

[1] Damien Quenson, "Wavelength Tunable Semiconductor Lasers," Undergraduate Training Period Report, Dublin City University, Glasnevin, Dublin, Ireland, 2007.

[2] ITU-T, Recommendation G.694.1, "Spectral grids for WDM applications: DWDM frequency grid," Jun. 2002.

[3] Gert Sarlet, Geert Morthier,and Roel Baets, "Control of widely tunable SSG-DBR lasers for dense wavelength division multiplexing," *J. Lightw. Technol.,* vol. 18, pp. 1128-1138, Aug. 2000.

[4] Intune AltoNet 1200 FTL Tx Module [Online]. Available: http://www.intunenetworks.eu/site/

[5] JDSU Tunable Laser Module 3205/3206 Series [Online]. Available: http://www.jdsu.com

[6] Bookham LambdaFLEX™ iTLA TL5000 Integrated Tunable Laser Assembly [Online]. Available: http://www.bookham.com/index.cfm

[7] J. Gripp, M. Duelk, J.E. Simsarian, A. Bhardwaj, P. Bernasconi, O. Laznicka and M. Zirngibl, "Optical switch fabrics for ultra-high-capacity IP routers," *J. Lightw. Technol.,* vol: 21, pp. 2839- 2850, Nov. 2003.

[8] Beck Mason, Jonathon Barton, Greg A. Fish, Larry A. Coldren and Steven P. DenBaars, "Design of sampled grating DBR lasers with integrated semiconductor optical amplifiers," *IEEE Photon. Technol. Lett.*, vol. 12, pp. 762-764, Jul. 2000.

[9] Larry A. Coldren, G. A. Fish, Y. Akulova, J. S. Barton, L. Johansson, and C.W. Coldren, "Tunable semiconductor lasers: a tutorial," *J. Lightw. Technol.,* vol. 22, pp. 193-202, Jan. 2004.

[10] J. Dunne, T. Farrell and R. O'Dowd, "Fast generation of optimum operating points for tunable SG-DBR laser over 1535-1565 nm range," in *Proc. Conf. on Lasers and Electro-Optics (CLEO99),* Baltimore, May 1999, pp. 147-148.

[11] T. Farrell, J. Dunne and R. O'Dowd, "Complete wavelength control of

GCSR lasers over EDFA band," in *Lasers and Electro-Optics Society Ann. Meet. (LEOS 1999)*, San Francisco, Nov. 1999, vol. 1, pp. 329-330.

[12] ITU-T, Recommendation G.692, "Optical interfaces for multichannel systems with optical amplifiers," Oct. 1998.

[13] Hongtao Han, B. Hammond, R. Boye, Bingzhi Su, J. Mathews, B. TeKolste, A. Cruz, D. Knight, B. Padgett and D. Aichele, "Development of internal wavelength lockers for tunable laser applications" in *Proc. Electron. Compon. and Technol. Conf.*, New Orleans, May 2003, pp. 805-808

[14] J.E. Simsarian and Liming Zhang, "Wavelength locking a fast-switching tunable laser," *IEEE Photon. Technol. Lett.*, vol. 16, pp. 1745-1747, Jul. 2004.

[15] G. Sarlet, G. Morthier and R. Baets, "Wavelength and mode stabilization of widely tunable SG-DBR and SSG-DBR lasers," *IEEE Photon. Technol. Lett.*, vol. 11, pp. 1351-1353, Nov. 1999.

[16] H. Ishii, F. Kano, Y. Yoshikuni and H. Yasaka, "Mode stabilization method for superstructure-grating DBR lasers," *J. Lightw. Technol.,* vol. 16, pp. 433-442, Mar 1998

[17] M.C. Larson, M. Bai, D. Bingo, N. Ramdas, S. Penniman, G.A. Fish and L.A. Coldren, "Mode control of widely-tunable SG-DBR lasers" in *Proc. Eur. Conf. Optical Commun. (ECOC02),* Copenhagen, Sep. 2002, vol. 3, pp. 1- 2.

[18] J.E. Simsarian M.C. Larson H.E. Garrett Hong Xu and T.A. Strand, "Less than 5-ns wavelength switching with an SG-DBR laser," *IEEE Photon. Technol. Lett.,* vol.18, pp. 565-567, Feb. 2006.

[19] D. Sadot and I. Elhanany, "Optical switching speed requirements for terabit/second packet over WDM networks," *IEEE Photon. Technol. Lett.,* vol.12, pp. 440-442, Apr. 2000.

[20] Jens Buus, Markus-Christian Amann and Daniel J. Blumenthal, *Tunable Laser Diodes and Related Optical Sources*, Wiley-Interscience, 2005, Chapter 10, "Communication applications and requirements," pp. 285–324.

[21] Y. Yu and R. O'Dowd, "Influence of mode competition on the fast wavelength switching of an SG-DBR laser," *J. Lightw. Technol.,* vol. 20, pp. 700-704, Apr. 2002.

[22] P.J. Rigole, M. Shell, S. Nilsson, D.J. Blumenthal and E. Berglind, "Fast wavelength switching in a widely tunable GCSR laser using apulse pre-distortion technique" in *Proc. Optical Fiber Commun. Conf. (OFC1997),* Dallas, Feb. 1997, pp. 231-232.

[23] S.A. Wood, R.G.S. Plumb, D.J. Robbins, N.D. Whitbread and P.J. Williams, "Time domain modelling of sampled grating tunable lasers" in *IEE Proc.-Optoelectron.,* vol. 147, pp. 43-48, Feb. 2000.

[24] San-Liang Lee, National. Ching-Yun Chien, Hen-Wai Tsao and Jingshown Wu, "Practical Considerations of Using Tunable Lasers for Packet Routing in Multiwavelength Optical Networks," in *Proc. 2003 Inter. Conf. on Parallel Process. Workshops* (ICPPW'03), Kaohsiung, Taiwan, Oct. 2003, pp. 325- 331

[25] J. Regan, W. Lynds and L. Coldren, "Widely tunable lasers for slow and fast switching applications," in *Proc .Photon. Switch. Conf. (PS 2003),* Versailles, Sep. 2003, paper no. PS.Mo.A1, pp. 11-13.

[26] Efraim Buimovich and Dan Sadot. "Physical limitation of tuning time and system considerations in implementing fast tuning of GCSR lasers," *J. Lightw. Technol.,* vol. 22, pp. 582-588, Feb. 2004.

[27] Yonglin Yu and O'Dowd, R., "Interpretation of wavelength switching effects of widely tunable lasers," *IEEE Photon. Technol. Lett*., vol. 14, pp.1397- 1399, Oct. 2002.

[28] A. Dantcha, L.P. Barry, J. Murphy, J.Dunne, T. Mullane, and D. McDonald, "BER performance in wavelength packet awitched WDM systems during nano-second wavelength switching events," *Elsevier Journal of Optics Commun.,* vol. 242, pp. 171-177, Aug. 2004.

[29] V. Polo, A. Ausiro, J. Prat and G. Junyent, "GCSR laser frequency drift compensation using optimized current waveform on one single electrode," in *Proc. 7th Inter. Conf Transparent Optical Networks (ICTON 2005),*

Barcelona , Jul. 2005, vol. 2, pp. 17- 20.

[30] A.J. Ward, D.J. Robbins, G. Busico, E. Barton, L. Ponnampalam, J.P. Duck, N.D. Whitbread, P.J. Williams, D.C.J. Reid, A.C. Carter and M.J. Wale, "Widely tunable DS-DBR laser with monolithically integrated SOA: design and performance," *IEEE J. Sel. Topics Quant. Electron*., vol. 11, pp. 149-156, Jan./Feb. 2005.

[31] T. Wipiejewski, Y.A. Akulova, G.A. Fish, P.C. Koh, C. Schow, P. Kozodoy, A. Dahl, M. Larson, M. Mack, T. Strand, C. Coldren, E. Hegblom, S. Penniman, T. Liljeberg and L.A. Coldren, "Performance and reliability of widely tunable laser diodes" in *Proc. Electron. Compon. and Technol. Conf.*, New Orleans, May 2003, pp. 789 – 795.

[32] L. Ponnampalam, N.D. Whitbread, R. Barlow, G. Busico, A.J. Ward, J.P. Duck and D.J. Robbins, "Dynamically controlled channel-to-channel switching in a full-band DS-DBR laser," *IEEE J. Quantum Electron.*, vol. 42, pp. 223-230, Mar. 2006.

[33] A Primer by Guy Foster, SyntheSys Research, Inc., "Anatomy of an Eye Diagram",
http://www.bertscope.com/Literature/White_Papers/Eye_Anatomy.pdf

Chapter 4 – TL Module Frequency Drift Investigation

The performance requirements of TL modules for use in current and future DWDM systems will depend on the particular network architecture used, with parameters such as channel spacing, packet length and number of wavelengths being of concern. As the demand for broadband connectivity increases, it may be expected that TLs will be employed in access networks within ultra dense wavelength-division-multiplexed (UDWDM) systems that have many channels with spacing less than 50 GHz. Such systems would be able to provide significant capacity in order to maximize the number of users. This reduction in channel spacing, however, puts more stringent requirements on the devices used in the system. In terms of the TL module, the wavelength *or* frequency stability becomes very important, since even a small drift could cause serious cross-channel interference.

In this chapter, the possibility of using TLs in UDWDM wavelength packet switched networks is investigated. The experimental work presented is based around the same TL module [1] as used in Chapter 3. As previously demonstrated, in order to minimize interference with other channels, due to spurious output during the switching process, the laser output is blanked for ~60 ns after a transition between wavelength channels is initiated. After blanking, the module is specified to give an output within 15 GHz of the target wavelength channel. The integrated wavelength locker then locks the laser to the target wavelength. The wavelength locker comprises an etalon filter for wavelength monitoring followed by a servo-loop controller, as outlined in section 3.1.2.

Superior locking mechanisms exist that can better reduce the magnitude of wavelength drift and lock in a faster time [2]. These solutions, however, are more complex and costly. This is particularly so when used in tunable lasers as opposed to single frequency lasers, with the former requiring a frequency comb to provide a reference for all possible wavelength channels. The focus of this work is to examine the drift associated with an existing, practical locking mechanism that is likely to be used in initial TL modules. The instantaneous frequency drift of a TL module immediately after the blanking period is measured. The impact that such a drift would have on a neighboring data channel in a two-channel pseudo-UDWDM network when the channel spacing was set to 12.5 and 25 GHz is then examined. It is also investigated how performance degradation, encountered as a result of the measured frequency drift, can be mitigated to improve UDWDM system performance.

4.1 Tunable Lasers in Future Optical Access Networks

With the introduction of an increased number of broadband applications, the demand from both residential and business customers for increased bandwidth connectivity has continued to grow. With respect to optical access schemes this connectivity can be grouped into different levels based on the proximity of the fibre-end to the customer, and is, in general, referred to as fibre to the X (FTTx), with X representing the home, the business, the cabinet or the curb [3]. Optical access technology has best met this demand by using passive optical networks (PONs) to deliver fibre closer to the end user. In such schemes a single optical fibre from a local exchange, the optical line terminal (OLT), is shared over a number of optical network units (ONUs), with each ONU representing a customer or a group of customers.

In initial PONs the optical fibre from the local exchange fed a splitter with an individual fibre link to each ONU [4]. The bandwidth of the fibre was divided between each customer using a time division access protocol. Later versions incorporated limited use of coarse WDM to increase the network capability [5]. To

fully exploit the available bandwidth of the fibre, as has occurred in the core and metropolitan networks; future optical access networks may utilize DWDM techniques. The wavelength domain could be used as an overlay to TDM-PON, increasing the network capacity and capability to satisfy future growth in bandwidth demand [3]. As access networks ultimately serve a relatively small amount of customers in comparison to the larger metropolitan and core networks, large-scale cost sharing associated with the later will be reduced. Accordingly the cost effectiveness of increased capacity FTTx networks utilizing DWDM has attracted much interest from researchers.

In WDM/TDM hybrid PONs proposed in [6, 7] a wavelength selective branching device such as an AWG is used in place of a splitter to efficiently divide the fibre between the different ONUs. A dedicated wavelength is assigned to each ONU in such a way that a virtual point-to-point connection is established between the local exchange and the ONU. Multiple tunable lasers, based at the exchange and used as downstream transmitters, can be used to reduce costs and support network reconfigurability [8] – varying customer demand levels can be satisfied by dynamically allocating bandwidth to different ONUs by simply tuning the TL wavelength. Costs can be kept modest by using colourless or wavelength agnostic ONUs, in which reflective SOAs are used to modulate upstream information on to a continuous wave carrier, of the appropriate wavelength, generated by TLs at the local exchange [9, 10]. Additional network capacity may be grown gracefully by increasing the number of TLs at the exchange, and adjusting the number of time slots allocated to each customer. The network capacity can also be cost-efficiently increased by using spectrally efficient narrowly spaced UDWDM wavelength channels. This allows for an increased number of customers, and bandwidth utilization, while still operating on modest channel bit rates, thus reducing the ONU cost. Once again, with such narrow channel spacing, the frequency stability of the TLs used in such future access networks will be of paramount importance.

4.2 Tunable Laser Drift Characterisation

In [11], DWDM transmission results were presented showing the degradation of an adjacent channel on a 50 GHz spaced grid due to the thermal drift of an unlocked SGDBR TL during wavelength switching. The drift was caused by the over compensation of a temperature controller to the initial thermal drift from the tuning current injection. The drift was characterised over timescales of hundreds of microseconds to seconds, eventually stabilising from a max drift of ~7.5 GHz to within +/-3 GHz after 3.5 s. In subsequent work, with a DSDBR TL [12], the thermally induced wavelength drift was controlled with a phase section wavelength locker. After a locking time of 2 μs, Q factor degradation of <1 dB, demonstrating error free performance, was reported for a 50 GHz spaced set-up.

In the work presented here, a TL module with an integrated wavelength locker capable of locking in 200 ns is used. The magnitude and duration of the laser output frequency during this initial locking period is characterised. UDWDM system transmission experiments are then presented, ultimately demonstrating error free performance, even during wavelength locking, with a power penalty of ~1.1 dB at a reference BER of 1×10^{-9}. This represents a four-fold reduction in channel spacing to 12.5 GHz compared to the standard 50 GHz currently available, for systems employing tunable laser switching.

The optical output of the TL module is suppressed by the SOA blanking during the main switching transient. Upon emerging from this blanking period the wavelength locker is turned on to lock the optical output to the target ITU channel. After a time of 200 ns, measured from the start of the wavelength switch, the output is specified to settle and remain within +/-2.5 GHz of the target channel. This stability is sufficient for UDWDM systems; the frequency drift/evolution during the initial locker settling time may, however, adversely impact adjacent channels in such systems and thus will be the focus of the following experimental investigation. The optical output of the TL module is measured using two methods. Initial characterisation is performed using an optical filter as a frequency discriminator.

The results obtained are then verified using an optical self-heterodyning technique.

4.2.1 Optical Filter Technique

The frequency drift of the module output, after the end of the blanking period, was measured with a tunable optical filter. Using the experimental setup shown in Fig. 4.1, a detuned FBG filter, with a 3 dB bandwidth of 27.5 GHZ, was operated as a sloped frequency discriminator [13, 14]. This allowed for the conversion of the optical frequency drift to an optical power drift. Using a fast digital oscilloscope, the power through the filter, and falling on a photodiode, was measured as a function of time – thus giving a time resolved trace of the power drift of the TL output. A power reference measurement is also taken (indicated by the dashed line in Fig. 4.1) by recording the power falling on the photodiode with no filter included. This is used to compensate the previous power trace measurement for any power variation during the switching time, thus ensuring that variation in the trace is due only to frequency variation of the module output.

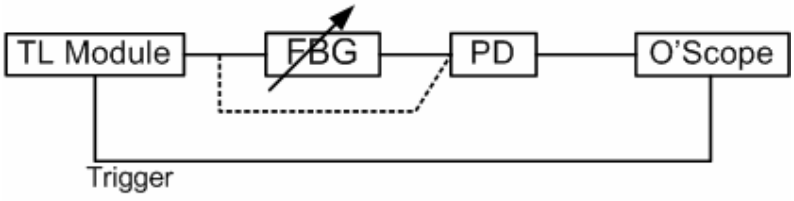

Figure 4.1 Experimental set-up used to measure the magnitude and duration of the frequency drift after the TL comes out of blanking using an optical filter as a frequency discriminator.

For a particular channel transition, the measurement was carried out with the TL settling into a target wavelength which was set at the middle of the logarithmic slope of the bandpass characteristic of the FBG (shown in Fig. 4.2); this is achieved by tuning the centre wavelength of the FBG. Operating at this point, further down the filter profile, gives an extended range over which the full extent of the frequency drift can be measured. This is in comparison with the work undertaken in [13, 14], and is deemed necessary given the relatively large frequency drift of +/-15 GHz specified for the TL module. This extended range can be seen by comparing

the range (represented by the horizontal lines on the filter profiles) offered by the logarithmic method (Fig. 4.2(a)) and the linear method (Fig. 4.2(b)). However, this increased range is at the expense of a lower signal-to-noise ratio and a more complex nonlinear wavelength drift to power transmission mapping. From the filter profile the power transmission as a function of frequency is known – this allows for the power to frequency conversion of the recorded trace to give the frequency drift of the TL output.

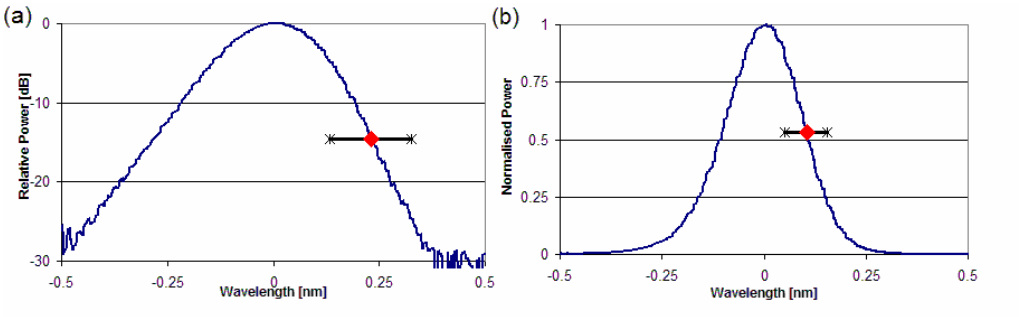

Figure 4.2 Frequency response of the FBG filter (a) using logarithmic scale, showing the positioning of the TL target wavelength (b) using linear scale.

The frequency drift measurement was performed for a number of channel transitions. The transition between Channel 42 (1548.915 nm) and Channel 52 (1544.924 nm) was found to have one of the larger drifts. The calculated frequency drift for this transition is presented in Fig. 4.3, which shows the frequency deviation of the module output from the target ITU channel as a function of time. As the TL emerges from blanking, it is ~6 GHz from the target channel. The wavelength locker can be seen to turn on ~30 ns after the TL comes out of blanking. The locker causes a fast fluctuation in output wavelength for a small period of time (~15 ns), after which the wavelength drift is characterized by a damped oscillation.

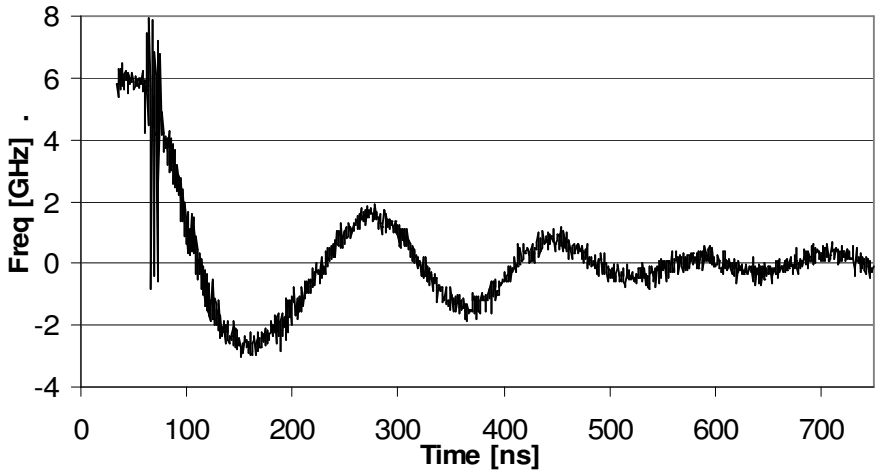

Figure 4.3 Measured frequency drift of TL module for channel transition 42-52 using tunable optical filter

4.2.2 Optical Self-Heterodyne Technique

A temporal frequency measurement technique presented in [15] is used to confirm the frequency measurement described in the previous section. Using a single tunable laser source an optical heterodyne system was set up using the experimental layout shown in Fig. 4.4. The output of a switching TL module was optically split into two paths before being recombined on a photo-detector. One of the paths was delayed using a length of fibre, while the other path was optically attenuated to ensure equal power upon recombination. Setting the delay duration greater than the laser switching time allowed the set up to operate as an optical self-heterodyne system, in which the delayed signal from the TL was essentially mixed with a continuous wave local oscillator, i.e. the TL already tuned to its target wavelength. For any frequency difference between the light signals detected at the photodiode, from each fibre output, a beating signal is generated. The frequency of this electrical signal corresponds to a difference in frequencies between the two signals. A low pass filter (LPF) was then used, to pass the beating signal only when below a certain margin (set by the LPF cut-off frequency), before recording a trace on an oscilloscope.

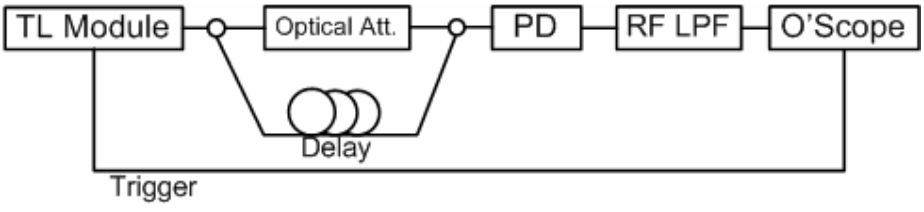

Figure 4.4 Experimental set-up used characterise the frequency drift after the TL comes out of blanking using an optical self heterodyne measurement.

For the oscilloscope trace presented in Fig. 4.5 the detected photocurrent was passed through a low pass filter with a 3 dB bandwidth of 117 MHz. This measurement is for the same channel transition as that presented in Fig. 4.3. Both figures represent approximately the same portion of the tuning cycle, with the time measured from within the blanking period. As the module emerges from the blanking period (at time T0) the heterodyne signal was of a frequency greater than 117 MHz (as is clearly presented in Fig. 4.3), therefore it was filtered out and no signal was observed on the oscilloscope. As the laser settles to its target wavelength the frequency of the heterodyne signal decreases and the filter passes the resultant RF signal. The laser crosses its target wavelength and overshoots four times before finally settling to its target at time T1.

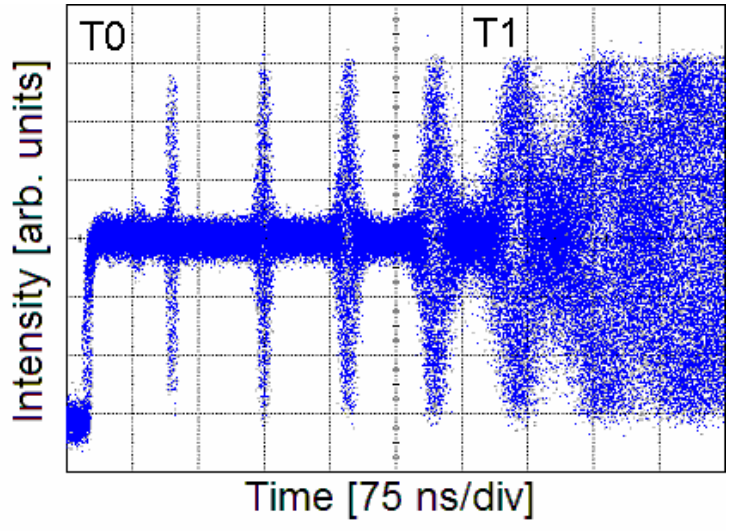

Figure 4.5 Frequency drift characterisation of TL module for channel transition 42-52 using self heterodyne technique

This measurement was repeated several times to give a discrete characterization of the time-frequency evolution of the laser tuning process. The electrical signal was filtered using a number of LPFs with different cut-off frequencies. The time it takes for the beating signal to settle was observed from each trace, thus giving the tuning time required to achieve stability at the different cut-off frequencies. These results compare well with the drift measurement using the FBG filter. This is evident from Fig. 4.6, in which the discrete measurements are given along with the magnitude of the wavelength drift measured using the FBG set-up.

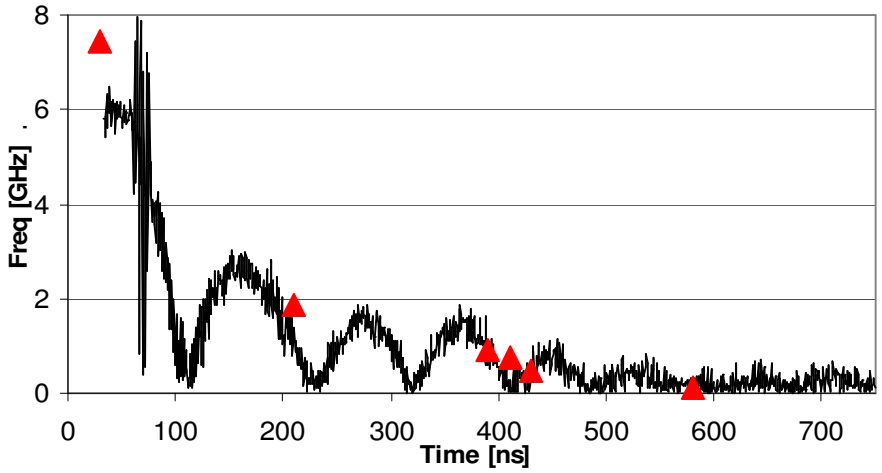

Figure 4.6 Discrete characterisation of the time-frequency evolution of the TL module for channel transition 42-52 using self heterodyne technique (▲) in comparison to measurement using optical filter (represented by the solid line)

4.3 Impact of Drift on UDWDM System

In the previous section a wavelength drift of the TL module was measured over the initial tens and hundreds of nanoseconds as the laser emerges from blanking and locks to the ITU target wavelength channel. This module drift could potentially cause the optical signal to fall inside the transmission band of, and corrupt, a neighbouring wavelength channel, when narrow channel spacing is used. The experimental set-up illustrated in Fig. 4.7 was used to evaluate the impact of TL module wavelength drift, during tuning, on an adjacent channel in a UDWDM

system. A two-transmitter test bed is used to simulate an array waveguide grating router based network, in which the interference from the TL module on an adjacent probe channel is investigated.

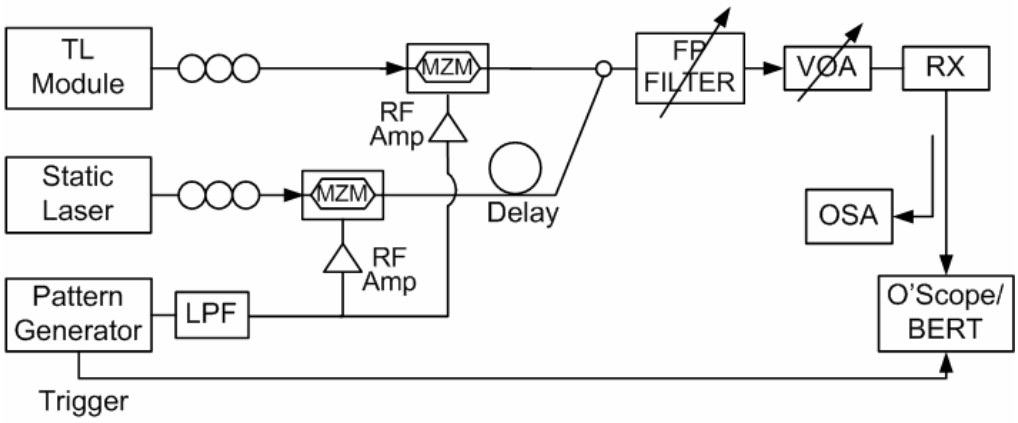

Figure 4.7 Two transmitter set-up used to investigate the effect of the measured wavelength drift on UDWDM transmission

4.3.1 Test Bed with 25 GHz channel Spacing

Initial investigation was performed for a channel grid with spacing of 25 GHz. The TL module was periodically switched in and out of channel 52 (1544.924 nm), using the same channel transition as is presented in section 4.2. A laser operating on a fixed wavelength, set 25 GHz away from the TL target channel at 1544.724 nm, was used as a probe channel. Each channel was externally modulated with an electrically amplified NRZ pseudo-random bit sequence generated by a pattern generator. A pattern length of 2^7-1 at a data rate of 2.5 Gbit/s was used. The same data was used for both lasers; it was therefore necessary to de-correlate the information carried in each channel. This was achieved by passing the probe channel through a fibre length of 3 m, which provided a delay of one quarter of the pattern length. The power of the fixed laser was set slightly higher than that of the TL module to allow for the loss over this fibre delay. The two power matched channels were then combined onto the same fibre using a 3 dB coupler.

One port of a 25 GHz spaced wavelength routing node was simulated by filtering the desired (probe) channel using an optical filter centred on the probe channel. A Fabry-Perot tuneable filter with a 3 dB bandwidth of 6 GHz was used. The demultiplexed probe channel was then passed through a variable optical attenuator (VOA) before entering the receiver, which consisted of an EDFA, an optical filter, a photodiode and an electrical amplifier. An oscilloscope and an error detector were used to examine the eye diagram and the BER of the detected channel. An optical spectrum analyser was used to monitor the FP filter operation and the signal spectrum at various points through out the set-up.

To quantify the impact of the module drift, the BER of the probe channel was measured as a function of the received optical power for various module switching configurations – when the interfering TL was (i) set to channel 42 (1548.915 nm) (>500 GHz away from filtered channel), (ii) set to channel 52 (25 GHz from filtered channel) and (iii) switching from channel 42 to channel 52. The TL was set to switch into channel 52 at a rate of 5 kHz.

As can be seen from the results presented in Fig. 4.8 there was a minimal power penalty (<0.1 dB) when the TL was static at channel 52 (i.e. 25 GHz from the probe channel) compared to when the TL was static at channel 42. This demonstrates that the optical filter was capable of selecting out a channel from a 25 GHz spaced DWDM system with no interference from an adjacent channel. When the TL was switching into channel 52, the adjacent channel, there was no additional power penalty or degradation in system performance. This is expected as at a channel separation of 25 GHz the measured drift of the TL as it comes out of blanking is too small to fall within the passband of the filtered channel.

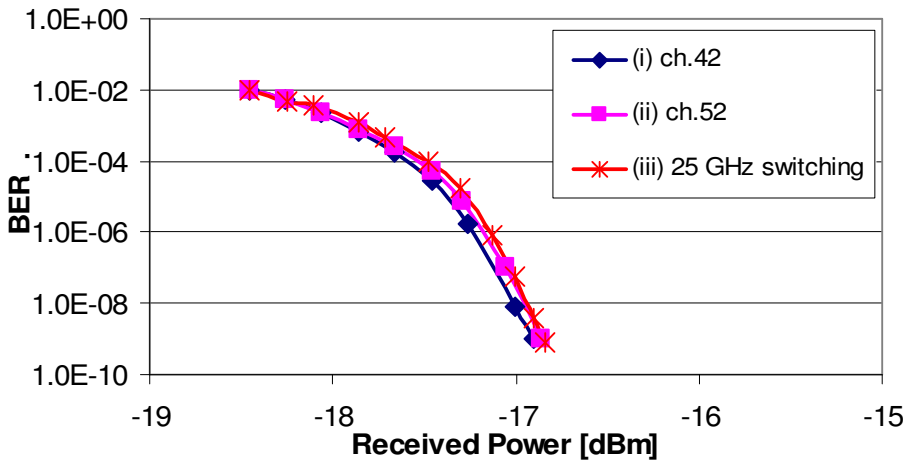

Figure 4.8 BER results on a probe channel in a 25 GHz spaced UDWDM test bed, using FP filter (3 dB bandwidth of 6 GHz), for different TL module channel settings, (i) static at distant channel, (ii) static at adjacent channel, (iii) switching into adjacent channel.

In earlier work an additional power penalty was observed due to interference from the switching TL module [16]. This work used a very similar set-up as is presented above – using the same type of TL module [1], the same data rate and the same switching time. An FBG filter with a 3 dB passband of 15 GHz was, however, used to demultiplex the probe channel. This wider passband, more typical of that found in 25 GHz AWG routers [17], resulted in a power penalty of around 1.5 dB at a reference BER of 1×10^{-9} when switching into the adjacent channel. This is due to the small amount of errors created by the frequency drift of the TL entering the passband of the FBG. As can be seen from the measured BER results given in Fig. 4.9, the penalty reduced and was eventually dominated by the errors due to thermal noise of the receiver at low received powers. It should be noted that, as with the FP filter, there was no significant power penalty for the measurements with the TL module static at a channel adjacent to the probe channel.

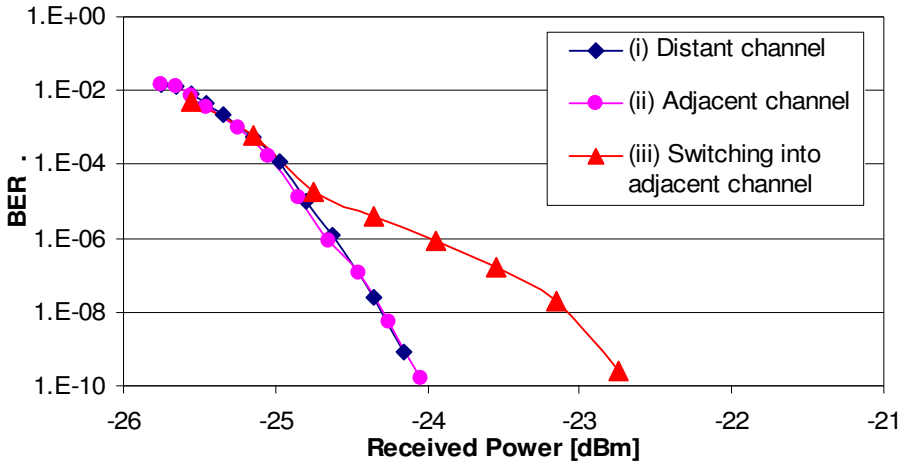

Figure 4.9 BER results on a probe channel in a 25 GHz spaced UDWDM test bed, using FBG filter (3 dB bandwidth of 15 GHz), for different TL module channel settings, (i) static at distant channel, (ii) static at adjacent channel, (iii) switching into adjacent channel.

4.3.2 Test Bed with 12.5 GHz Channel Spacing

To investigate the effect of the frequency drift on a 12.5 GHz channel spaced system, the experimental set-up (given in Fig. 4.7) was slightly modified. The wavelength of the static laser was tuned to 1544.824 nm, to operate as an adjacent probe channel 12.5 GHz away from the TL module target wavelength channel. The centre wavelength of the Fabry-Perot filter was also tuned accordingly. The BER measurements of the filtered channel vs. received optical power were repeated using the same TL configurations as for the 25 GHz channel spacing analysis.

These results along with the switching result from the 25 GHz spaced measurements are presented in Fig. 4.10. There was only a minimal power penalty (<0.1 dB) when the TL was static at channel 52 (i.e. 12.5 GHz from the fixed channel) compared to when the TL was static at channel 42, thus demonstrating the suitability of the optical filter for 12.5 GHz channel spacing. However when the TL switches between channels 42 and 52 the wavelength drift, after blanking, degrades the system performance and introduces an error floor at a BER of 10^{-7}.

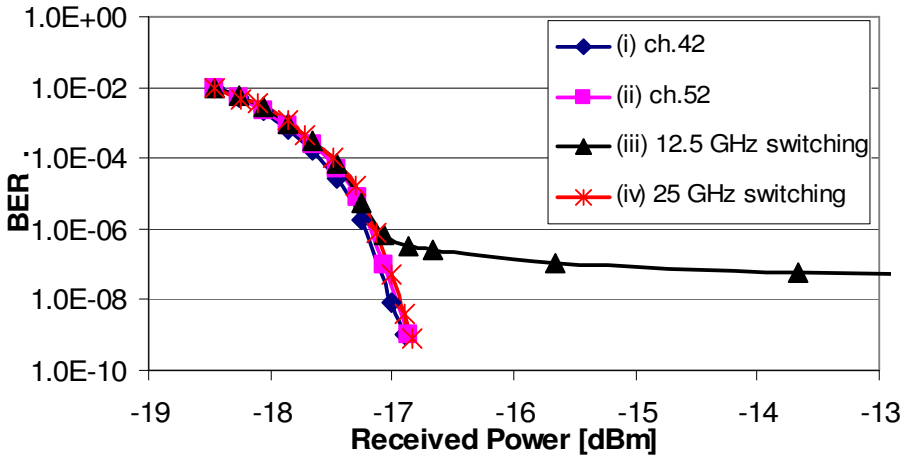

Figure 4.10 BER results showing impact of locker turn on transient on a probe channel in a 12.5GHz spaced UDWDM test bed for different TL module channel settings, (i) static at distant channel, (ii) static at adjacent channel, (iii) switching into adjacent channel. (iv) For comparative purposes the result is also given for switchcing into an adjacent channel in a 25 GHz spaced set-up.

The data signal was not gated during these tests, so that the BER measured on probe channel was dominated by the periodic errors caused by the switching channel. These errors were aggregated over the full switching period, made up of (a) the time at the beginning of the data transmission when the TL is settling into channel 52, (b) the time when the TL is settled into channel 52, (c) the time when the TL is at channel 42 and (d) the time when the TL is blanked. The switching TL causes a burst of errors only at the beginning of the data stream, as it emerges from blanking and begins to settle into channel 52. At this time the drift is large enough such that it enters the filter passband of the fixed channel. As the TL approaches its target wavelength the errors reduce, eventually giving no errors when the TL is within ~3 GHz of its target wavelength.

The measured wavelength drift of the TL module as it emerges from blanking is small enough not to cause problems in 50 GHz channel spaced DWDM networks. However, it is shown that as channel spacing decreases this issue becomes more important, resulting in power penalties at 25 GHz spacing and critical error floors at

12.5 GHz spacing. It is expected that this system degradation will become even greater if the bit rate of the data carried by the laser is increased. Thus if the TL can be locked with less drift, this interference can be reduced. The wavelength transient could potentially be reduced by optimising the servo loop controller settings. The TL module, however, does not allow for access to the control electronics and thus this is not an option for the investigation presented here. Alternatively, the impact of increasing the blanking time duration on the locker turn of transient was investigated, and is presented in the following section.

4.4 Extended Blanking

The laser blanking time, after the wavelength transition is initiated, was increased from the default value of 60 ns. This was done in anticipation that the module output would be closer to the ITU target wavelength channel upon emergence from the blanking period. The drift of the TL module as it comes out of blanking was measured for the channel transition 42 to 52, using various blanking times. The frequency drift using an adjusted blanking time of 260 ns, measured using the optical filter technique described in section 4.2.1, is presented in Fig. 4.11.

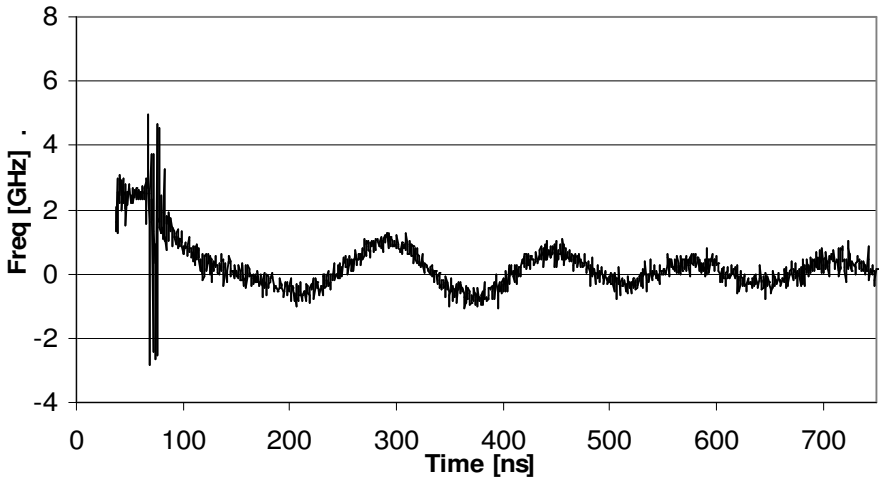

Figure 4.11 Measured frequency drift of TL module, for channel transition 42-52 with extended blanking time of 200 ns, using tunable optical filter.

It can be seen that using an extended blanking time resulted in an expected reduction in the frequency drift of the laser output – the magnitude of the drift is halved in comparison with the drift presented Fig. 4.3. Once the blanking time ends, and the module begins to emit light, the output is ~3 GHz from the target channel. The wavelength locker is delayed accordingly, and as previously can be seen to turn on ~30 ns after the blanking time ends. The locker, again, causes a fast fluctuation in output wavelength after which the wavelength settles to its target wavelength.

The same experimental set-up and method, as used in section 4.3, was used to investigate if this reduction in initial wavelength drift improves the performance of an adjacent channel in a 12.5 GHz spaced system as the TL module transitions. The BER results presented in Fig. 4.12 demonstrate such an improvement. With the extended blanking time the system performs with a residual power penalty of ~1.1 dB (relative to the case when the TL laser is static), at a reference BER of 10^{-9}, due to interference from the adjacent TL channel. This is in comparison with an error floor at a BER of 10^{-7}, shown in Fig. 4.10, for the case when the default blanking time is used. The best system performance was achieved with this setting of 260 ns, and this is believed to be the optimal extended blanking time as the power penalty did not reduce by further increasing the blanking time. This supports the hypothesis that beyond this blanking time, the power penalty measured is primarily due to the fast fluctuation in frequency drift when the locker turns on.

Although extending the module blanking time can reduce the initial wavelength drift, thus improving UDWDM system performance, it is not an ideal solution as it also results in a corresponding increase in the effective TL switching time, thereby reducing network throughput. This will be particularly limiting in future optical packet switched systems, which will require the fastest tuning times. An alternative solution may be to reduce the impact of the drift, rather than reducing the drift itself. This idea is explored in the following section by using sub-carrier

multiplexing.

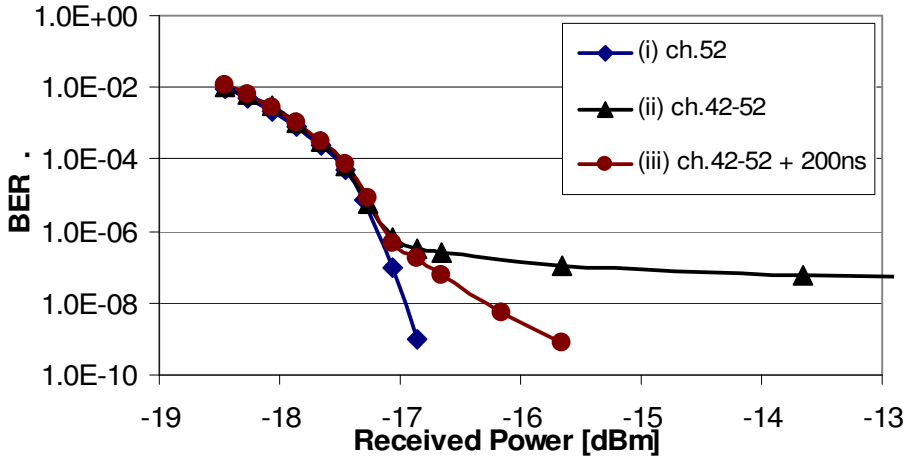

Figure 4.12 BER results showing impact of locker turn on transient on a probe channel in a 12.5GHz spaced UDWDM test bed for different TL module channel settings, (i) static at adjacent channel, (ii) switching into adjacent channel with default blanking duration (iii) switching into adjacent channel with blanking duration extended by 200 ns.

4.5 Sub-Carrier Multiplexing

The use of sub-carrier multiplexing (SCM) and relatively simple electrical heterodyne detection [18] was investigated for a 12.5 GHz spaced system. This SCM scheme is used as a means to reduce the impact of the initial wavelength drift on an adjacent channel. Using a similar two transmitter test-bed to that presented in Fig. 4.7, the impact of the module wavelength drift on an adjacent channel was examined for a set-up employing conventional base-band (BB) amplitude shift keying intensity modulation and for a set-up using SCM, displayed respectively in Fig. 4.13 (a) and Fig 4.13 (b). The SCM signal is demodulated with a mixer based analogue circuit using the same local oscillator (LO) as was used at the transmitter, to emulate performance from a phase locked LO at the receiver. Both systems used the same optical filter with bandwidth of 10.8 GHz, as shown schematically in Fig. 4.14; this determines the detection bandwidth for the BB case.

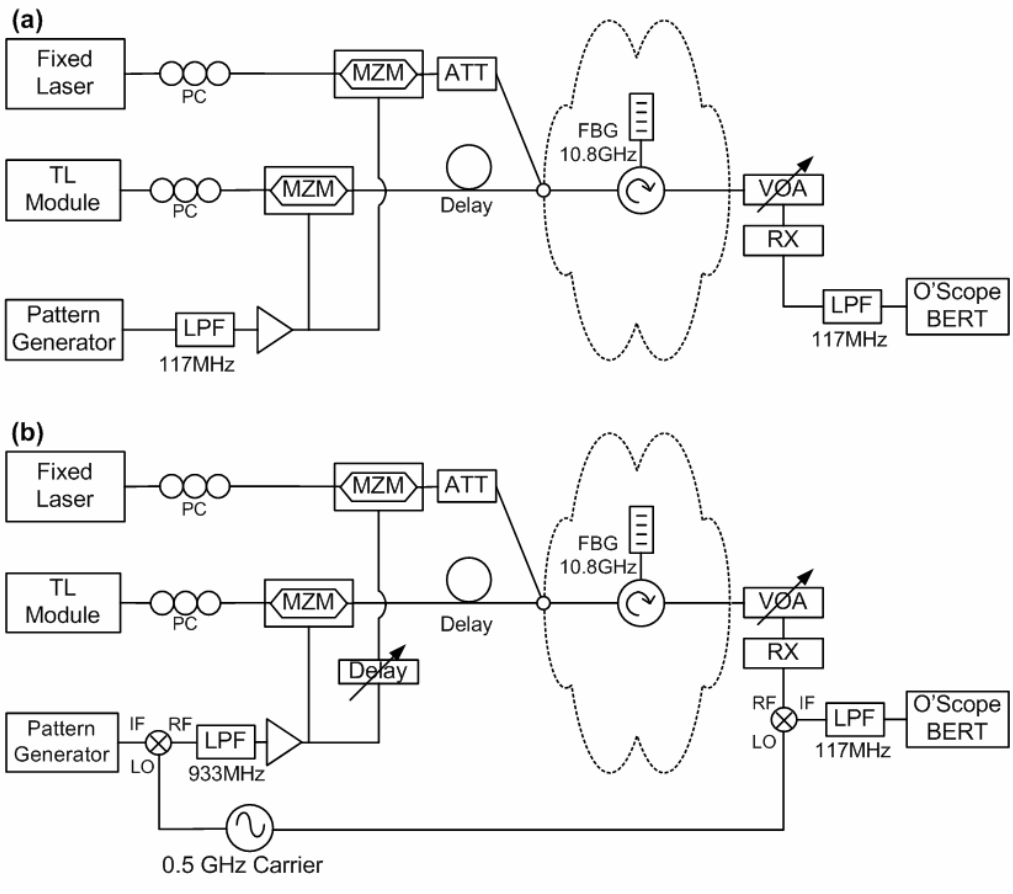

Figure 4.13 (a) Base-band experimental set-up (b) Sub-carrier experimental setup

Since the dynamic drift of the TL module (shown by a dashed line) is sufficiently large to make the signal fall inside the optical filter, the BB detected data (Fig. 4.14(a)) will experience interference due to the intensity demodulation used. In the SCM case (Fig. 4.14(b)), however, in-band interference does not impact the detected data signal as the demodulation process is phase selective and BER degradation only becomes significant if the interferer falls within the detection bandwidth of the demodulation circuit. In the tested scenario with short data bursts that periodically use the channel adjacent to the static channel, it is expected that SCM will out perform the BB system. The goal of this investigation, then, is to quantitatively compare SCM and BB systems with an aggressive switching regime.

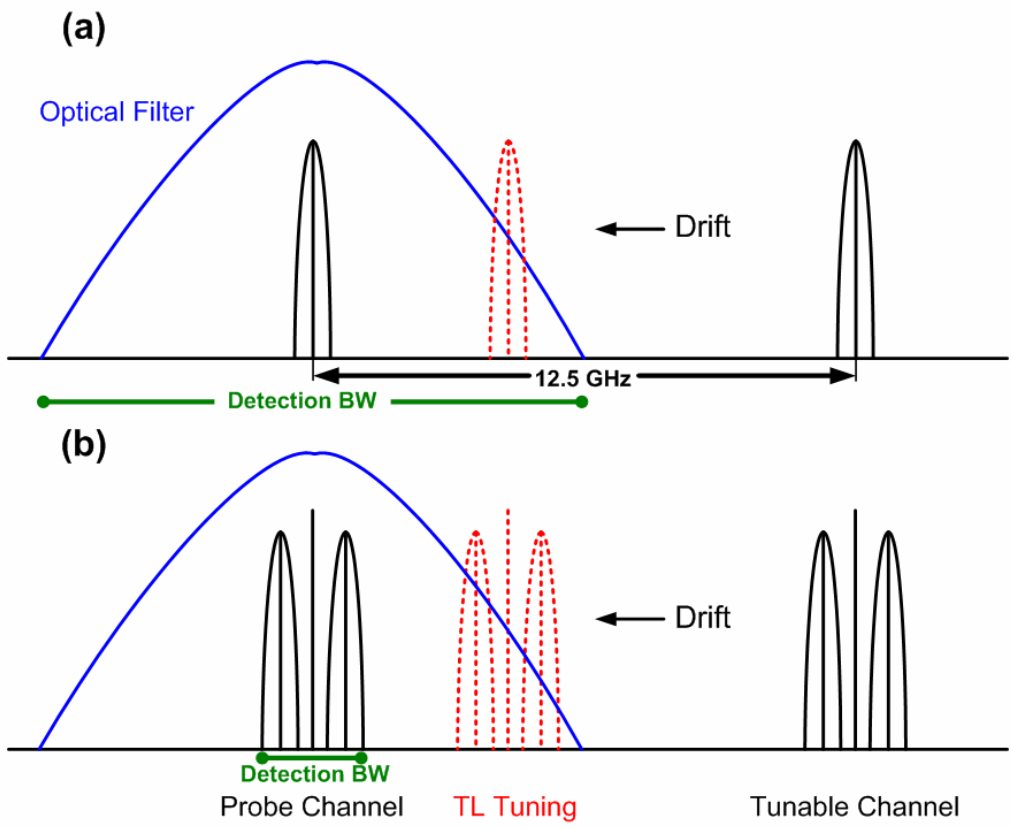

Figure 4.14 (a) Base-band optical spectra scheme (b) Sub-carrier multiplexed optical spectra scheme

4.5.1 Experimental Procedure and Results

As in the experiments described in section 4.3, a laser operating on a fixed wavelength represents a probe channel to be filtered out, and an interferer is produced by using a TL module that switches periodically between a distant channel and a channel adjacent to the probe channel. The same channel transition was used, with the TL module switching into channel 52 from channel 42 at a rate of 500 kHz. The fixed laser positioned 12.5 GHz from channel 52 to simulate an UDWDM system. Both lasers were externally modulated, using 2.5 GHz electro-optic modulators biased at quadrature, with a 155 Mbit/s NRZ PRBS pattern of length of 2^7-1. The interfering channel was de-correlated using 40 m of fibre, and the power levels were matched using an optical attenuator.

One port of a 12.5 GHz spaced wavelength routing node was simulated by filtering

the probe channel using a Fibre Bragg Grating (FBG) with a bandwidth of 10.8 GHz. The output optical spectrum, measured using an OSA, of the filtered probe channel with the interferer in static mode 12.5 GHz away is given in Fig. 4.15. The demultiplexed channel was then passed through a variable optical attenuator before entering the direct detection receiver which consists of an EDFA, an optical filter, a photo diode and an electrical amplifier. After detection the BB signal was filtered using a LPF and fed directly to an error detector. As a reference, base-band data was transmitted using a 117 MHz electrical filter in the transmitter, and processed in the receiver with an identical low pass filter (Fig. 4.13 (a)). For the SCM system, at the transmitter the 155 Mbit/s data was binary phase shift keyed (BPSK) modulated onto a 500 MHz local oscillator before double side band electro-optic modulation, whilst the received signal was demodulated to base-band using a second mixer before low pass filtering (Fig. 4.13(b)). A variable electrical delay was used before modulation to set the RF carrier of the probe channel to be in quadrature with that of the interferer.

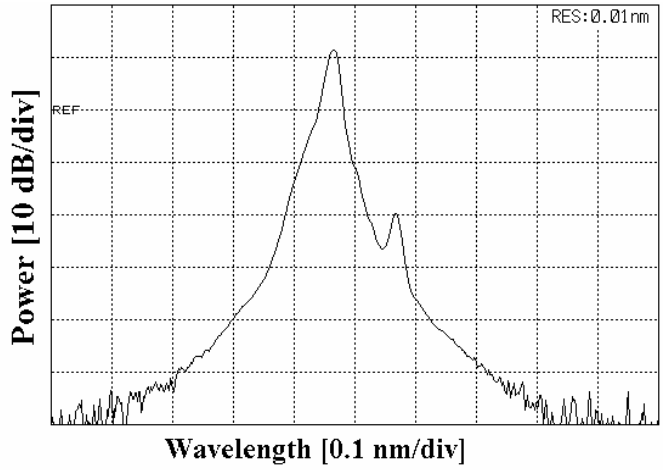

Figure 4.15 Optical spectrum of the filtered probe channel using a FBG fiter (3dB bandwidth 10.8 GHz) with the TL module, in static mode, 12.5 GHz away

In order to characterize the adjacent channel interference due to the wavelength drift of the TL the Bit Error Rate (BER) of the probe channel (static laser) was measured for three different modes of TL operation: (i) when TL was static at

channel 42 (>500 GHz away from the probe channel), (ii) when TL was static at channel 52 (12.5 GHz away from the probe channel) and (iii) when TL was switched repetitively between channel 42 and 52 every 1 μs. The BER vs. received optical power plot for the BB data is shown in Fig. 4.16. It can be seen that there is a negligible power penalty on the desired laser channel when the TL is in static mode at channel 52 (12.5 GHz away) in comparison to when it is at channel 42 (512.5 GHz away). It can also be seen that, when the TL is switched repetitively as described above, wavelength drift of the TL causes an adjacent channel interference, which places an error floor on the performance characteristic of the signal above 1e-4.

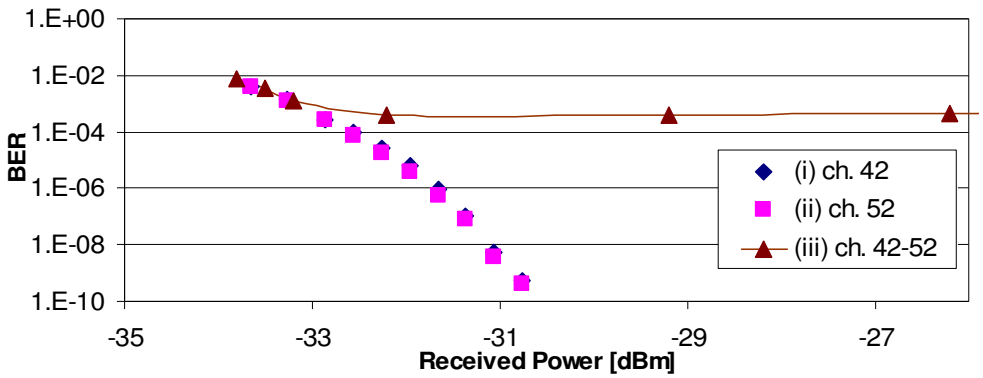

Figure 4.16 BER results showing impact of locker turn on transient on a probe channel in a 12.5GHz spaced base-band UDWDM test bed for different TL module channel settings, (i) static at distant channel, (ii) static at adjacent channel, (iii) switching into adjacent channel.

The same BER measurements were performed for the SCM data and are presented in Fig. 4.17. In this case error free performance was achieved in all three cases, with a residual power penalty of 1.2 dB at a reference BER of 1e-9 replacing the error floor when the interfering channel is switched repetitively.

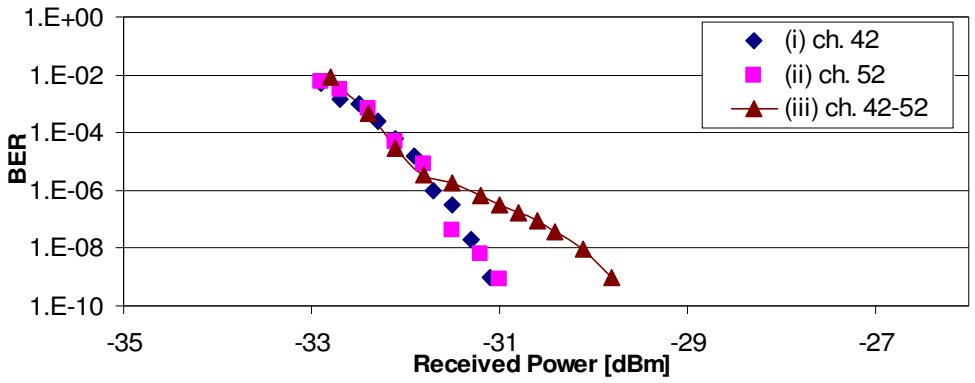

Figure 4.17 BER results showing impact of locker turn on transient on a probe channel in a 12.5GHz spaced sub-carrier multiplexed UDWDM test bed for different TL module channel settings, (i) static at distant channel, (ii) static at adjacent channel, (iii) switching into adjacent channel.

These results show that the impact of the wavelength drift from the TL module is significantly reduced for the SCM data (Power Penalty of 1.2 dB at 1e-9) compared to the BB data (BER > 1e-4). This is despite the separation between the SCM signals being even smaller than that between the BB data. The improved performance can be explained as follows: The 3 dB bandwidth of the optical filter used to select out the probe channel is 10.8 GHz, and based on the drift measurement, it is believed that the light from the interfering TL module will drift within this filter's pass band as the module tunes to an adjacent wavelength channel. For the BB DWDM system any light that leaks through the filter will interfere with the data carried by the probe channel. However, in the case of SCM DWDM system, the interference is suppressed by the phase selective heterodyne detection at the receiver. The drift has to fall within the detection bandwidth of the SCM system, resulting in spectral overlap of the side bands of the two lasers, before significant degradation of the quality of the signal transmitted by the probe laser is observed.

These results indicate that using SCM in a low bit rate DWDM access PON with TLs would enable wavelength channels to be more closely spaced without a significant increase in ONU complexity. The Korean experiences discussed in [19]

show the real deployment of relatively low bit rate systems and, of particular interest here, discussed the use of 125 Mbit/s WDM-SCM-PON systems for residential access.

Conclusion

The magnitude and duration the TL module wavelength drift, as it emerges from the blanking and locks into its target wavelength, has been investigated. The measured drift (7.5 GHz) has been shown to cause power penalties for 25 GHz channel-spaced UDWDM set-ups. However, as the channel spacing decreases this issue becomes more important, resulting in critical error floors at 12.5 GHz spacing due to cross-channel interference. Two approaches, the use of an extended blanking time and the use of sub-carrier multiplexed transmission, have been demonstrated to overcome this drift, and allow for error free transmission in a 12.5 GHz spaced system. These results demonstrate the feasibility of using TLs at the local exchange in PONs using very narrow channel spacing, thus allowing for an increased number of users on a single fibre.

References

[1] Intune AltoNet 1200 FTL Tx Module [Online]. Available: http://www.intunenetworks.eu/site/

[2] C. C. Renaud, M. Duser, C. F. C. Silva, B. Puttnam, T. Lovell, P. Bayvel, and A. J. Seeds, "Nanosecond channel-switching exact optical frequency synthesizer using an optical injection phase-locked loop (OIPLL)," *IEEE Photon. Technol. Lett*., vol. 16, pp. 903–905, Mar. 2004.

[3] R. Davey, J. Kani, F. Bourgart, and K. McCammon, "Options for future optical access networks," *IEEE Commun. Mag.,* vol. 44, pp. 50-56, Oct. 2006.

[4] ITU-T, Recommendation G.983.1, "Broadband optical access systems based on Passive Optical Networks (PON)," Jan. 2005.

[5] F.J. Effenberger, H. Ichibangase and H. Yamashita, "Advances in broadband passive optical networking technologies," *IEEE Commun. Mag.,* vol. 39, pp.118-124, Dec. 2001.

[6] Fu-Tai An, Kyeong Soo Kim, David Gutierrez, Scott Yam, Eric (Shih-Tse) Hu, Kapil Shrikhande and Leonid G. Kazovsky, "SUCCESS: A next-generation hybrid WDM/TDM optical access network architecture," *J. Lightw. Technol.,* vol. 22, pp. 2557-2569, Nov. 2004.

[7] C. Bock, J. Prat and S. D. Walker, "Hybrid WDM/TDM PON using the AWG FSR and featuring centralized light generation and dynamic bandwidth allocation," *J. Lightw. Technol.,* vol. 23, pp. 3981-3988, Dec. 2005.

[8] Fu-Tai An, Kyeong Soo Kim, Yu.-Li. Hsueh, Matthew S. Rogge, Wei-Tao Shaw and L. G. Kazovsky, "Evolution, challenges and enabling technologies for future WDM-Based optical access networks" presented at *2nd Symposium on Photonics, Networking and Computing*, Cary, NC, Sep. 2003, pp. 1449-1453.

[9] Ton Koonen, "Fiber to the home/fiber to the premises: what, where, and when?," *Proc. IEEE*, vol. 94, pp. 911–934, May 2006.

[10] H. Takesue, T. Sugie, "Wavelength channel data rewrite using saturated SOA modulator for WDM networks with centralized light sources," *J. Lightw. Technol.,* vol. 21, pp. 2546-2556, Nov. 2003.

[11] B. Puttnam, M. Dueser and P. Bayvel, "Experimental investigation of the signal degradation in WDM transmission through coherent crosstalk caused by a fast tunable SG-DBR laser," in *Proc. Optical Fiber Commun. Conf. and National Fiber Optic Eng. Conf. (OFC /NFOEC 2005),* Anaheim, Mar. 2005, vol. 3, pp. 444-446.

[12] B. Puttnam, M. Dueser, B. Thomsen, P. Bayvel, A. Bianciotto, R. Gaudino, G. Busico, L. Ponnampalam, D. Robbins and N. Whitbread, "Burst mode operation of a DS-DBR widely tunable laser for wavelength agile system applications," in *Proc. Optical Fiber Commun. Conf. and National Fiber Optic Eng. Conf. (OFC/NFOEC 2006),* Anaheim, Mar. 2006, vol. 24, pp. 1-3.

[13] J.E. Simsarian and Liming Zhang, "Wavelength locking a fast-switching tunable laser," *IEEE Photon. Technol. Lett*., vol. 16, pp.1745-1747, Jul. 2004.

[14] V. Polo, A. Ausiro, J. Prat and G. Junyent, "GCSR laser frequency drift compensation using optimized current waveform on one single electrode," in *Proc. 7th Inter. Conf Transparent Optical Networks (ICTON 2005),* Barcelona , Jul. 2005, vol. 2, pp. 17-20.

[15] H. Joseph and D. Sadot, "A novel self-heterodyne method for combined temporal and spectral high-resolution measurement of wavelength transients in tunable lasers," *IEEE Photon. Technol. Lett*., vol. 16, pp. 1921–1923, Aug. 2004.

[16] E. Connolly, A. Kaszubowska-Anandarajah and L.P.Barry, "Cross channel Interference due to wavelength drift of tuneable lasers in DWDM networks," *Proc. Inter. Conf Transparent Optical Networks (ICTON 2006),* Nottingham, Jun. 2006, vol. 4, pp. 52–55.

[17] Yoon-Suk Hurh, Gyo-Sun Hwang, Jin-Young Jeon, Kyung-Goo Lee, Kyung-Woon Shin, Sang Soo Lee, Keon Young Yi, and Jae-Seung Lee, "1-

Tb/s (100×12.4 Gb/s) transmission of 12.5GHz-spaced ultradense WDM channels over a standard single-mode fiber of 1200 km," *IEEE Photon. Tech. Lett.,* vol. 17, pp. 696-698, Mar. 2005.

[18] C. Bock, M.P. Thakur, C. Arellano, J.J. Lepley, I. Tsalamanis, S.D. Walker and J. Prat, "Wavelength independent RSOA-based ONU for FTTH PON implementation of switched Ethernet services," in *Proc. Eur. Conf. Optical Commun. (ECOC05),* Glasgow, Sep. 2005, vol. 1, pp. 85-86.

[19] C-H. Lee, S-M. Lee, K-M. Choi, J-H. Moon, S-G. Mun, K-T Jeong, J-H Kim and B Kim, "WDM-PON experiences in Korea," OSA J. Opt. Networking, Vol. 6, pp. 451-462, May 2007.

Chapter 5 – Tunable Lasers in SCM Optical Labelled Switched System

In the previous chapter the use of fast tunable laser modules in UDWDM systems was investigated. The modules were used to provide narrowly spaced wavelength channels carrying relatively low data rates, typical of access networks. This chapter is concerned with DWDM transmission in future high capacity "backbone" or core networks, which transmit large amounts of information between large population centres. Deployed networks of this type utilize wider channel spacing, capable of supporting up to 128 channels on a 50 GHz grid or 64 channels on a 100 GHz grid, with individual channels supporting respective data rates of up to 10 Gbit/s and 40 Gbit/s [1]. The challenge of the core network, to more efficiently meet the increased future demand, has led to the development of architectures such as optical burst switching (OBS) [2] and optical packet switching (OPS) [3, 4]. In such schemes electrical processing of the payload traffic is relegated to the network edges, and the payload is kept in optical format during its time in such "all optical" networks. This is done to increase traffic transparency and overcome the potential mismatch between the fibre capacity and optical-electronic-optical processing speeds required for cross connects in conventional intermediate network nodes.

As in the more modest access networks discussed in Chapter 4, OPS traffic can be transmitted on destination specific wavelengths and wavelength filtering can to be used for traffic forwarding. Fast wavelength tunability at internal nodes allows for an added level of intelligence and autonomy to be incorporated into the optical network. As with internet protocol (IP) packets in the electronic domain, the intelligence is provided by each individual optical packet carrying its own routing information. At intermediate nodes a dynamic wavelength routing decision can be

made based on this packet information to efficiently forward the payload to its destination. This allows for the more efficient use of network capacity and resources.

5.1 Optical Label Switching

Pure OPS in which header recognition, processing and control are performed optically for each packet is beyond the reach of current OPS test beds, with optical signal processing still in its infancy, there is however ongoing research into the area [5]. Current OPS implementations therefore combine optical switching and transport with electronic control and processing. In order to enable such OPS networks optical label switching (OLS) has been proposed [6]. This involves the separation of the optical packet, and the routing information while within the OPS network, with the former transmitted as the payload and the latter transmitted as an associated optical label. The payload is kept in the optical format throughout the network, thus allowing for transparency of the payload data rate, protocol and modulation format. The shorter optical label can be transmitted at a lower data rate for low cost processing with readily available electronics at intermediate network nodes, thus allowing for optical switching of the payload data to overcome potential electronic bottlenecks.

In such OLS networks when IP packets from the client networks arrive at the "ingress" node the IP header is examined and a destination dependent optical label and wavelength are assigned to the packet. Using a fast tunable laser the IP packet and its optical label are transmitted into the OPS network on the appropriate wavelength. At each node a portion of the signal is tapped and the optical label is extracted for processing. Label swapping [7] can be used at this stage to update the routing information. This allows for better network scalability [8] but will add to node cost and complexity in comparison to a simpler deterministic routing algorithm scheme in which the original label is kept. The optical packet can be converted to a new wavelength, determined by the processed label information, to allow for routing to the next node. This can be achieved by setting a fast tunable

laser, and using, for example, a semiconductor optical amplifier (SOA) based wavelength converter [9, 10]. On reaching its destination "egress" node at the other side of the core network, the optical payload is converted back to electronic format and the IP packet is routed as normal using electronic routing hardware.

5.1.1 Optical Label Encoding

Several different techniques for optical label coding have been reported, for either label swapping or deterministic routing algorithms, with the technique used influencing the node architecture and general system performance [11, 12]. The main labelling implementations are bit-serial, WDM, orthogonal modulation and SCM.

- In the bit-serial approach the payload and label at base-band are time division multiplexed together and are transmitted on the same wavelength channel with a guard-band used for separation. This method offers simple transmission with low interference between payload and label, however the need for strict time synchronisation adds to receiver complexity.
- WDM labelling involves the transmission of the labels on a single or multiple dedicated label wavelength channels. The use of individual transceivers for label and payload channels allows for simple label processing, however this is at the cost of a high component count and poor spectral efficiency. Chromatic dispersion can cause timing misalignment of the payload and label over large distances, due to different propagation speeds of various wavelength channels in the fibre.
- In orthogonal modulation labelling the payload and the label are modulated onto different dimensions of the optical carrier. The label could be phase or frequency modulated, while the payload could be intensity modulated onto the same wavelength channel. This offers very good spectral efficiency, although crosstalk between the payload and the label is an issue and a compromised payload extinction ratio is required to maintain label presence throughout.
- For SCM labelling the label is modulated onto a sub-carrier but within the

same wavelength channel bandwidth of the payload, which is transmitted at base-band.

SCM labelling is used for the experimental work presented in this chapter.

SCM Labelling

Optical SCM labels are one of the possible methods for label coding [8, 13, 14, 15]. The label data is placed on a radio-frequency sub-carrier and used to intensity modulate the laser resulting in two sidebands containing the label information, centred on the optical carrier, which contains the payload data. The SCM label can be read by detecting the entire multi wavelength signal and then down converting the label [8], or by extracting the label using an optical bandpass filter and detecting it directly [16]. The advantages of SCM labels over other methods are that they are very easily generated and detection is simple. Also, there are no strict timing and synchronisation requirements. However, the technique is less spectrally efficient than other methods and SCM labels suffer both from dispersion-induced fading, and from inter-modulation distortion, which can lead to degradation of the label signal.

A spectrally efficient SCM scheme based on optical carrier suppression and separation (OCSS) is presented in [17]; however this requires three Mach Zehnder modulators (MZM) at the transmitter. In this chapter a novel scheme for spectrally efficient optical sub-carrier labelling, which requires only a single MZM, is proposed and demonstrated using a single channel experimental set-up. This scheme is then employed in a 100 GHz spaced DWDM subsystem to investigate the detrimental effect that switching events of a tunable laser module may have on such a system. Degradation in system performance of a static channel, as a transmitter is tuned into an adjacent channel, is characterized in terms of the frequency drift of the tunable laser using time resolved BER measurements.

5.2 Transmitter

The transmitter set-up used in the following experimental work, to enable spectrally compact label controlled switching with low system penalty, is presented in Fig. 5.1. This is a novel scheme for deterministic optical sub-carrier labelling based around the use of single MZM driven by a combined electrical drive signal consisting of the label and payload data. This approach compares favourably to the use of independent payload and label modulation in series [18], as it does not require a compromised payload extinction ratio to avoid label degradation. The scheme enables the simultaneous generation of an amplitude modulated phase shift keyed (AM-PSK) payload and a non-return to zero (NRZ) sub-carrier multiplexed label, offering a compact spectrum compatible with a 40 Gbit/s payload data on a 100 GHz channel spacing grid. Payload receiver sensitivities between -26 and -30 dBm, requiring approximately 10 dB less optical power in the payload compared to the OCSS presented in [17], are demonstrated. Low crosstalk measured between the payload and labels allows for the use of a high data rate (2.5 Gbit/s) label, ensuring good address scalability when using a deterministic routing algorithm. It is also anticipated that the AM-PSK payload will offer additional advantages such as high dispersion tolerance.

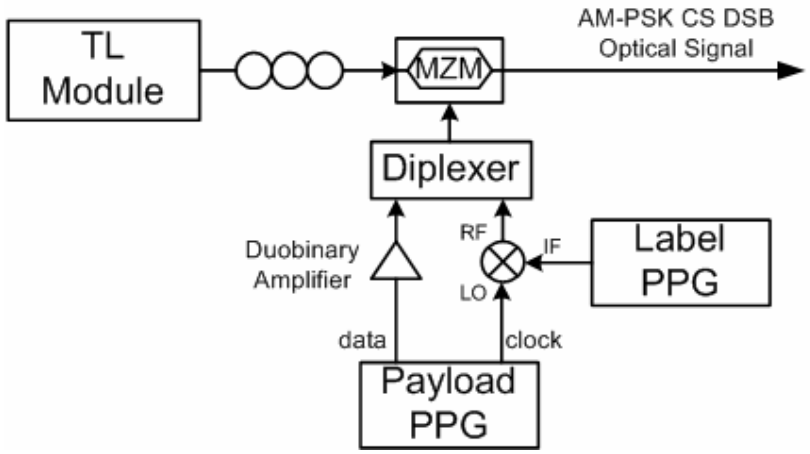

Figure 5.1 Single-modulator transmitter set-up for payload signal using SCM optical labelling

A TL module [19] of the same type as was used in the experiments presented in the previous chapters is used as the optical source for the transmitter. The MZM used to externally modulate the laser is driven by the combination of the payload and label data. To maintain a high payload data rate, while at the same time transmitting labels, it was necessary to use spectrally efficient modulation of the optical source. In this way, the transmitter set-up used allows for the enhanced network flexibility and capacity utilization offered by labelling without compromising the individual data rate per channel.

5.2.1 Electrical Signal

A spectrally compact electrical payload signal was achieved by passing NRZ digital data from the Payload pulse pattern generator (PPG) through a duobinary amplifier, which converts the two-level electrical signal into a multi-level electrical duobinary signal through extreme low pass filtering (LPF). Duobinary coding has previously been used in [20] to increase the spectral efficiency of a packet routing system. The filtering, accounting for the reduced spectral width, can be achieved through digital bit delay and add or through the use an electrical LPF with a 3 dB bandwidth of approximately 25 % of the NRZ data rate [21]. In this way each binary NRZ data bit, “0” or “1”, is correlatively mapped onto a three-level duobinary symbol, “0”, “1” or “2”, depending on the preceding data bit. An example of a three level electrical eye generated by passing a NRZ PRBS at data rate of 418 MHz through a LPF with a 3 dB cut off of 117 MHz is given in Fig. 5.2.

The compact payload spectrum enables a closely spaced sub-carrier signal to be used. This SCM signal was produced by amplitude modulating a base band NRZ label from the Label PPG onto a high frequency clock signal using an RF mixer. The clock signal from the Payload PPG was used, thus synchronising the sub-carrier to the data signal, enabling closer spectral separation between the label and the payloads by having a fixed relationship between them. The electrical duobinary payload and the SCM label were passively combined in the electrical domain using a diplexer to generate the combined modulator drive signal.

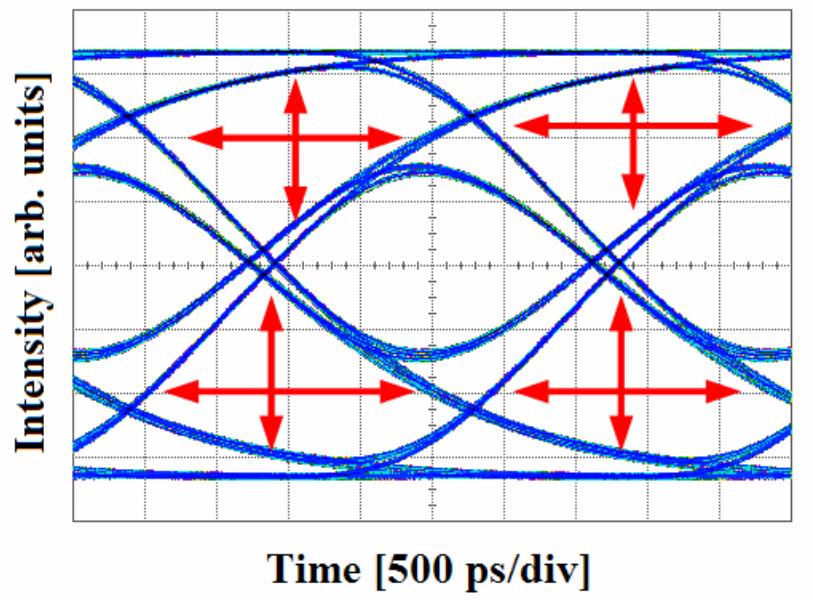

Figure 5.2 Duobinary electrical eye showing three symbol levels, with the eye opening indicated with arrows.

5.2.2 Optical Signal

Optimum performance was obtained for both payload and label signals with the MZM biased at extinction. In the case of the payload, driving the MZM around its minimum transmission point allows the three-level electrical signal to be modulated onto the phase and amplitude of the optical carrier, thus generating a narrow spectrum AM-PSK signal from the narrow spectrum duobinary payload drive signal [21, 22, 23]. This can be understood from Table 5.1, which presents the mapping of the different levels of the electrical duobinary signal to the optical domain. An advantage of this modulation format is that the optical signal can be received using conventional NRZ direct detection.

At the receiver, however, the square law detection cannot differentiate between variation in the optical phase, giving only two levels, 0 and E^2, [24] as per Table 5.1. Thus the detected data would appear not be equal to the transmitted NRZ data. Accordingly differential coding is necessary so that the detected data corresponds to the transmitted data. Differential encoding is performed at the transmitter rather

than decoding at the receiver so as to avoid error propagation in the detected signal. In the experimental work presented the use of differential encoding is not required as, for the Payload PPG used, a differential encoded PRBS is simply a delayed version of the original sequence and the error detector (ED) at the receiver can adjust to this delay [25]. The enhanced spectral efficiency of this modulation technique can be seen from Fig. 5.3 (a), in which the optical spectra of a 42.6 Gb/s payload signal is shown for both AM-PSK modulation and conventional NRZ intensity modulation. It can be clearly seen that the spectral width of the AM-PSK signal is narrower than that of the NRZ signal.

Electrical Level	Optical Level	Detected Level
0	-E	E^2
1	0	0
2	E	E^2

Table 5.1 Mapping of electrical duobinary signal to optical AM-PSK signal to detected electrical signal

In the case of the label signal, extinction biasing enabled suppression of the optical carrier by up to 15 dB. Carrier suppression improves the modulation depth of the sub-carrier signal allowing for increased receiver sensitivity [26, 27]. In the following experiments the drive amplitudes of the payload and label were optimised to minimise crosstalk. The optical spectrum of the transmitted AM-PSK carrier suppressed double side band (CS DSB) signal for the single channel experimental investigation (outlined in the section 5.4) is shown in Fig. 5.3 (b).

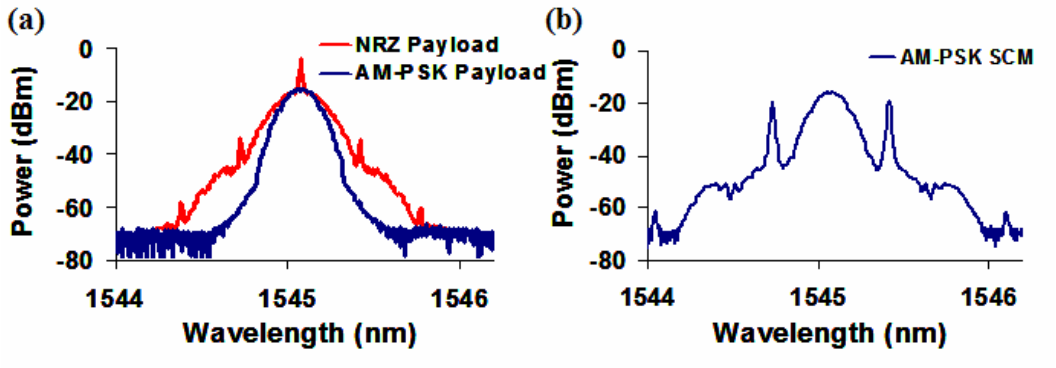

Figure 5.3 (a) Spectral comparison of NRZ modulation and AM-PSK modulation for 42.6 Gb/s Payload, (b) Transmitted optical signal consisting of combined AM-PSK payload and double side band SCM labels.

5.3 Receiver

The receiver set-up for the experimental work is given in the Fig. 5.4. Upon entering the receiver the combined signal was optically pre-amplified with an EDFA and passed through an AWG specified for 100 GHz spaced systems. This filters out the desired channel and minimises the amplified spontaneous emission noise introduced by the optical pre-amplification. A second EDFA was then used to boost the signal before optically separating the payload from the DSB sub-carrier label. This was done using an asymmetrical Mach-Zehnder deinterleaver (AMZD) with a free spectral range (FSR) of 82.5 GHz.

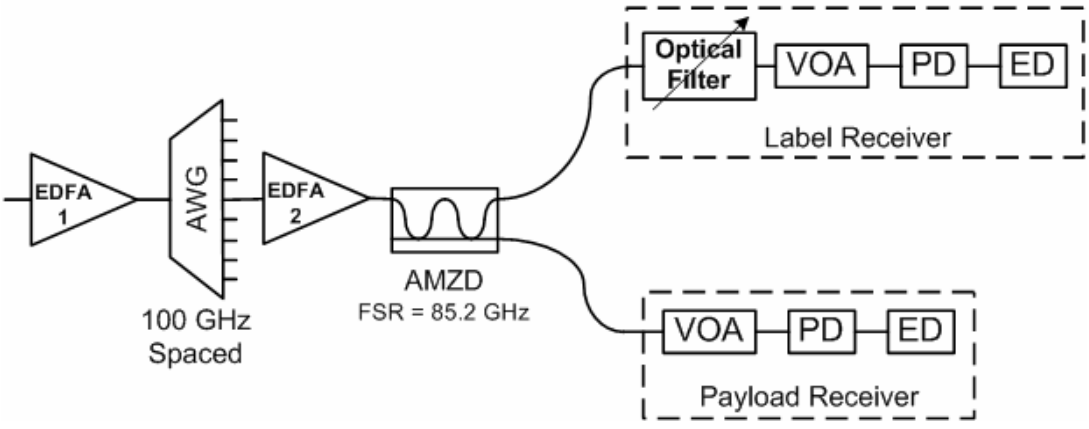

Figure 5.4 Receiver set-up, using AMZD to separate payload and optical SCM label

The payload was suppressed on one of the AMZD output ports and the DSB labels were passed to the label receiver, represented by the upper path in Fig. 5.4. The inverse happened on the other output port, represented by the lower path in the figure, and the payload was directed to the payload receiver, consisting of a variable optical attenuator (VOA) a photodiode (PD) and an ED. The optical spectra of the outputs from the AMZD, for the single channel experimental investigation (outlined below in section 5.4) are shown in Fig. 5.5. In the label receiver additional filtering was performed on the DSB label, a narrowband tunable optical filter was used to extract a single label. This allows for simple direct detection of the label with a receiver optimised for the label bit rate. In addition the filter eliminates any dispersion-induced carrier fading that may occur due to fibre transmission [28], and it also minimises any spectral interference between the label and residual payload that may have passed through the AMZD. The detected label is then sent to an ED for bit error rate (BER) testing.

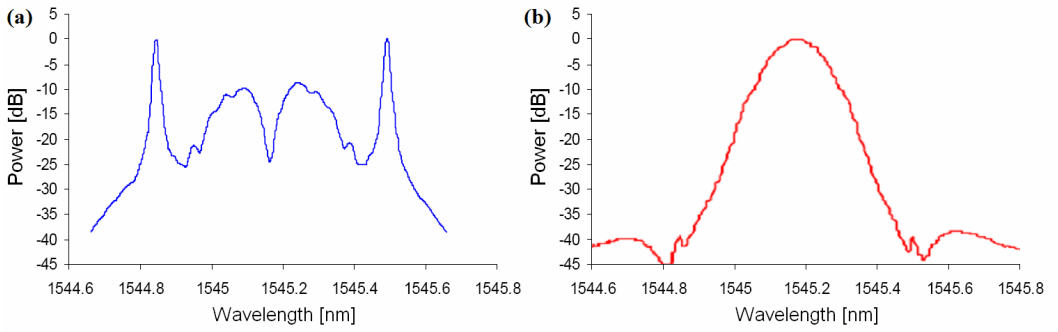

Figure 5.5 Optical spectra of the AMZD output ports showing (a) the extracted DSB label, and (b) the extracted payload.

5.4 Single Channel Experimental Investigation

5.4.1 Experimental Setup

A single channel experimental investigation was performed to measure the receiver sensitivities of the payload and of the label using the transmitter and receiver

configuration described above. The impact of the label on the payload receiver sensitivity and the impact of the payload on the label receiver sensitivity were measured for various pattern lengths. In this set of experiments the TL module was set in static mode at channel 51 (1545.322 nm). The drive signal amplitudes for the payload and for the label were set at approximately Vπ and 0.7 Vπ, respectively. This was done in order to reduce any crosstalk between the payload and label, and gave optical power in each sideband label of ~6 % of the total transmitted optical power. The combined optical signal was transmitted through 1 km of standard single mode fibre (SSMF). At the receiver, the signal power was monitored using a power meter and an optical spectrum analyser, thus allowing the individual power levels of the payload and labels to be determined. The optical spectrum of the signal at the receiver is presented in Fig. 5.3 (b). A 100 GHz spaced AWG with a flat-top profile and a 3 dB bandwidth of 80 GHz was used to select out the combined signal. In the label receiver a tunable Fabry-Perot filter with a 3 dB bandwidth of 6.25 GHz was used to select out a single side band of the label. The optical spectrum of the filtered single sideband, used for direct detection, is shown in Fig. 5.6.

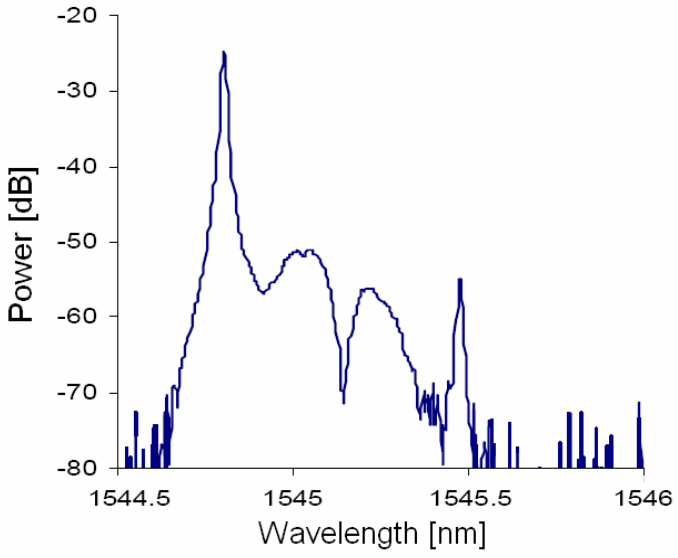

Figure 5.6 Extracted Label using tunable Fabry-Perot filter with a 3 dB bandwidth of 6.25 GHz

5.4.2 Payload receiver Sensitivity

The payload was modulated with a PRBS of pattern length 2^7-1. The performance of the payload was analysed by measuring its BER as a function of the received payload power, with no label transmitted, and then when labels of various PRBS pattern lengths were also transmitted. Label pattern lengths of 2^7-1, 2^{15}-1 and 2^{31}-1 were used. From the results presented in Fig. 5.7 (a) it can be seen that adding the label, only marginally impacted on the receiver sensitivity of the payload, introducing a power penalty of <1 dB. It can also be seen that there was no observable power penalty for the payload receiver sensitivity for different label pattern lengths. This low pattern sensitivity is to be expected, since each payload bit period is much shorter than the bit period of the label, so that increasing the length of consecutive uniform bits in the pattern would not further impact the payload integrity. The optical power required for a payload BER of 10^{-9} was ~10 dB less than that reported in [17] for the OCSS scheme.

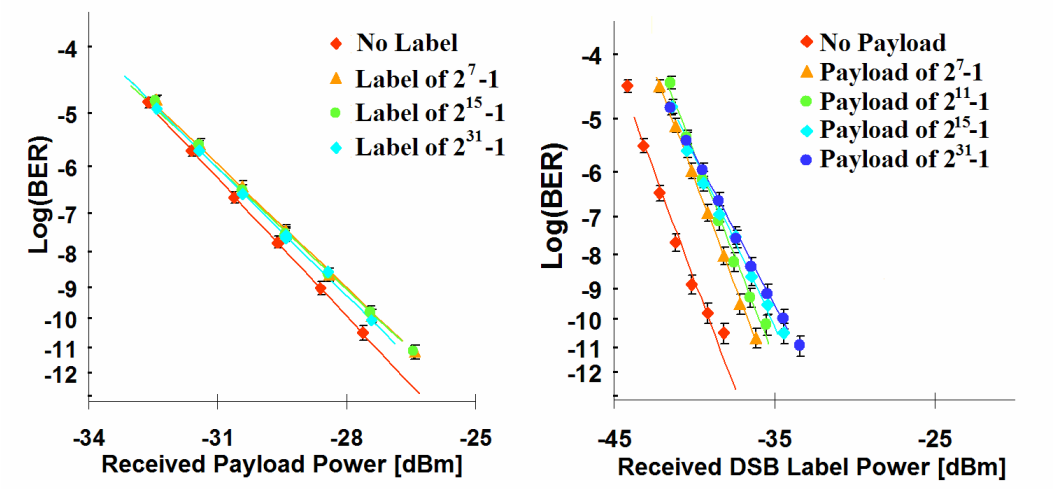

Figure 5.7 BER performance characteristic for (a) payload, and (b) label, showing impact resulting from addition of, and variation of pattern length, for label and payload, respectively.

5.4.3 Label Receiver Sensitivity

The impact of the payload on the label was then analysed by measuring the BER of the label as a function of the received DSB label power. These measurements were

performed when no payload was transmitted and then when payloads of different pattern lengths were also transmitted. The label was modulated with a PRBS of pattern length 2^7-1, while pattern lengths of 2^7-1, 2^{11}-1, 2^{15}-1 and 2^{31}-1 were used for the payload. It can be seen from the results presented in Fig. 5.7 (b), that the presence of the AM-PSK payload introduced a power penalty of ~2.5 dB on the label sensitivity for a label pattern length of 2^7-1. The label power penalty progressively increased as the payload pattern length was increased, with a maximum increase of ~1.5 dB measured for a pattern length of 2^{31}-1. In this case the label is sensitive to variation of the payload pattern length because each label bit is impacted upon by up to 17 payload bits, thus the effective bias point for the sub-carrier signal may be slightly modulated by the low frequency content of the payload data. This can result in a variation in the optical power of the label, leading to a vertical closing of the label eye for long strings of '0' data bits. Using Manchester encoding on the payload data may reduce this penalty, as this would reduce the low frequency component of the payload data [29].

5.5 Multi Channel Experimental Investigation

5.5.1 Experimental Setup

The experimental set-up used to investigate the SCM labelling scheme (described in the previous sections) in a multi-channel system on a 100 GHz spaced grid is given in Fig. 5.8. The set-up is based around the same transmitter and receiver configuration as was used in the single channel experiment. System performance analysis was carried out on a two-channel system by monitoring the impact on a static channel as a TL module, supporting a second channel, was tuned into an adjacent channel. The light from two TL modules was externally modulated with a combined electrical data signal consisting of a 40 Gbit/s duobinary base-band payload and a synchronised 40 GHz sub-carrier, ASK-modulated with 155 Mbit/s NRZ labels. This gives a two channel OLS system with a spectral efficiency of 0.4 b/s/Hz. The PRBS pattern length of both payload and label was 2^7-1.

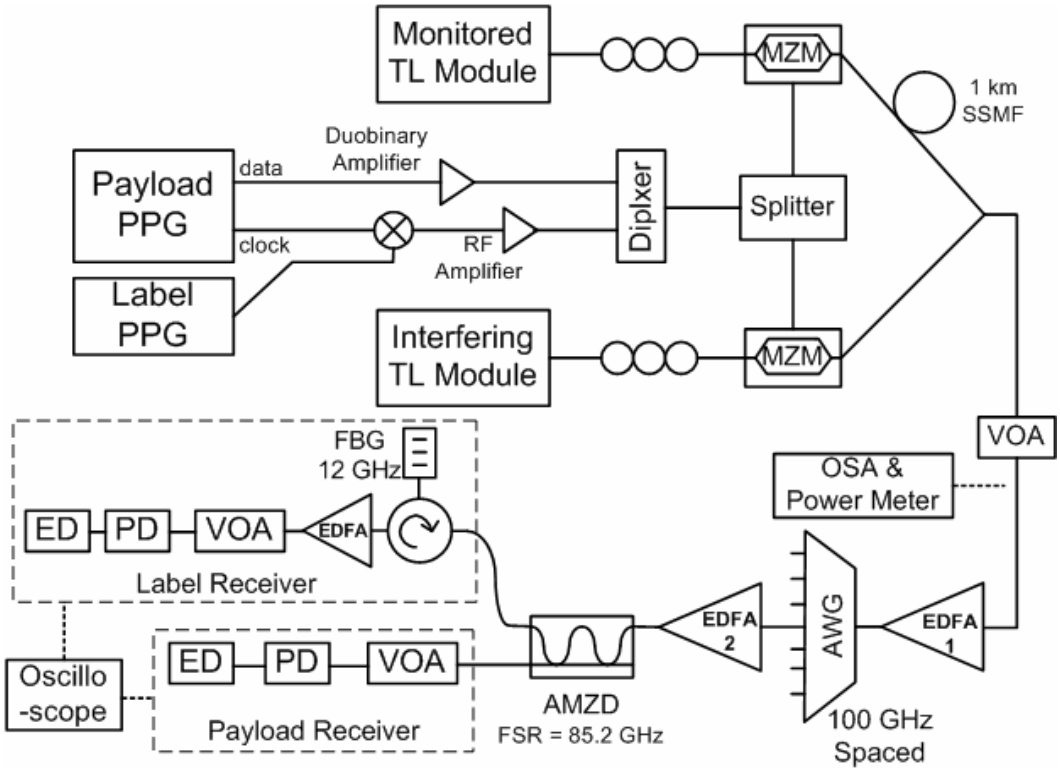

Figure 5.8 Multi-channel experimental set-up used to evaluate impact, on a monitored static SCM labelled signal, from a second SCM labelled signal.

Due to equipment limitations a lower data rate was used for the label, in comparison with the single channel analysis, and the same data was used to modulate both channels. This was done by power splitting the diplexer output, and sending half the power to each of the MZ modulators. The payload drive voltage to each modulator was approximately 0.9 $V\pi$ and the peak-to-peak drive amplitude of the sub-carrier was less than 0.5 $V\pi$, this gave each channel an optical power distribution of 93% in the payload and 7% in the labels. One of the channels was passed through 1 km of SSMF in order to de-correlate the data patterns; this corresponds to ~6.1 word lengths for the label and ~1574.8 word lengths for the payload. The two channels were then coupled together using a wide band optical coupler.

The optical spectrum measured at the input to the receiver, showing the two

transmitted channels, is shown in Fig. 5.9. The TL modules are in static *or* locked mode and are spaced by 100 GHz, at channel 49 (1546.12, 193.9 THz) and channel 51 (1545.32, 194.0 THz). After pre-amplification channel 51 was selected using a 100 GHz spaced Gaussian profiled AWG with a 3 dB bandwidth of 65 GHz. The demultiplexed channel was then separated into its component parts using the AMZD.

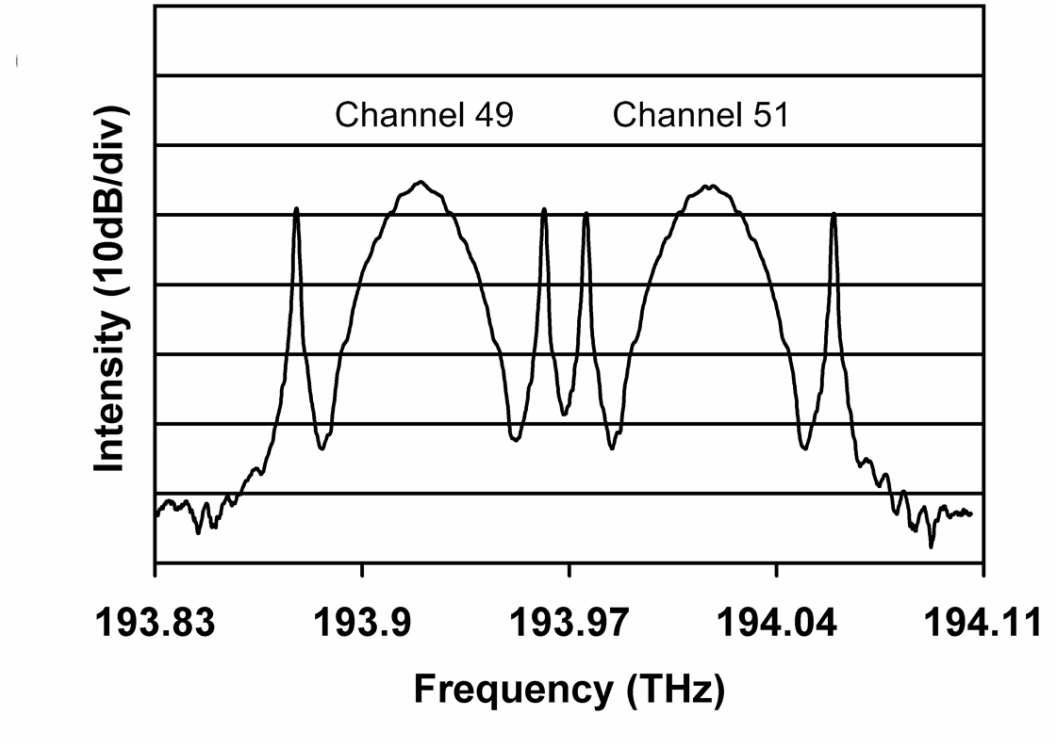

Figure 5.9 Optical Spectrum of adjacent 100 GHz spaced AM-PSK double side band SCM labelled signals at channel 49 and channel 51.

The spectra of the AMZD extracted payload and label are given in Fig. 5.10 (a) and Fig. 5.10 (b), respectively. Suppression of approximately 30 dB is shown on the label signal at the payload output (lower output port of AMZD), however the higher frequency label from the adjacent channel can be seen to leak through. Approximately 10 dB of payload suppression is seen at the label output (upper output port of AMZD).

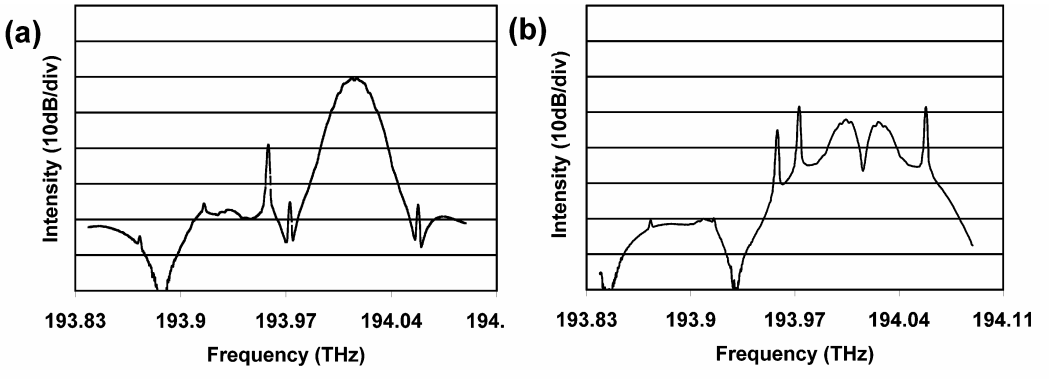

Figure 5.10 Optical spectra of the AMZD output ports showing (a) the extracted payload, and (b) the extracted DSB label, when a second signal is positioned at an adjacent 100 GHz spaced channel

The extracted payload was sent for photo-detection and BER testing while, as in the single channel experiment, the DSB label underwent additional optical filtering in the label receiver to allow for direct detection. In this case a tunable fibre Bragg grating (FBG) was used to perform the filtering; the input arm of a circulator was connected to an FBG with a 3 dB reflection bandwidth of approximately 12 GHz. This bandwidth is wide enough to ensure correct detection of the label even in the case of wavelength drift of the tuneable laser.

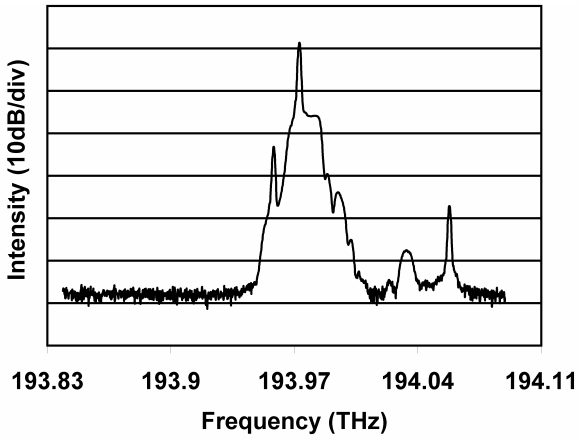

Figure 5.11 Extracted Label using tunable FBG filter with a 3 dB bandwidth of 12 GHz

The filter was tuned to reflect the lower frequency label of the extracted channel, to gauge the impact of any interference from that may arise from a signal at an adjacent channel. The reflected label, shown in Fig. 5.11 was directly detected, electrically amplified and low pass filtered before being sent for BER testing.

5.5.2 BER Performance of Monitored Static Channel

The system performance was analysed by measuring the BER of the payload and label as a function of the total (payload and label) received optical power, using different scenarios. Initially the interfering TL module was set to a distant channel, (channel 13 – 1560.60 nm), 1.9 THz from the filtered channel, this ensured that there would be no power leakage through the AWG. As in the previous section, the impact of the label on the payload, and the impact of the payload on the label were examined. This was done by performing the BER measurements on the payload with the label turned off and on, and then performing the BER measurements on the label with the payload turned off and on. As can be seen in Fig. 5.12 (a) the presence of the label (Δ) had only a minimal impact on the performance of the payload alone (○). However as can be from the results presented in Fig. 5.12 (b) (showing the performance with only the label transmitted (○) and the performance with the combined signal of payload and label (Δ) transmitted) the presence of the duobinary payload had a detrimental impact on the label, introducing a power penalty of approximately 13 dB. An OSA was used to measure the proportion of the transmitted channel power in the labels with the payload turned off (~48.5% in each label) and with the payload turned on (~3.5% in each label). This reduction in the label power accounted for ~11.4 dB of the label penalty. The remaining 1.6 dB penalty was attributed to the aggregate modulation of the bias position of the 40 GHz sub-carrier by the payload data (averaged over 258 bits). This figure is comparable to the 2.5 dB label power penalty observed in the single channel experiment with the payload turned on (Fig. 5.7 (b)).

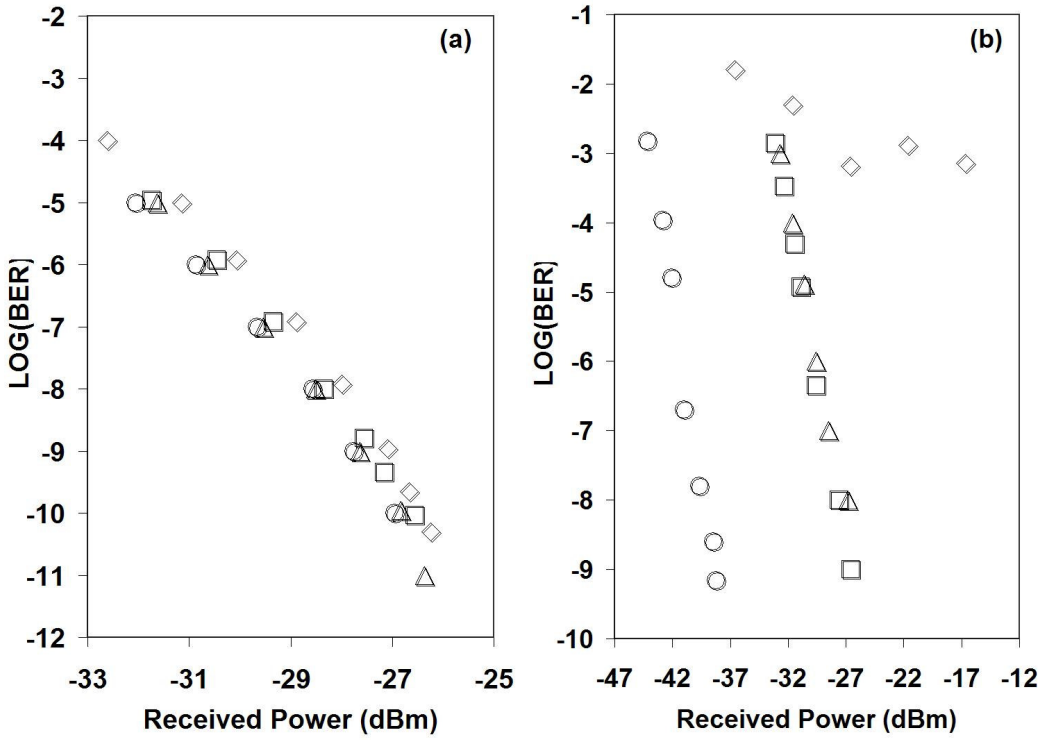

Figure 5.12 (a) BER of the monitored static channel payload versus total received power for four cases: labels turned off, with the interfering TL signal set at a distant channel (○); labels turned on, with the interfering TL signal set at a distant channel (Δ); labels turned on, with the interfering TL signal set at adjacent channel (□); labels turned on, with the interfering TL signal switching into adjacent channel (◊). (b) BER of the monitored static channel label versus total received power for four cases: payload turned off, with the interfering TL signal set at a distant channel (○); payload turned on, with the interfering TL signal set at a distant channel (Δ); payload turned on, with the interfering TL signal set at adjacent channel (□); payload turned on, with the interfering TL signal switching into adjacent channel (◊).

The impact of adjacent channel interference on the system was then investigated by measuring the BER performance of the payload and label as a function of the total received optical power for the following cases. The first case was with the interfering TL module set to channel 49, thus creating two adjacent channels spaced by 100 GHz (i.e. at channel 49 and channel 51) as described in the experimental set-up and illustrated in Fig. 5.8. The received eye diagrams, for this case, of the payload and label data are given in Fig. 5.13 (a) and Fig. 5.13 (b), respectively. The

second case was with the interfering TL module switching into the adjacent channel (channel 49) from the distant channel (channel 13) every 520 ns. This final case used a channel transition with one of the largest initial frequency drifts for the particular TL module used, and the switching time used represents the fastest switching time possible for the module. The results for the payload and label performance measurement are included with the previous results in Fig 5.12 (a) and Fig. 5.12 (b), respectively.

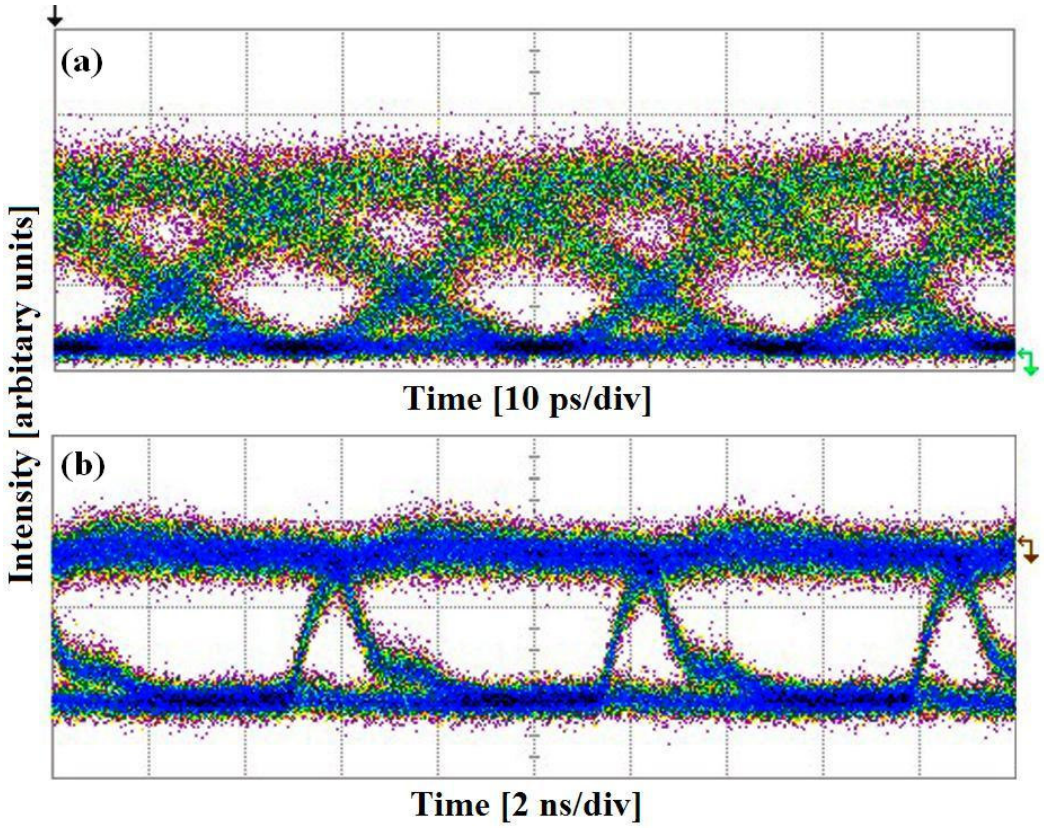

Figure 5.13 Eye diagrams for directly detected (a) AMZD extracted duobinary payload, and (b) FBG extracted ASK label

It can be seen from the results for the payload BER measurements (Fig 5.12 (a)) that by simply having two channels adjacent to each other in static mode (□), a power penalty of approximately 0.5 dB is introduced on the performance characteristic of the monitored payload for the case when the interfering TL was set

at the distant channel (Δ). This is due to cross talk from the label of the adjacent channel (clear from Fig. 5.10 (a)) and could potentially be reduced, or even eliminated, by optimising the profile of the AWG which is used to select the channels. Further degradation for the case when the interfering TL module is switching into the adjacent channel is minimal (◊). This behavior is expected as the maximum wavelength drift that the TL module is specified to experience (+/-15 GHz) is less than spacing between the extremity of the interfering signal (i.e. the higher frequency label), and the edge of the band pass characteristic of the payload port of the AMZD, used to select out the static payload.

This relative spacing decreases for the case when the performance of the monitored label is analysed, and is reflected in the associated BER measurements given in Fig. 5.12 (b). As with the payload, the presence of an adjacent static channel (□) only results in a minor power penalty on the label performance characteristic in comparison to the case with distant positioning of the interfering TL (Δ). However, when the interfering TL module is switching into the adjacent channel, an error floor, greater than 5×10^{-4}, is introduced on the performance characteristic of the monitored static label (◊). This is due to the label of the interfering signal falling under the filter pass band of the monitored label. This can be better understood from the work carried out in the previous chapter on the time evolution of the TL module output frequency, directly after channel tuning. The interference leading to the error floor is due to the wavelength drift of the label, from the interfering TL, around its target wavelength as the TL module locker is activated. Comparing time resolved BER measurements with the module frequency drift, as explained in the following section, supports this understanding.

5.4.3 Time Resolved Bit Error Rate Measurement

The performance of the monitored label was measured as a function of time for the case when the modulated interfering TL is tuned into channel 49, i.e. adjacent to the monitored channel. Time resolved BER measurements were performed by gating the error detector with a gate signal, synchronised to the TL channel transition, and

progressively delaying the gate for each BER measurement. The measurements were performed at a received optical power of -28.5 dBm, using a gating period of 8 ns, and are presented in Fig. 5.14. The time resolved frequency of the higher frequency label from the switching laser is also displayed. This was indirectly obtained from a measurement of the instantaneous frequency of the TL module, while un-modulated, for the particular channel transition under test (channel 13-49). The instantaneous frequency was extracted from the complimentary outputs of the 85.2 GHz AMZD, while biased at quadrature. This was achieved by using the measured frequency response of the AMZD to resolve the TL Module output frequency. For reference purposes the frequency of the monitored label and the target frequency for the interfering label are emphasized in the figure.

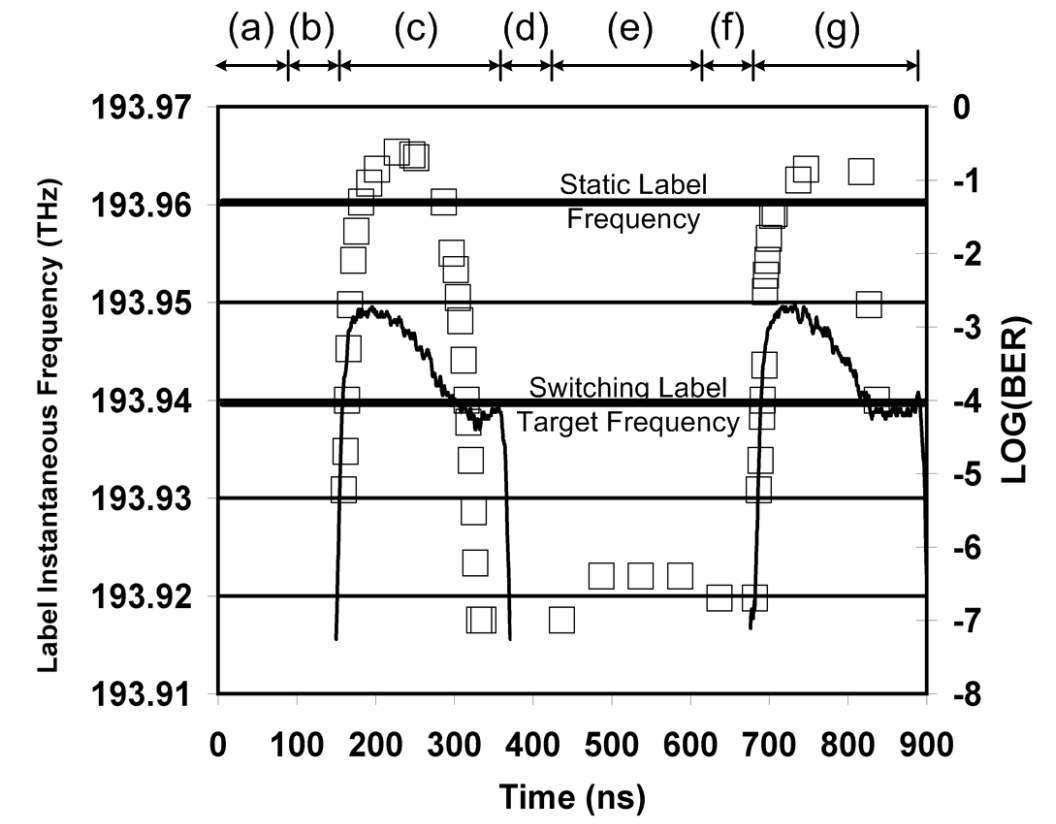

Figure 5.14 Time Resolved bit error rate measurements for the extracted label (□) and instantaneous frequency of the interfering TL's label (line).

It can clearly be seen that the instantaneous frequency of the TL module corresponds to the time intervals when there are significant errors on the received label data. To improve the figure clarity (i.e. Fig. 5.14), the time axis is divided into the following periods based on the condition of the interfering TL module:

(a) TL module at distant channel (channel 13),

(b) TL module blanked for 60 ns,

(c) TL module settling into target channel (channel 49) for 200ns,

(d) TL module blanked for 60 ns,

(e) TL module at distant channel (channel 13),

(f) TL module blanked for 60 ns,

(g) TL module settling into target channel (channel 49) for 200ns.

The device used to gate the bit error rate tester had an inherent delay of ~130 ns and so no measurements could be taken for time periods (a) and (b). While the module is blanked and also while it sits at the distant channel, the error rate drops considerably to become error free for a short time. This low error regime has a maximum error rate of ~4 x 10^{-7}. However as the TL module tunes towards its target wavelength, and the higher frequency label to 193.94 THz the error rate initially increases dramatically and then begins to fall off, mimicking the instantaneous frequency measurement of the module output.

From this result we can conclude that the error floor on the performance characteristic of the label for the TL module tuning case, as illustrated in Fig 5.14, is due to the initial wavelength drift of the TL module falling under the reflection band of FBG filter used to select out the monitored label. This is an important result as it can be used in formulating a method to achieve error-free performance for an SCM labelled system while using fast tunable lasers.

Conclusion

This chapter examined the use of a tunable laser module as the optical source for an optical label switched high data rate payload, typical of future high capacity all optical networks. With the transmitter set up used the combined label and the payload data was modulated onto the same optical carrier using a single MZ modulator. The use of a spectrally efficient duobinary payload allowed for closely spaced sub-carrier labels, thus giving the benefits of labelling without compromising the individual data rate per channel. It has been shown that wavelength drift of the tunable laser module can cause interference between adjacent labels in a DWDM system, which could result in the incorrect routing of packets in an OLS system.

In a single channel setup using 42.6 Gbit/s payload data and 2.5 Gbit/s label data it was shown that the payload introduced a pattern length dependent penalty on the label receiver sensitivity. To date, most of the literature on OLS systems has primarily looked at single-channel systems. Performance of a two channel system using 40 Gbit/s payload data and 155 Mbit/s label data on a 100 GHz spaced grid was investigated. Error-free transmission was reported for both the payload and label of a probe channel with the presence of an adjacent channel. It has however been shown that severe interference between the labels of adjacent channels can be caused by wavelength switching effects of the TL modules, with the introduction of an error floor on the performance characteristic of the probe label. Time resolved BER measurement has shown that the errors are localised immediately after a channel transition, corresponding with the initial wavelength drift of the laser as it emerges from blanking and is locked to its target wavelength. This result allows for the easier development of a method to overcome the problem.

The results presented from these set of experiments are specific to the transmitter and receiver scheme used, they could however be used to improve the future performance of this and other similar systems using fast tunable lasers. The module blanking time could be increased to reduce the initial wavelength drift (as used in

section 4.4) to allow for error free switching performance in a multi channel OLS system. Increasing the channel spacing could also eliminate the measured error floor. Both of these solutions would however reduce the network throughput. More attractive solutions would include optimised channel and label filter profiles or the use of single side band sub-carrier generation [26, 27] to eliminate interference between labels of adjacent channels, and optimisation of the TL module locking mechanism.

References

[1] P. Hofmann, E. E. Basch, S. Gringeri, R. Egorov, D. A. Fishman and W.A. Thompson, "DWDM long haul network deployment for the Verizon GNI nationwide network," in *Proc. Optical Fiber Commun. Conf. and National Fiber Optic Eng. Conf. (OFC /NFOEC 2005),* Anaheim, Mar. 2005, vol. 2, Paper OTuP5.

[2] T. Battestilli and H. Perros, "An introduction to optical burst switching," *IEEE Commun. Mag.,* vol. 41, pp. S10-S15, Aug. 2003.

[3] D.J. Blementhal, T. Ikegami, P.R. Prucnal and L. Thylen, "Guest editorial photonic packet switching technologies, techniques, and systems," *J. Lightw. Technol.,* vol. 16, pp. 2065-2067, Dec. 1998.

[4] D.J. Blumenthal, J. E. Bowers, L. Rau, H.-F.Chou, S. Rangarajan, W. Wang and H.N. Poulsen, "Optical signal processing for optical packet switching networks," *IEEE Commun. Mag.,* vol. 41, pp. S23-S29, Feb 2003.

[5] H. J. S. Dorren, M. T. Hill, Y. Liu, N. Calabretta, A. Srivatsa, F. M. Huijskens, H. de Waardt and G. D. Khoe, "Optical packet switching and buffering by using all-optical signal processing methods," *J. Lightw. Technol.,* vol. 21, pp. 2-12, Jan. 2003.

[6] F. Xue and S. J. B. Yoo, "High capacity multiservice optical label switching for the next generation internet," *IEEE Optical Commun.*, vol.2, pp. S16-S22, May 2004.

[7] D. J. Blumenthal, B. E. Olsson, G. Rossi, T. E. Dimmick, L. Rau, M. Masanovic, O. Lavrova, R. Doshi, O. Jerphagnon, J. E. Bowers, V. Kaman, L. A. Coldren and J. Barton, "All-optical label swapping networks and technologies," *J. Lightw. Technol.,* vol. 18, pp. 2058-2075, Dec. 2000.

[8] B. Meagher, G. K. Chang, G. Ellinas, Y. M. Lin, W. Xin, T. F. Chen, X. Yang, A. Chowdhury, J. Young, S. J. Yoo, C. Lee, M. Z. Iqbal, T. Robe, H. Dai, Y. J. Chen and W. I. Way, "Design and implementation of ultra-low latency optical label switching for packet-switched WDM networks". *J. Lightw. Technol.,* vol.18, pp. 1978-1987, Dec. 2000.

[9] D.J. Blumenthal, "Photonic packet and all-optical label switching technologies and techniques," in *Proc. Optical Fiber Commun. Conf.* (OFC 2002), Anaheim, Mar. 2002, pp. 282-284.

[10] D. Nesset, T. Kelly, and D. Marcenac, "All-optical wavelength conversion using SOA nonlinearities," *IEEE Commun. Mag.,* vol. 36, pp. 56-61, Dec. 1998.

[11] Zuqing Zhu, V. J. Hernandez, Min Yong Jeon, Jing Cao, Zhong Pan and S. J. Ben Yoo, "RF photonics signal processing in subcarrier multiplexed optical-label switching communication systems," *J. Lightw. Technol.,* vol. 21, pp. 3155-3166, Dec. 2003.

[12] I. T. Monroy, A. M. J. Koonen, J. Zhang, N. Chi, P. V. Holm-Nielsen, C. Peucheret, J. J. Vegas Olmos and G.-D. Khoe, "Techniques for labeling of optical signals in burst switched networks," in First Inter. Workshop on Optical Burst Switch. (WOBS'03), Dallas, October 2003.

[13] A. Martinez, D. Pastor, J. Capmany, B. Ortega, P.-Y. Fonjallaz, M. Popov, T. Berceli and T. Banky, "Experimental demonstration of subcarrier multiplexed optical label swapping featuring 20 GB/s payload speed and 622 Mb/s header conveyed @18.3 GHz," in *Proc. Eur. Conf. Optical Commun. (ECOC05),* Glasgow, Sep. 2005, vol. 4, pp. 959-960.

[14] M. Y. Jeon, Z. Pan, J. Cao, and S. J. B. Yoo, "BER performance of all optical subcarrier label swapping with 2R regeneration," *IEEE Photon. Technol. Lett.,* vol. 16, pp. 323-235, Jan. 2004.

[15] D. J. Blumental, A. Carena, L. Rau, V. Curri, and S. Humphries, "All optical label swapping with wavelength conversion for WDM-IP networks with subcarrier multiplexed addressing," *IEEE Photon. Technol. Lett.*, vol. 11, pp. 1497-1450, Nov. 1999.

[16] H. J. Lee, S. J. B. Yoo, V. K. Tsui, and S. K. H. Fong, "A simple alloptical label detection and Swapping technique incorporating a fiber Bragg grating filter," *IEEE Photon. Technol. Lett.,* vol. 13, pp. 635-637, Jun. 2001.

[17] Gee-Kung Chang, Jianjun Yu, Arshad Chowdhury and Yong-Kee Yeo, "Optical carrier suppression and separation label-switching techniques," *J.*

Lightw. Technol., vol. 23, pp. 3372-3387, Oct. 2005.

[18] N. Chi, J. Zhang and P. Jeppesen, "All-optical subcarrier labeling based on the carrier suppression of the payload," *IEEE Photonics Technol. Lett.,* vol.15, pp. 781-783, May 2003.

[19] Intune AltoNet 1200 FTL Tx Module [Online]. Available: http://www.intunenetworks.eu/site/

[20] M. Deulk, J. Gripp, J. Simsarian, A. Bhardwaj, P. Bernasconi, M. Zirngibl, and O. Laznicka, "Fast packet routing in a 2.5 Tb/s optical switch fabric with 40 Gb/s duobinary signals at 0.8 b/s/Hz spectral efficiency" in *Proc. Optical Fiber Commun. Conf. (OFC 2003)* , Georgia, Mar. 2003, vol. 3, postdeadline paper PD8-1-3.

[21] Peter J. Winzer and Renè-Jean Essiambre, "Advanced modulation formats for high-capacity optical transport networks," *J. Lightw. Technol.,* vol. 24, pp. 4711-4728, Dec. 2006

[22] G. Charlet, "Progress in optical modulation formats for high-bit rate WDM transmissions," *IEEE J. Sel. Topics Quant. Electron*., vol. 12, pp. 469-483, Jul./Aug. 2006.

[23] Takashi Ono, Yutaka Yano, Kiyoshi Fukuchi, Toshiharu Ito, Hiroyuki Yamazaki, Masayuki Yamaguchi and Katsumi Emura, "Characteristics of Optical Duobinary Signals in Terabit/s Capacity, High-Spectral Efficiency WDM Systems," *J. Lightw. Technol.,* vol.16, pp.788-797, May 1998.

[24] Eric Tell, "Modulation formats for digital fiber transmission", 6 Aug. 2005, http://www.dtr.isy.liu.se/OKkurs/OKpresentation_EricT.ppt

[25] Hari Shankar, "Duobinary modulation for optical systems," Lightwave, 1 June 2006
http://lw.pennnet.com/display_article/256526/13/ARTCL/none/none/Duobinary-modulation-for-optical-systems/

[26] Rongqing Hui, Benyuan Zhu, Renxiang Huang, Christopher T. Allen, Kenneth R. Demarest, Douglas Richards, "Subcarrier multiplexing for high-speed optical transmission," *J. Lightw. Technol.,*vol. 20, pp. 417-427, Mar. 2002.

[27] Shijun Xiao and Andrew M. Weiner, "Optical carrier-suppressed single sideband (O-CS-SSB) modulation using a hyperfine blocking filter based on a virtually imaged phased-array (VIPA), " *IEEE Photonics Technol. Lett*., vol. 17, pp.1522-1524, Jul. 2005.

[28] V. Hernandez, V.K. Tsui, S.J.B Yoo and H.J. Lee, "Simple, polarisation-independent, and dispersion-insensitive SCM signal extraction technique for optical switching systems applications," *Electronics Letters,* vol. 37, pp.1240-1241, Sep. 2001.

[29] Jianfeng Zhang, Nan Chi, P.V. Holm-Nielsen, C. Peucheret and P. Jeppesen, "Performance of Manchester-coded payload in an optical FSK labeling scheme," *IEEE Photonics Technol. Lett*., vol. 15, pp. 1174-1176, Aug. 2003.

Chapter 6 - Conclusion

The electronically tunable semiconductor laser, although still regarded as an emerging technology, is set to become a key component in optical networking over the next few decades. High-volume TL manufacturing is currently underway and initial deployment has begun, thus far, however, only for sparing applications in current DWDM point-to-point networks. With the growth of advanced broad band applications and the market desire for triple play services, TLs will begin to impact network architectures in the coming decade. This is because the design of the current optical layer is too rigid to meet such demand. It is only at the stage of development of optically switched burst and packet networks, that the TL switching time will be of importance to network and service providers. This thesis investigated the use of fast switching TL modules in experimental set-ups designed to examine the module operation for future optically switched networks of this type.

A significant problem associated with TLs, is the generation of undesired spectral components during wavelength switching events. These spurious modes where shown to result in interference on channels in WDM systems if emitted at such channel wavelengths. This issue becomes more important as the switching interval time is reduced. It has been demonstrated in Chapter 3, that a viable solution to this problem is the use of an SOA at the output of the TL to blank the output during the transition to attenuate the spurious components that may be generated during that time. However, if a large number of TL's are employed in a network, then the system penalties due to this effect may be non-negligible, as shown in the experiments with three TLs. In WDM networks employing a large number of TLs, therefore, it may be necessary to increase blanking levels to prevent performance

degradation due to wavelength switching events

The magnitude and duration of the TL wavelength drift, as it emerges from the SOA blanking and locks into its target wavelength, has been investigated in Chapter 4. The measured drift (~7.5 GHz) has been shown to cause problems in low capacity systems, typical of future access schemes, utilizing channel spacing of 12.5 GHz. The drift was shown to cause critical error floors on the BER vs. received power performance characteristic of data channels adjacent to the TL target channel. It has been shown that by using an extended blanking time the wavelength drift can be significantly reduced, thus allowing error free performance. It was also shown that the use of SCM transmission and electrical heterodyne detection, which is less sensitive to the TL wavelength drift than a conventional BB scheme, can be used to achieve error free performance. Through using very closely spaced wavelength channels, as was examined in this work, in an access type environment, it is possible to serve more end users from a single fibre. These techniques, coupled with the use of reflective SOAs at the customer premises for upstream data, could therefore be used to overcome the "tunable premium" and allow for TLs to be used in future wavelength switched access networks.

In the penultimate chapter the use of TLs in high capacity optical labelled switched systems was investigated. Using a spectrally efficient OLS system employing SCM labels and a 40 Gbit/s duobinary payload, the tunable laser module drift, after wavelength switching, was shown to result in interference between the labels of two adjacent channels on a 100 GHz spaced grid. Using time resolved BER measurements it was shown that the interference was consistent with the measured wavelength drift of the tunable laser. As with the low capacity UDWDM experimental work, the blanking time could be extended to reduce the wavelength drift and allow for error free transmission. This option is however not as attractive an option for the case of a high capacity channel as the increased switching time would significantly increase the packet overhead, leading to a greater reduction in network throughput. In this case other options such as a delayed locker turn on time

or optimisation of the locker electronic control should be considered.

One must bear in mind that with optical circuit switched systems only currently beginning to see widespread deployment, and with optical burst and packet based networks still at the test-bed level, initial deployment of such networks may be someway off. A full migration from real-time based to IP based traffic is also not expected for the midterm. Accordingly the future optical layer will more probably be a based on a hybrid circuit and burst or packet switched structure capable of supporting multiple services of varying quality requirement. Overtime this hybrid structure will become predominately burst and packet based, thus the use of fast tunable lasers, upon which this thesis is based, will become increasingly important.

Appendix A - List of Publications

Referred Journals

Cross-Channel Interference due to Wavelength Drift of Tunable Lasers in DWDM Networks

E. Connolly, F. Smyth, A.K. Mishra, A. Kaszubowska-Anandarajah and L.P. Barry, *IEEE Photonics Technology Letters*, vol 19, no. 8, pp. 616 – 618, April 15 2007.

Demonstration of Wavelength Packet Switched Radio-Over-Fiber System

A. Kaszubowska-Anandarajah, E. Connolly, L.P. Barry and P. Perry, *IEEE Photonics Technology Letters*, vol 19, no. 4, pp. 200 – 202, February 15 2007.

Spectrally Compact Optical Subcarrier Multiplexing with 42.6 Gbit/s AM-PSK Payload and 2.5 Gbit/s NRZ Labels

A.K. Mishra, A.D. Ellis, D. Cotter, F. Smyth, E. Connolly and L.P. Barry, *Electronics Letters*, vol 42, no. 22, pp. 1303 – 1304, October 26 2006

Effects of Crosstalk in WDM Optical Label Switching Networks Due to Wavelength Switching of a Tunable Laser

F. Smyth, E. Connolly, A.K. Mishra, A.D. Ellis, D. Cotter, A. Kaszubowska-Anandarajah and L.P. Barry, *IEEE Photonics Technology Letters*, vol 18, no. 20, pp. 2177 – 2179, October 15 2006.

Fast Wavelength Switching Lasers Using Two-Section Slotted Fabry–Pérot Structures

F. Smyth, E. Connolly, B. Roycroft, B. Corbett, P. Lambkin and L.P. Barry, *IEEE Photonics Technology Letters*, vol 18, no. 20, pp. 2105 – 2107, October 15 2006.

Cross-Channel Interference Due to Wavelength Switching Events in Wavelength Packed Switched WDM Networks

E. Connolly, A. Kaszubowska-Anandarajah, L.P. Barry, J. Dunne, T. Mullane and D. McDonald, *Optical Communications*, vol. 267, no. 1, pp. 88 – 91, 1 November 2006

Impact of Tunable Laser Wavelength Drift in a Base-Band and Sub-Carrier Multiplexed System

E. Connolly, A. Kaszubowska-Anandarajah, P. Perry, L. P. Barry, submitted for publication.

Reviewed Conference Papers

Frequency Drift Characterisation of Directly Modulated SGDBR Tunable Lasers

R. Maher, P. Anandarajah, E. Connolly, A. Kaszubowska and L.P. Barry, *Lasers and Electro-Optics Society Annual Meeting (LEOS2007)*, Orlando, paper no. WJ 3

Adjacent Channel Interference due to Wavelength Drift of a Tunable Laser in Base-Band and Subcarrier Multiplexed System

E. Connolly, A. Kaszubowska-Anandarajah and L.P. Barry, *Lasers and Electro-Optics Society Annual Meeting (LEOS 2006), Montreal,* pp. 968 – 969

Characterisation of Fast Tunable Lasers for Applications in Optical Packet Switching Networks

A. Kaszubowska-Anandarajah, E. Connolly and L. P. Barry; *China-Ireland International Conference on Information and Communications Technologies (CIICT 06)*, Hang Zhou, China, 18-19 Oct 2006

SCM optical label switching scheme in a WDM packet transmitter employing a switching SG-DBR laser

F. Smyth, A. Mishra, E. Connolly, A. Ellis, D. Cotter, A. Kaszubowska and L. Barry, *Photonics in Switching Conference (PS 2006)*, Crete, Oct 2006

Spectrally Compact Optical Subcarrier Multiplexing for Label-Switched Networks with 42.6 Gb/s Duobinary Payload and 2.5Gb/s NRZ Labels

A.K. Mishra, A.D. Ellis, D. Cotter, F. Smyth, E. Connolly and L.P. Barry, *European Conference on Optical Communication (ECOC 2006*), Cannes, paper no. Th. 1.4.6, 24-28 September 2006

Cross Channel Interference due to Wavelength Drift of Tuneable Lasers in DWDM Networks

E. Connolly, A. Kaszubowska-Anandarajah and L.P. Barry, *International Conference on Transparent Optical Networks (ICTON 2006)*, Nottingham, vol. 4, pp. 52 – 55, 18-22 June 2006

Fast Tunable Lasers in Radio-over-Fiber Access Networks

A. Kaszubowska-Anandarajah, E. Connolly, L.P. Barry and D. McDonald, , *International Conference on Transparent Optical Networks (ICTON 2006)*, Nottingham, vol. 1, pp. 228 – 231, 18-22 June 2006

Cross-channel interference due to wavelength switching events in wavelength packet switched WDM networks

E. Connolly, A. Kaszubowska-Anandarajah, L.P. Barry, J. Dunne, T. Mullane and D. McDonald, *European Conference on Optical Communication (ECOC 2005*), vol. 3, pp. 359 – 360, 25-29 Sept. 2005.

Appendix B – TL Module Channel Assignment

AltoNet 1200 frequency plan assignments

The AltoNet 1200 can support all channels in the C-band of wavelengths, as defined by ITU-T G.692, which is equivalent to 80 channels on the 50 GHz frequency grid. The channel numbers assigned to each frequency for the AltoNet 1200 module are specified below, where the wavelength in vacuum has been specified. Channels 13 and 93 indicate the edge of the standardised ITU grid of frequencies according to the current channel identification scheme. Lasing frequencies from channel 8 to 94 are, by default, supported on C-band versions of the AltoNet 1200.

Table 2. Frequency Assignments

Channel number	Channel frequency (THz)	Channel wavelength (nm)	Channel number	Channel frequency (THz)	Channel wavelength (nm)
1	191.5	1565.496	**52**	194.05	1544.924
2	191.55	1565.087	**53**	194.1	1544.526
3	191.6	1564.679	**54**	194.15	1544.128
4	191.65	1564.271	**55**	194.2	1543.730
5	191.7	1563.863	**56**	194.25	1543.333
6	191.75	1563.455	**57**	194.3	1542.936
7	191.8	1563.047	**58**	194.35	1542.539
8	191.85	1562.640	**59**	194.4	1542.142
9	191.9	1562.233	**60**	194.45	1541.746
10	191.95	1561.826	**61**	194.5	1541.349
11	192	1561.419	**62**	194.55	1540.953
12	192.05	1561.013	**63**	194.6	1540.557
13	192.1	1560.606	**64**	194.65	1540.162
14	192.15	1560.200	**65**	194.7	1539.766
15	192.2	1559.794	**66**	194.75	1539.371
16	192.25	1559.389	**67**	194.8	1538.976
17	192.3	1558.983	**68**	194.85	1538.581
18	192. 35	1558.578	**69**	194.9	1538.186
19	192.4	1558.173	**70**	194.95	1537.792
20	192.45	1557.768	**71**	195	1537.397
21	192.5	1557.363	**72**	195.05	1537.003
22	192.55	1556.959	**73**	195.1	1536.609
23	192.6	1556.555	**74**	195.15	1536.216
24	192.65	1556.151	**75**	195.2	1535.822
25	192.7	1555.747	**76**	195.25	1535.429
26	192.75	1555.343	**77**	195.3	1535.036
27	192.8	1554.940	**78**	195.35	1534.643
28	192.85	1554.537	**79**	195.4	1534.250
29	192.9	1554.134	**80**	195.45	1533.858
30	192.95	1553.731	**81**	195.5	1533.465
31	193	1553.329	**82**	195.55	1533.073
32	193.05	1552.926	**83**	195.6	1532.681
33	193.1	1552.524	**84**	195.65	1532.290
34	193.15	1552.122	**85**	195.7	1531.898
35	193.2	1551.721	**86**	195.75	1531.507
36	193.25	1551.319	**87**	195.8	1531.116
37	193.3	1550.918	**88**	195.85	1530.725
38	193.35	1550.517	**89**	195.9	1530.334
39	193.4	1550.116	**90**	195.95	1529.944
40	193.45	1549.715	**91**	196	1529.553
41	193.5	1549.315	**92**	196.05	1529.163
42	193.55	1548.915	**93**	196.1	1528.773
43	193.6	1548.515	**94**	196.15	1528.384
44	193.65	1548.115	**95**	196.2	1527.994
45	193.7	1547.715	**96**	196.25	1527.605
46	193.75	1547.316	**97**	196.3	1527.216
47	193.8	1546.917	**98**	196.35	1526.827
48	193.85	1546.518	**99**	196.4	1526.438
49	193.9	1546.119	**100**	196.45	1526.050
50	193.95	1545.720	**101**	196.5	1525.661
51	194	1545.322			

Note: For use with G.653 type fibers, please consult the factory with your required frequency plan.